Assessment of Individual Trees using Aerial Laser Scanning in New Zealand Radiata Pine Forests

---

A thesis submitted in partial fulfilment
of the requirements for the Degree of
Doctor of Philosophy
in Forestry by

David Pont

School of Forestry

University of Canterbury

2016

I am told there are people who do not care for maps,

and I find it hard to believe.

Robert Louis Stevenson, Treasure Island

Table of Contents

List of Figures

Figures

List of Tables

Abstract

Forest managers aim to maximise the productivity, profitability, health, and sustainability of New Zealand's plantation forests. There is an increasing need for high quality information about forest stands to support effective management. This is exemplified in the concept of precision forestry, which maps variation at a fine scale to allow targeted management, and in the concept of tree-level phenotyping, which quantifies the genetic and environmental drivers of tree growth. Remotely sensed data, in particular airborne laser scanning (ALS), was identified as having strong potential to provide tree level information to assist in attaining the goals of phenotyping and precision forestry. Tree-based, rather than area-based, analyses of ALS were identified as being essential to separate and quantify genetic and environmental factors on individual tree growth, and therefore critical to the development of novel phenotyping methods supporting precision forestry. The aim of this study was therefore to develop methods to characterise individual trees using remotely sensed airborne laser scanning data.

The research was focussed on evaluating the utility of ALS data to estimate key operationally relevant tree attributes for New Zealand plantation-grown radiata pine. Review of the literature identified three key research questions within which to frame the study. The first research question addressed the need to obtain accurate estimates of tree size, form, wood quality and disease attributes from ALS. A set of 36 individual tree crown metrics were derived from ALS data and evaluated for their correlations with ground measurements of the attributes. The second research question was aimed at evaluating the utility of tree-level ALS data in the analysis of genetic and environmental variance components and the estimation of genetic parameters, including genetic gains. The third research question evaluated the effects of ALS pulse density on estimates obtained from tree-level analyses of ALS data.

Strong correlations were established between morphological crown metrics and tree size attributes (r=0.90, 0.82, and 0.84 for *H*, *DBH* and *V* respectively), but not for tree form and wood quality attributes. A moderate correlation (r=0.50) with the level of Dothistroma

infection was attributed to the effect of the disease on tree growth, indicating potential for disease phenotyping using remote sensing. Accurate estimates of variance components and genetic parameters were obtained from ALS for tree size attributes, but not for tree form, wood quality and disease attributes. For *H*, *DBH*, and *V* crown-based versus ground-based estimates of narrow sense heritabilities were within 5.0%, 19.5% and 23.9%, and estimates of genetic gains (96 tree selection level) were within 19%, 25%, and 25% respectively. Manually corrected tree segmentations were found to provide negligible improvements to correlations and estimates of genetic parameters, supporting the operational use of automated methods. Exponential reductions in tree detection accuracy, correlations, and estimates of genetic parameters were observed with reducing pulse density. A minimum pulse density of 6 $Pu.m^2$ was recommended for tree-based analysis of ALS in New Zealand radiata pine stands, and results indicated exponential increases in pulse density will be required to significantly improve estimates.

This study has successfully addressed the research questions and produced important findings regarding tree-based analysis of remotely sensed ALS data. Morphological crown metrics have been derived, representing allometric relationships, which are therefore are expected to have general utility in estimating tree size attributes. Novel features of this research included: the wide range of operationally relevant tree attributes including tree size, form, wood quality and disease; quantification of genetic and environmental factors from ALS; comparison of the effects of automated and manually corrected tree delineations; and the quantification of the effects of pulse density on tree-based analyses. This research provides significant findings in support of the use of remotely sensed ALS data for phenotyping trees in genetics and research trials, and the development precision forestry methods, nationally and internationally.

Acknowledgments

Firstly I would like to express my sincere appreciation to my supervisors Dr Justin Morgenroth, School of Forestry, and Dr Michael Watt, Scion, for their expert guidance and assistance throughout my studies.

I also want to extend sincere thanks to Heidi Dungey for providing access to the genetics trial data and invaluable support on analyses using ASReml-R. I must also recognise the important contribution made by the examiners, whose valuable comments helped improve the thesis. I would like to thank Rod Brownlie, Rodrigo Osorio, Toby Stovold, Mark Miller, Kane Fleet, and Jody Wharekura for collection of the GNSS test data and measurements of the genetics trial used in this study. Thanks are also extended to Jeanette Allen at the School of Forestry for easing my way through administrative matters.

Grateful acknowledgement is made to Scion for the opportunity and the financial support to carry out this study. The research was also supported by the 'Growing Confidence in Forestry's Future' programme which is jointly funded by the New Zealand Ministry of Business, Innovation and Employment and the New Zealand Forest Growers Levy Trust. In addition I would like to recognise Timberlands Ltd for access to the forest, LiDAR and stand records, and the New Zealand Radiata Pine Breeding Co-operative for provision of the data on Dothistroma infection.

Glossary

Additive variance. (σ_a^2) The similarity of offspring to their parents is due to additive effects of genes on phenotype. Additive variance is the component of total phenotypic variance (σ_P^2) attributed to additive genetic effects. It is used to estimate narrow sense heritability (h^2) and genetic correlations (r_g).

ALS. Airborne Laser Scanning. An active remote sensing technology that uses the time of flight of laser pulses along with accurate positioning and orientation information to derive a three dimensional description of the terrain and covering vegetation below. The data produced can be in the form of discrete points (a point cloud) or a digitised representation of the reflected signal (waveform).

ABA. Area-based analysis. An area-based approach to the analysis of remotely sensed data. With ALS this is done by analysis of square patches of LiDAR data, typically of the order of 20 by 20 metres. Metrics derived from these patches are typically related to averaged tree attributes such as mean top height, basal area, and stem volume.

ASReml. A statistical package that provides methods for using restricted (or residual, or reduced) maximum likelihood (REML) methods to fit linear mixed effects models for large, unbalanced trial data sets (VSN International Ltd, Hemel Hempstead, HP1 1ES, UK www.vsni.co.uk). ASReml-R is a package allowing the use of ASReml from the R statistical software.

Breeding value. The genetic value of an individual or group determined by the mean values of its progeny. Can be based on individual attributes or a composite selection index.

CHM. Canopy Height Model. A digital surface model representing the difference between the upper surface of the canopy and the underlying terrain surface. Used in this study to carry out tree detection, crown delineation and derivation of individual tree crown metrics.

CITC. Calibrated individual tree crown. A methodological solution to the problem of inherent bias commonly incurred in individual tree crown (ITC) analysis, where a preponderance of omission or commission errors in uncalibrated approaches lead to large biases in estimates of tree counts and derived measures such as stand basal area and volume, or crown metrics.

Commission error. In tree detection it is a falsely detected tree. One common form of commission is when a single tree crown is separated and counted as though it were two or more crowns. Another common form of commission is the detection of image features that are not trees, such as undergrowth or terrain features.

Crown metrics. Measures determined for individual tree crowns. In this study crown metrics were derived from a segmented CHM image.

Dilution of precision. DOP. The additional multiplicative effect of navigation satellite geometry on positional measurement precision. A number of variants are used for precisions of: geometric (GDOP), position (PDOP), horizontal (HDOP), vertical (VDOP), and time (TDOP) estimates.

Fusion. A software package providing a number of functions for the viewing and analysis of ALS and associated data, principally for forestry applications (U.S. Department of Agriculture, Forest Service, Pacific Northwest Research Station, University of Washington, Box 352100, Seattle, WA 98195-2100).

Genetic correlation. (r_g). An estimate of the additive genetic effect (see additive variance) shared between two traits. The derivation is analogous to that of a Pearson's correlation, but using additive genetic variance rather than total phenotypic variance.

Genetic gain. (ΔG) The change realised by selection in a specific attribute. Gain is influenced by selection intensity, the level of variation and level of heritability.

Genotype. The specific set of genes possessed by an individual, which can be expressed or recessive. Interaction of the genotype with the environment results in the observed phenotype.

GIS. Geographic Information System. Software, widely used in forestry, to store, present, and analyse various forms of spatial data, including remotely sensed information.

GNSS. Global Navigation Satellite System. The generic term for satellite systems that provide global positioning information. This includes the GPS (United States), GLONASS (Russian), Galileo (European), and Beidou (Chinese) systems. Orbiting satellites transmit signals that allow a GPS receiver to calculate its position by triangulation, typically from four or more satellites.

GPS. Global positioning system. A system of American satellites used to determine global positions. See GNSS.

Heritability. The degree to which progeny resemble their parents. Broad sense heritability (H^2) is the proportion of total phenotypic variance (σ_P^2) attributable to genetic (additive and non-additive) effects (σ_g^2). Narrow sense heritability (h^2) is the proportion of total phenotypic variance attributable to additive genetic effects (σ_a^2).

Incomplete block. A trial design where all treatments do not occur within each block. These are commonly used in tree and plant breeding, where a large number of breeds are to be evaluated and trial size must be limited to contain costs and reduce unwanted environmental effects.

ITC. Individual tree crown. An approach to analysis of remote sensing data, including ALS, where individual trees are detected and characterised. This is contrasted with the area-based approach (see ABA).

ITD. Individual tree detection. The detection of individual trees from remotely sensed data. Generally applied to data collected from satellite or aircraft, notably ALS data.

LAStools. A software suite with a number of tools to view and process LiDAR data, principally ALS data (rapidlasso GmbH, http://rapidlasso.com/LAStools).

LiDAR. Light detection and ranging. An active remote sensing technology that uses the time of flight of laser pulses along with accurate positioning and orientation information to derive a three dimensional description of the objects in the field of view. LiDAR systems can mounted on manned and unmanned aircraft and ground vehicles and can also be tripod mounted or hand-held.

Multipath error. GNSS signals can reach receivers by multiple paths due to atmospheric interference or reflections from terrain, buildings or vegetation. This causes error in perceived positions.

Non-additive variance. The component of the genetic variance which has a nonlinear effect, such as dominance, epistasis, or gene-environment interactions.

Omission error. In tree detection it is the failure to detect a tree. A common cause of omission is the failure to detect small or completely supressed trees.

Pedigree. The record of ancestry. In tree breeding a partial pedigree is common due to the use of trees from open-pollinated seed.

Phenotype. The observable attributes of an individual. Phenotype is the results of the genotype interacting with the growth environment.

Phenotyping. The process or methods to obtain measures of attributes.

Point cloud. The data set resulting when LiDAR returns are digitised as discrete points. Very large numbers of points are created, lying on the surfaces of objects in the field of view.

Point density. The number of ALS points (returns) per unit ground area (points m^{-2}).

Point spacing. The mean horizontal distance between ALS points (returns) projected onto a horizontal plane (m).

Precision forestry. The use of new technology and tools to obtain detailed information for use in improved forest management. Current examples are the use of remote sensing, navigation systems and geographic information systems. The aim is to use information based decision making to improve forestry processes such as production and sustainability.

Pulse density. The number of ALS laser pulses, determined by considering first or last returns, per unit ground area ($Pu.m^{-2}$).

Point spacing. The mean horizontal distance between ALS laser pulses, determined by considering first or last returns, projected onto a horizontal plane (m).

REML. The restricted (or residual, or reduced) maximum likelihood approach is a form of maximum likelihood estimation for use in fitting linear mixed effects models with unbalanced data such as found in incomplete block designs.

Remote sensing. The collection of information without making physical contact. In forestry this typically takes the form of aerial and satellite imagery, and more recently ALS data. It also refers to data collected by sensors carried on UAVs, robots, vehicles or personnel.

Segmentation. The processing of an image to divide it into multiple parts (segments) representing objects or features.

Selection differential. The difference between a selected tree, family, or clone and the average of the population it was selected from. Used to quantify the improvement in an attribute due to selection from the population.

TBA. Tree-based analysis. Analysis of ALS data at the individual tree level, using individual tree crown (ITC) methods. A term used to differentiate from area-based analysis (ABA) of ALS.

Variance components. Variance is a statistical measure of variability. The total observed variance is referred to as phenotypic variance, this can be segregated into genetic (additive and non-additive) and environmental variance.

Chapter 1 Introduction

Accurate measurements of tree attributes such as diameter and height provide the foundations for forest research and management. Recent advances in remote sensing technology and associated data processing capabilities have made available new forms of information for use in forest assessment. There is strong potential to develop methods to extract information about individual trees from remotely sensed airborne laser scanning (ALS), a form of data that is becoming more widely available in the forestry sector. These methods, and the tree level information they create, will have applications in the development of a precision forestry approach for researchers, tree breeders and forest managers. Such methods can make an important contribution to commonly recognised goals of increased productivity, profitability, health, and sustainability of New Zealand's forests (NZ Forest Owners Association 2012; Scion 2014).

1.1 Precision forestry

The concept of precision forestry has been adopted from precision agriculture, where crop researchers and farmers have used modern technologies to map variation in order to manage inputs such as fertiliser and herbicide. Management is targeted on a site-specific basis, in order to increase production and maintain environmental quality (Cobb et al. 2013; Dhondt et al. 2013). In forestry, accurate maps of forest stand variables such as tree spacing, size, quality, and disease levels could be used to plan management actions such as re-stocking, thinning, fertilisation and harvesting (Holopainen et al. 2014; McRoberts et al. 2010; Pont et al. 2013). Geographic information systems can then be used to collate, present and analyse the mapped information for use in decision making processes (Goulding 1998). Such detailed information can also establish better general forest records, improve traceability for forest certification, and provide the basis for sustainable management practices (Becker 2001; Holopainen et al. 2014).

1.2 Sources of variation in tree growth

The need for precision forestry originates with variability in the resource, which demands appropriate management in order to maximise outcomes. There are a number of factors which contribute to variation in the attributes of trees. Observed attributes such as tree diameter and height can be viewed as the result of a tree's genetic program interacting with the growing environment (Cobb et al. 2013; Visscher et al. 2008). Both the genetic program and the environment are complex, and the tree attributes observed at one point in time are the cumulative result of interactions between these two sources of variation. Due to an operational rotation length of 20 to 30 years for radiata pine (*Pinus radiata D. Don*) in New Zealand, the interactions between these dynamic effects are integrated over long time periods making them more difficult to understand.

Radiata pine breeding has been underway for over 60 years in New Zealand (Dungey et al. 2009). Despite successful improvements in growth and wood quality traits over that time, the trees are still at an early stage of domestication and the species has considerable genetic variability (Burdon 2001, 2008; Dungey et al. 2006; Jayawickrama 2001; Mead 2013). Radiata pine, like *Pinus* species in general, is tolerant of a range of different site conditions (Burdon 2001). The species has noted phenotypic plasticity for several traits, including height, branching, stem form and wood properties (Burdon 2001). The variability exhibited by the species, from both genetic and environmental origins, offers opportunities and challenges. The range of genetic variation offers useful selection options for tree breeders. Phenotypic plasticity, evident as wide variation in stem form, growth, and wood properties, in response to site and silviculture, confers site tolerance and management options. Reducing the variability of the crop is, however, a major issue for forest managers and tree breeders (NZ Forest Owners Association 2012). The challenge is to carry out research to analyse and understand the drivers of tree growth and quality in order to better capitalise on them for forest management objectives.

1.3 The use of airborne laser scanning

A remote sensing technology which is having a major impact on forest assessment is airborne laser scanning (ALS), a form of laser scanning which can provide highly detailed information on the structure of forest cover and the underlying terrain (Maltamo et al. 2014; Næsset 2004; Næsset et al. 2004). The use of ALS for forest research and management purposes has grown significantly in the last two decades (Brosofske et al. 2014; Maltamo et al. 2014; Næsset 2002, 2004; White et al. 2013). The two major approaches to analysis of ALS are area-based analysis (ABA) and the use of individual tree crown (ITC) methods used to carry out tree-based analysis (TBA) (Maltamo et al. 2014). In ABA, metrics for use in modelling are generated for small areas, typically of the order of 0.04 to 0.08ha in size, a scale spanning many trees (Næsset and Økland 2002). In the TBA approach, individual trees are detected and metrics generated at the tree level.

1.3.1 The need for tree-based analysis of ALS

Area-based analysis of discrete return ALS is being widely developed and applied for forest management applications, internationally and in New Zealand, with proven success in estimating stand height, basal area, volume and biomass (Beets et al. 2012; Næsset 2002; Stone et al. 2011; Turner et al. 2011; Watt 2005; Watt and Watt 2013). However area-based methods are unsuitable for characterising individual trees, and yet methods to characterise individual trees from ALS data are essential to meet the research goals of phenotyping trees using remote sensing.

Tree breeders, tree growth researchers and forest managers are interested in the ability to measure individual trees using remote sensing, following the lead of agricultural researchers whom have developed so-called phenotyping (measurement) methods for individual crop plants (Cobb et al. 2013; Dhondt et al. 2013). Recent technological advances have provided methods to identify trees in ALS data collected for New Zealand radiata pine stands (Pont et al. 2015b), offering the potential to characterise individual trees. Tree-based analysis of ALS could therefore meet the need to characterise individual trees using remote sensing.

The availability of ALS data for New Zealand forests has increased over recent years as more forest owners adopt it for operational purposes such as roading and area-based inventory (Adams et al. 2011). Continuing technological advances are likely to result in increased availability and resolution of ALS. Developments such as LiDAR units on unmanned airborne vehicles (UAVs), ground-based vehicles, all-terrain vehicles (ATVs) as well as tripod mounted and hand-held units can produce very dense data and could provide cost-competitive alternative sources of data compared with the ALS collected from manned aircraft (Bilker and Kaartinen 2001; Pont and Lorraine 2015; Wallace et al. 2014a; Wallace et al. 2012). The growing availability and quality of LiDAR data, combined with methods to detect individual trees, offers potential for such data to play important roles in research and precision forestry applications.

There are a number of researchers investigating methods for tree delineation that point out the potential benefits of estimating tree-level measures from ALS (Chen and Zhu 2012; Lindberg et al. 2012; Lindberg et al. 2010; Vauhkonen et al. 2010). The main barrier to applications appears to be a lack of accurate and general methods (Breidenbach et al. 2010; Kaartinen and Hyyppa 2008; Kaartinen et al. 2012; Lindberg et al. 2010). In a study on *Pinus sylvestris* stands, significant bias in determining the number of stems with an ITC approach resulted in no improvement in estimation of tree size distributions, stand mean height and stand mean diameter compared with ABA estimates (Peuhkurinen et al. 2011). Accurate tree detection has also been reiterated as a barrier to developing methods to characterise trees using ALS in other recent research (Heinimann and Breschan 2012; Kankare et al. 2015; Tang et al. 2013).

1.3.2 Locational error under forest canopy

The ALS data routinely used in forestry is geo-referenced with high horizontal accuracy, having error < 100 mm (Maltamo et al. 2014; White et al. 2013), making it suitable for use in precision forestry applications. However in order to develop statistical relationships, crown metrics derived for individual trees detected in ALS data must be accurately matched with ground measurements made on the corresponding trees.

Positional information in the forest is routinely determined with GNSS (Global Navigation Satellite System) equipment. Errors, due to signal blocking and multi-pathing under typical radiata pine canopy, are likely prevent reliable location of single trees in the forest using GNSS equipment. The degree of canopy cover has been found to be a key variable affecting GPS accuracy and error of 7 m in young forest and 10 m under closed canopy using consumer-grade GPS was observed (Wing et al. 2005). In subsequent studies little improvement in error was found from using mapping-grade (post-corrected) GPS units under canopy (Valbuena et al. 2010; Wing and Eklund 2007).

One approach to locating individual trees in forest is to obtain an accurate location with high-grade GPS in a relatively open position, and then surveying to the tree with accurate distance and bearing (Jakubowski et al. 2013b) but this method is time-consuming and of uncertain accuracy. In some cases, typically research projects on sites of limited size, surveying methods are used to determine highly accurate positions of all trees, but this approach is onerous. In other cases, tree maps within plots are used with a GPS plot location to provide approximate tree locations for alignment with trees detected in the ALS (Flewelling 2006). It is concluded that quantification of GNSS error in New Zealand forest conditions, and a solution to the problem of matching ground and remotely sensed tree data are required.

1.3.3 Methods for tree segmentation

Various segmentation methods have been researched for tree detection, and comparative studies made on different forest types (Jakubowski et al. 2013b; Kaartinen et al. 2012; Vauhkonen et al. 2011; Wallace et al. 2014b). Detection algorithms applied to ALS data can be classified according to the form of the data they operate on. Point-based methods operate directly on the three-dimensional points, or use a voxel representation, where space is subdivided into a regular grid of cubical cells (voxels) and voxels containing points are recorded. Raster-based methods typically use a canopy height model (CHM), generally represented as a grayscale image (Figure 1.1). With each type of input data there are also a number of different algorithms used to detect trees, but the literature shows that watershed or

similar algorithms applied to CHM images are a widely used combination (Jakubowski et al. 2013b; Wu et al. 2016). Raster representations require less storage and processing, and have been shown to give acceptable results for tree detection, particularly for the planted conifer forest type which will be the focus of the planned research (Vauhkonen et al. 2011; Wallace et al. 2014a). Although there is active research into alternative methods, including point-based, hybrid, and more complex approaches, using techniques such as convex hull and alpha shapes, a recent review concluded these methods are much more difficult to implement, can be more dependent on laser point density, and be more sensitive to forest type (Zhen et al. 2016). It is therefore concluded that a raster-based approach using a watershed algorithm will provide a more stable, easy to implement, and efficient basis for tree detection and delineation.

A recently developed methodology has been shown to provide unbiased estimates of tree count by applying tree detection to canopy height model (CHM) images derived from ALS (Pont et al. 2012a; Pont et al. 2015a; Pont et al. 2015b). This methodology includes an assessment of detection accuracy in terms of omission and commission errors, thus meeting the requirements for comprehensive evaluation of tree detection accuracy as proposed in a recent review of ITC methods (Zhen et al. 2016). Utilisation of this tree detection methodology can provide a sound foundation for the development of methods to characterise trees from ALS (Figure 1.2 and Figure 1.3).

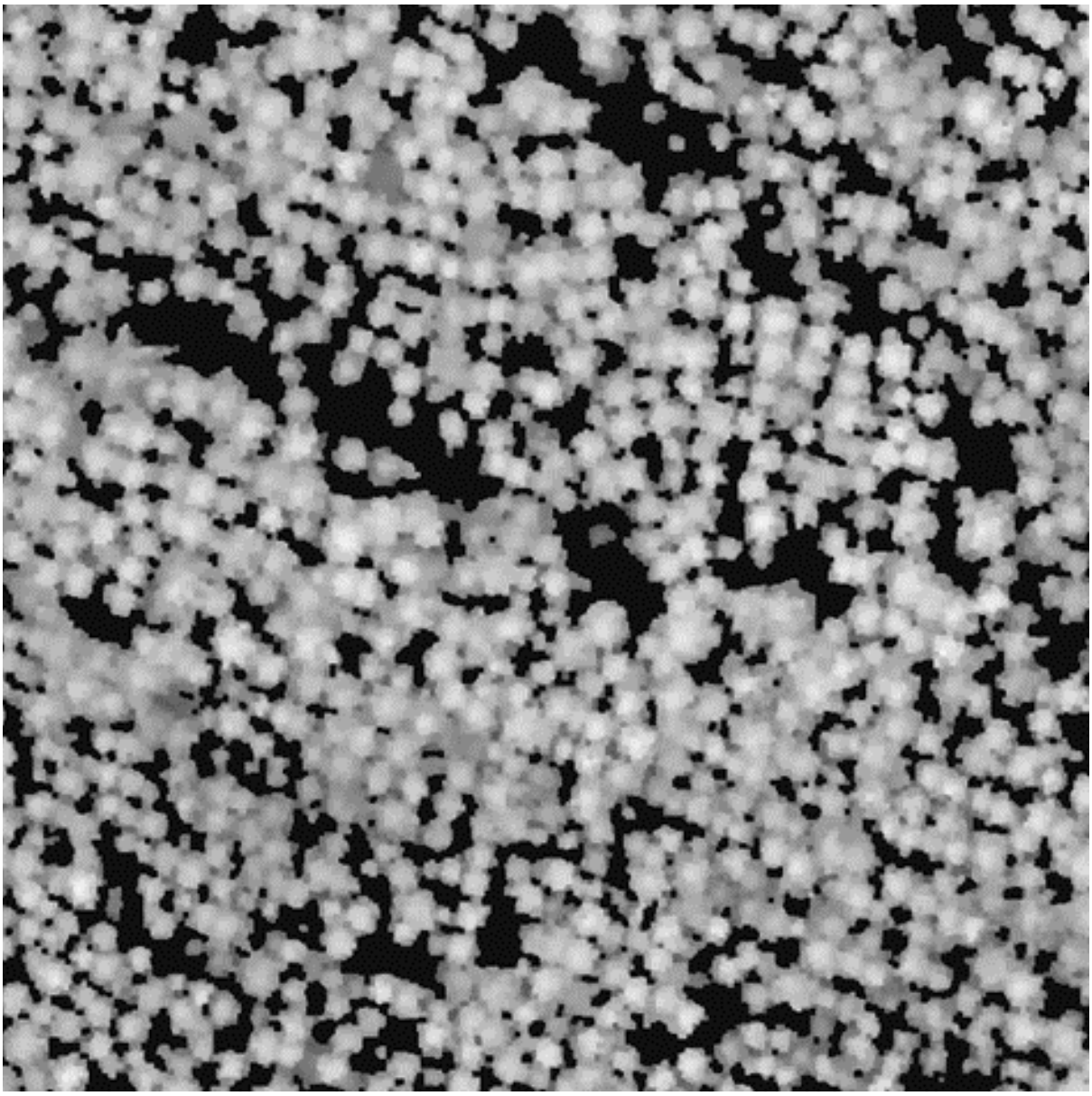

Figure 1.1. CHM image of a mature stand of radiata pine. Pixel size is 0.25 m and the image covers an area of 120 by 120 m, the vertical axis of the image is oriented to true north.

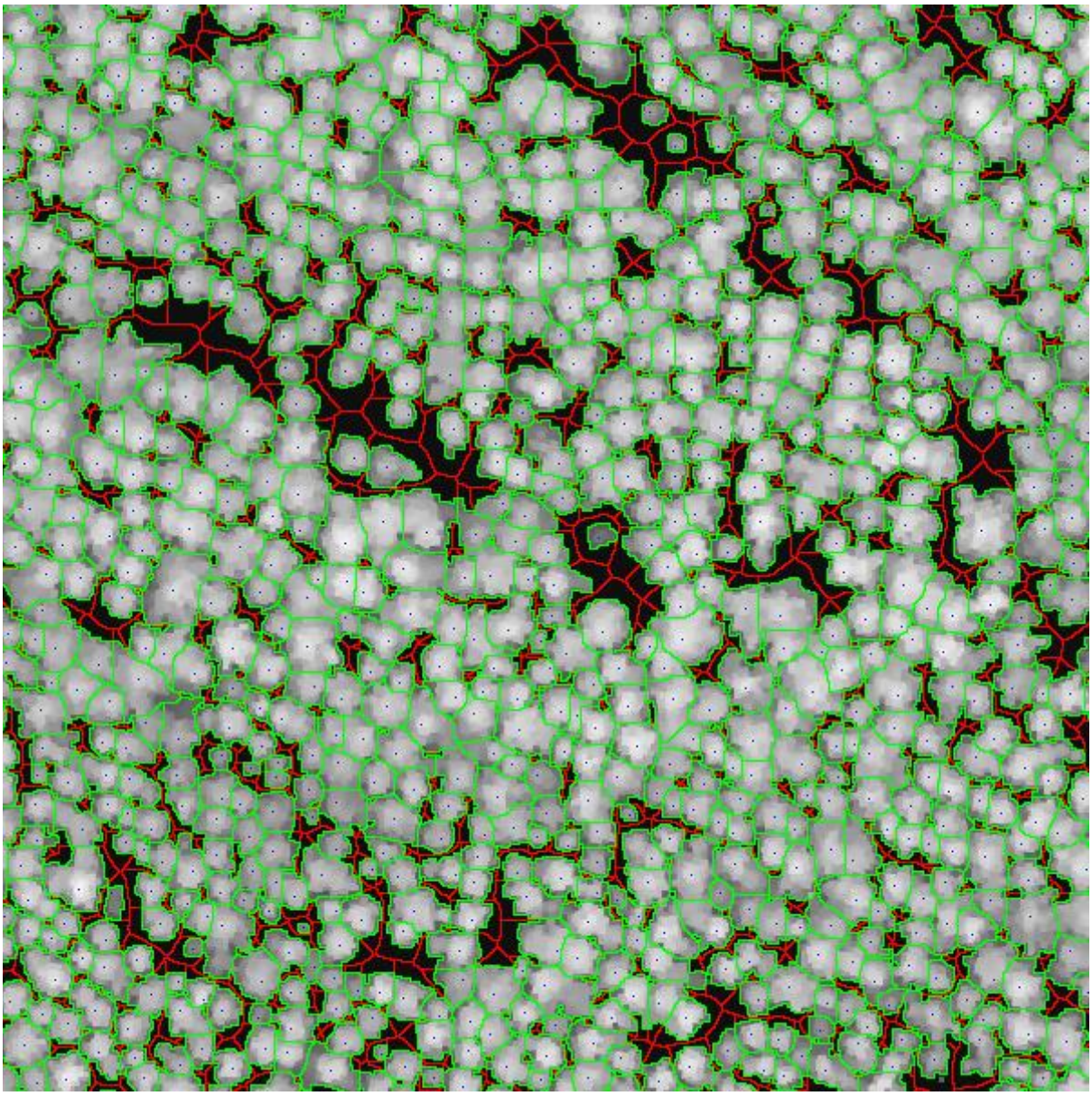

Figure 1.2. Tree detection result processed to delineate tree crowns. Individual tree boundaries are processed to define crown boundary in green and larger growth boundary extended out to include a portion of any adjacent gap in red.

1.3.4 Crown metrics

Because a CHM represents heights above ground, the area within each detected tree boundary can also be treated as a three-dimensional surface (see Figure 1.3) and analysed to generate further metrics such as crown depth and volume (Chen et al. 2007; Kaartinen and Hyyppa

2008; Lindberg et al. 2010; Packalen et al. 2013; Pont et al. 2012b; Xu et al. 2014). Once individual trees have been delineated, point-based analysis of ALS data at the tree level could be considered, particularly because of the successes of point-based methods in area-based analyses of ALS. In a recent review, tree-based analyses of ALS were shown to be widely researched but still in a relatively early stage of development, with a lack of standardised approaches or even methods for comparing results (Zhen et al. 2016). The authors noted the potential benefits of deeper analyses of the points belonging to individual trees but showed there is insufficient evidence to date for benefits of a point-based approach for tree-based analysis. Wallace et al. (2014a) showed that a raster-based approach was superior, and more sophisticated crown representations did not deliver concomitant benefits in estimation of crown width from derived crown metrics. In a study into estimation of height, DBH and volume for trees in boreal forest, crown volume metrics, easily derived from a CHM representation, featured strongly among a large set of candidate metrics evaluated (Vauhkonen et al. 2010). In a study comparing the use of raster- and point-based analyses to estimate crown dimensions of olive trees, the point-based approach provided only marginal benefits, while the raster-based approach was insensitive to reducing point density, indicating it as a more useful approach for operational purposes (Hadaś and Estornell 2016). Crown metrics derived from a CHM also used for tree detection were successfully used to estimate tree height and volume in a recent study applied to longleaf pine stands (Silva et al. 2016).

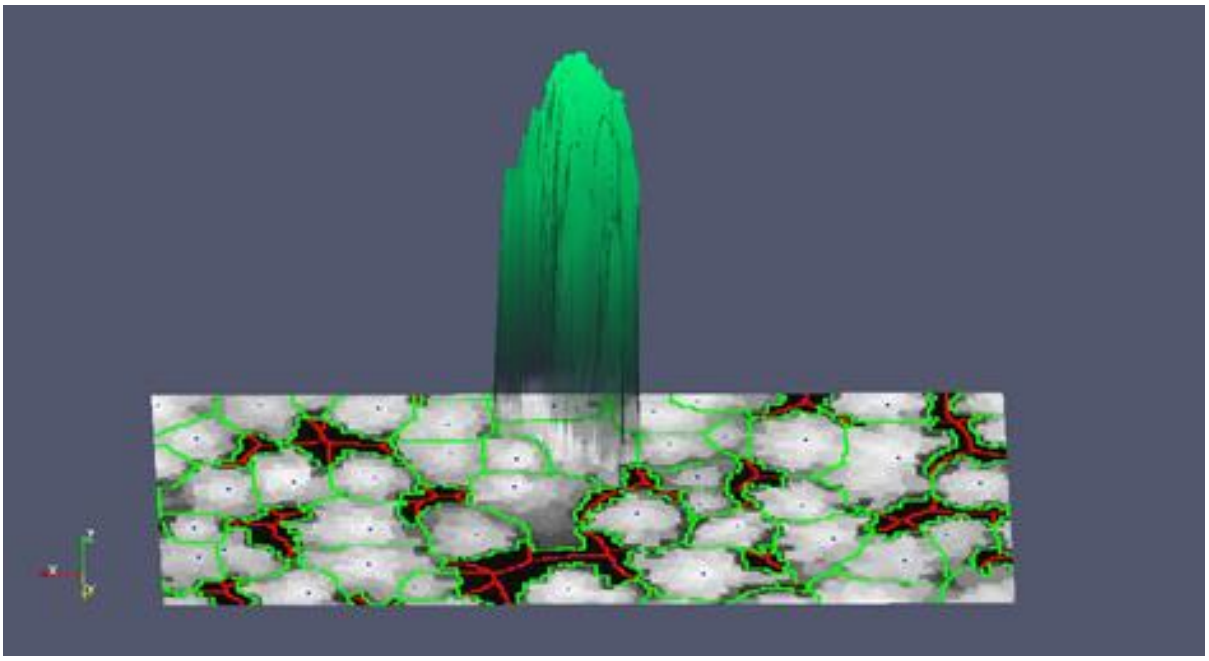

Figure 1.3. Derivation of crown metrics from a CHM image. Two-dimensional crown metrics can be derived using the crown (outlined in green) and tree detection boundaries (including a portion of any adjacent gap, outlined in red) delineated on the CHM image. The grayscale values in the CHM image represent height above ground and can be used to derive three-dimensional crown metrics from the enclosed crown envelope (transparent green surface above image).

It is important to note that point-based analysis of ALS is effectively the only option in the area-based approach. Raster-based analysis at a patch level, without any detection of trees, yields few metrics, effectively being limited to texture analysis methods. In typical area-based analysis of ALS, a point-based approach is routinely used to generate large numbers of canopy metrics and several researchers have applied techniques such as principal components analysis, best-subset regression, and canonical correlation analysis to determine a parsimonious set of metrics for modelling (Hudak et al. 2006; Lefsky et al. 2005; Næsset et al. 2005). In a useful insight into the utility of the various ABA metrics Lefsky et al. (2005) found just three point-based LiDAR metrics, describing canopy mean height, canopy depth and canopy closure, provided a concise description of canopy structure with clear biological interpretation and widespread utility in modelling. So while a point-based approach generated many metrics, a small subset were found to be the most useful across numerous studies, and it was apparent those metrics described canopy morphology. Once individual trees are delineated on a CHM

raster there are potentially many raster-based metrics that could be derived for each crown, and it is apparent that many of those metrics will effectively describe crown morphology, such as maximum height, crown area, and crown volume. It is concluded that raster-based methods used in tree-based analysis of ALS can provide a parsimonious approach (Zhen et al. 2016), with modest data storage and processing requirements, and potential to generate useful morphological crown metrics for use in estimating tree attributes. Researchers have already shown that measures of crown morphology, such as crown width, correlate strongly with tree size and quality through allometric relationships (Filipescu et al. 2012; Groot 2014; Groot et al. 2015; Groot and Schneider 2011; Lenz et al. 2012; Madgwick 1994).

The utility of crown metrics derived using the proposed raster-based approach will be dependent on the accuracy of tree detection, and subsequent crown delineation. Errors in tree detection and crown delineation will result in changes to delineated crown boundaries. For example undetected small tree crowns (omissions) could be merged with other tree crowns resulting in overestimation of crown size. Similarly, falsely detected trees (commissions) occur when crowns are erroneously subdivided, leading to underestimation of crown sizes. An investigation into the importance of accurate tree detection and delineation is seen as an important objective, requiring investigation in the proposed research.

1.4 Estimating tree attributes using airborne laser scanning

There are a number of tree attributes which are routinely assessed in forest inventory, research trials, and tree breeding programmes. Those attributes can be placed into four groups: tree size, tree form (determining tree and log quality), wood quality, and disease. There is potential for cost savings and new approaches to tree assessment if methods could be developed to evaluate attributes representing each of these groups using remotely sensed ALS data.

1.4.1 Tree size

Researchers have used crown metrics derived from ALS data to estimate individual tree height, DBH or volume in boreal and savannah forest types (Chen et al. 2007; Lindberg et al. 2012;

Vauhkonen et al. 2010; Yu et al. 2011), and for planted forests (Chen and Zhu 2012; Lo and Lin 2013). Estimates of tree height typically had higher accuracy than estimates of DBH and volume. Estimates of height, DBH and volume for trees in boreal forest in southern Sweden had RMSEs of 4%, 15% and 35% respectively (Lindberg et al. 2012). Very similar results were obtained in a study of boreal forest in southern Finland, where RMSEs on estimates of height, DBH and volume were 3%, 13%, and 31% respectively (Vauhkonen et al. 2010). While there is only limited international research, results indicate good potential for the use of crown metrics from ALS data to estimate tree size attributes in New Zealand radiata pine stands.

1.4.2 Tree and log quality

Stem form variables of interest in forest management are straightness, including absence of butt sweep, and absence of malformations, in order to maximise the merchantable volume and quality of the stem. Tree breeds with multi-nodal branching are also favoured as they tend to have smaller branches, as well as better growth rate and straighter, less malformed, stems (Burdon 2001). Trees with straight, defect-free stems and small branches achieve higher log grades and are therefore of higher value. A strong relationship was found between tree maximum branch diameter and crown radius measured from the ground in one study, and the potential to use ALS data for estimating branch size was proposed by the authors (Groot and Schneider 2011). However review of the literature found no examples of using ALS data to directly estimate stem form or branching attributes for individual trees.

1.4.3 Wood quality

Wood stiffness and density are key attributes for structural timber and are therefore important to forest managers and tree breeders. In a review paper the potential use of ALS data to estimate various wood quality variables for forest management purposes was discussed (Van Leeuwen et al. 2011). Moderate success has been achieved in estimating wood properties from ground measured crown variables and the authors suggested the possibility of using remote sensing data, such as ALS, in the future (Groot et al. 2015; Lenz et al. 2012).

There are some examples of estimating wood quality from ALS, although these studies are confined to estimates at the plot, rather than tree, level. In a pilot study (Pont et al. 2012b), crown metrics were used to estimate plot mean standing tree acoustic velocity, a measure which is highly correlated with timber stiffness, with an R^2 of 0.69 (Watt et al. 2013b). Wood fibre attributes, including wood density and microfibril angle, were estimated at the plot level with low to moderate precision (R^2 from 0.18 to 0.53 and RMSE from 2% to 14%) using metrics derived from ALS data (Luther et al. 2014). In a study using area-based metrics describing canopy height, canopy depth and canopy light zones, about half of the observed variance at the plot level was explained for fibre attributes (Hilker et al. 2012). Crown structural metrics derived from a canopy height model (CHM) from terrestrial laser scanning data were used to estimate plot mean wood fibre properties with R^2 from 0.63 to 0.72 for black spruce stands (Blanchette et al. 2015). In summary, a review of the literature has shown potential, but has not identified any research that has estimated wood quality metrics at the individual tree level from ALS data.

1.4.4 Disease

The negative impacts of defoliation on tree growth due to disease or pests is an important issue in New Zealand and internationally. Review of the literature found few studies using ALS data to characterise levels of infection or needle loss on individual trees. Metrics from area-based analysis of ALS data were found to be correlated with plot level assessments of needle loss due to pine beetle infestation (Coops et al. 2014). In a study of loblolly pine it was noted that crown metrics are known to be correlated with individual tree leaf area, but the ability to predict leaf area index (LAI) was limited by the ability to accurately detect tree crown diameters and lengths (Roberts et al. 2005). Nearest neighbour methods were used to establish relationships allowing determination of two defoliation classes for individual trees, to an accuracy of over 80%, based on ground measured training data and point cloud metrics (Kantola et al. 2013; Kantola et al. 2010). Several studies have investigated the use of laser scanning in the estimation of leaf area index or the related measure leaf area density, which might be used to quantify needle loss due to disease (Beets et al. 2011; Korhonen and Mosdorf 2014; Solberg et

al. 2006b; Tang et al. 2014). A number of those studies have relied on full waveform or terrestrial laser scanner data (Adams et al. 2012; Kato et al. 2013). Measurement of LAI for individual trees is very difficult (Breda 2003), and the few studies which looked at the individual tree level were for isolated trees, not groups of trees which had been delineated (Oshio et al. 2015). While the potential use of ALS data to quantify needle loss on individual trees has been recognised, to date there has been little research into methods to carry this out.

1.5 Understanding the drivers of tree growth

The ability to analyse the genetic and environmental effects on tree growth has uses in the development of elite tree breeds (NZ Forest Owners Association 2012; Scion 2014). Researchers wanting to create models for tree growth and quality also have a need to incorporate the effects of genetics, environment, and silviculture in models (Kimberley et al. 2015b). Such models would be valuable for operational forest management, helping plant the right breeds on sites, and to manage tree growth to increase productivity, value, health and sustainability (NZ Forest Owners Association 2012; Scion 2014). Therefore tree-based analysis of LiDAR data, combined with methods to partition environmental and genetic effects, provides opportunities to better understand and model the key drivers of tree growth. Such an approach may be applied to study trees in research trials and in forest stands.

It is important to note that tree-based analysis, as opposed to area-based analysis, is essential for precision forestry applications. There is a need to separate, quantify, analyse and model genetic and environmental factors affecting the growth of individual trees. While genetics are often described at higher levels of grouping, such as seedlot and family, in typical non-clonal New Zealand forest stands each tree is genetically distinct (Dungey et al. 2013; Mead 2013). Environmental factors affecting growth, such as temperature and soil moisture are also often described at higher levels, such as the regional scale, but can exhibit variation right down to the tree level (Watt and Zoric 2010). In order to separate and quantify the interactions of genetics and environment on tree growth it is therefore essential to characterise and analyse the growth of individual trees in relation to their environment.

1.6 The effects of varying LiDAR resolution

The required resolution of LiDAR scanning is an important consideration when considering the use of ALS data to characterise forest trees. LiDAR scanners emit pulses at high frequency and pulse density is a measure of the number of pulses (Pu.) per unit ground area ($Pu.m^{-2}$) (Gatziolis and Andersen 2008; Wehr and Lohr 1999; White et al. 2013). A number of parameters can be managed to vary pulse density achieved when collecting ALS data (Gatziolis and Andersen 2008). Tree-based analyses of ALS have been shown to require higher density ALS than area-based methods, and increased pulse density might offer higher quality data, but at increased cost (Gatziolis and Andersen 2008; Vauhkonen et al. 2008). It is therefore important to quantify the effects of varying pulse densities on estimates of tree characteristics obtained from tree-based analyses of ALS. This knowledge will used to guide cost-effective operational collection of ALS data with adequate resolution.

1.7 Research aims

The aims of the research are to develop and evaluate novel methods for analysing individual trees detected in ALS data in order to improve measurement, management, breeding, and knowledge about tree growth for New Zealand plantation-grown radiata pine. The assessment of individual trees from remote sensing can be used in genetics trials and forest stands as a novel phenotyping tool, supporting a new approach to improved tree breeding. Such methods can also be used to produce tree-level data, at an unprecedented scale and volume, for the development of a next-generation of individual tree growth and wood quality models. With the use of appropriate experimental designs and analytical methods to partition variance according to genetic and environmental sources, such tree growth models could incorporate the effects of genetics, site and silviculture, thereby reducing uncertainty from forest management (De Reffye et al. 1995; Wang et al. 2012). A tree-based approach can therefore be used to develop a better understanding of the drivers of tree growth. This requires the development of methods to delineate individual tree crowns, match them with ground measurements, extract individual crown metrics, estimate tree attributes, and to partition sources of variation. These methods will

be evaluated in terms of the utility of crown metrics in estimating tree attributes and their component sources of variation. The resolution of ALS data necessary to apply such methods is also an important consideration for operational applications and warrants quantification. Such methods could generate an unprecedented level of detail in describing trees in trials and forests, supporting precision forest research, tree breeding and management applications (Dungey et al. 2013; Scion 2014).

Review of the literature relevant to the use of ALS data for characterising individual trees has identified the opportunities and gaps in international research. The focus of the research is the use of crown metrics derived from ALS data to estimate key attributes, including size, form, wood quality, and disease, for individual New Zealand radiata pine trees. The review was used to guide the formulation of three key research questions, with associated objectives:

1. **Can methods be developed to estimate key attributes of individual trees using airborne laser scanning data?**

    - *Derive a set of individual crown metrics from raster-based analysis of ALS data in which individual trees have been detected.*

    - *Quantify correlations between LiDAR crown metrics and ground-based measures of tree size, form, wood quality, and disease expression.*

    - *Evaluate the effect of errors in tree detection and delineation by comparing estimates of correlations from automatic and manual segmentation of individual trees.*

2. **Can methods be developed to estimate variance components of individual trees using airborne laser scanning data to elucidate the genetic and environmental drivers of tree growth?**

- *Estimate genetic parameters for measures of tree size, form, wood quality, and disease expression using crown metrics and compare these with estimates from ground measurements.*

- *Evaluate the effect of errors in tree detection and delineation by comparing estimates of genetic parameters from automatic and manual segmentation of individual trees.*

3. **What is the effect of varying pulse density on the accuracy of estimates obtained from the analysis of discrete return LiDAR?**

    - *Quantify the effect of reducing pulse densities on the accuracy of tree detection.*

    - *Quantify the effect of reducing pulse densities on correlations between crown metrics and ground measurements of key tree attributes.*

    - *Quantify the effect of reducing pulse densities on estimates of heritabilities and genetic gains.*

1.8 Thesis structure

The Introduction (Chapter 1) defined the basic concept of precision forestry and identified applications and benefits of tree-based analysis of ALS data. Review of the international literature identified gaps and opportunities in relation to tree-based analysis of ALS, leading to the definition of the approach to be taken. Three key research questions were used to frame specific objectives to be achieved. Each research question and its associated objectives are addressed in a subsequent thesis chapter.

Chapter 2, Materials and Methods, describes the materials and methods utilised in the main thesis chapters. In order to carry out the tree-based analyses of LiDAR for this thesis a critical requirement was the ability to match trees identified in the LiDAR with trees measured on the ground. An investigation was made of GNSS positional accuracy under typical New Zealand forest canopy conditions to determine the suitability of this technology to provide accurate ground locations for trees. This investigation is reported in Appendix A.

In Chapter 3 the correlations between crown metrics and ground measurements are investigated to address the first research question. In Chapter 4 the relationships with crown metrics are then used to address the second research question regarding the estimation of correlations and variance components for key tree attributes. In Chapter 5 the third research question is addressed by evaluating the effects of reduced pulse densities on correlations and genetic parameters investigated in the prior chapters.

In Chapter 6 the research covered in the thesis is reviewed in terms of the objectives and research questions posed. The relevance and impact of the research is demonstrated in Appendix B by outlining the dissemination of results to international and national audiences.

Chapter 2 Materials and Methods

2.1 Introduction

The data sets utilised in the research covered in Chapter 3, Chapter 4, and Chapter 5 comprised ground measurements of individual trees in a genetics trial, and ALS data collected for that trial. This chapter documents the details of those data and of the processes used to derive crown metrics for individual trees from the ALS data. The results from investigations into GNSS error under forest canopy (see Appendix A) showed the error of that approach is too large for reliable identification of individual trees. This chapter also includes description of the methods used to locate individual trees for the analyses to be carried out in the subsequent chapters.

2.2 Genetics trial site

The study site was the genetics trial BC 35-3, established in 2007 by the Radiata Pine Breeding Company Ltd (RPBC) in compartment 76 at Kaingaroa forest (38.53° S, 176.66° E) in the central North Island of New Zealand (Figure 2.1). The trial was designed to evaluate Dothistroma resistance for breeds in the breeding programme lacking this information and used an incomplete block design with single tree plots. The trial site was relatively flat and sloped gently (< 5 degrees) to the southeast.

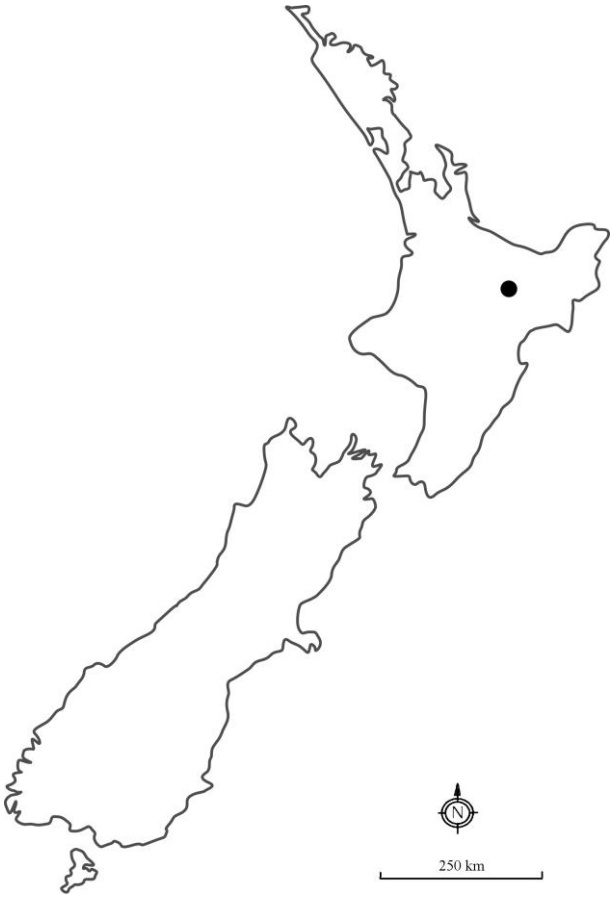

Figure 2.1. Trial location in the North Island of New Zealand.

The trial comprised 75 blocks with single tree plots representing a total of 96 families (Figure 2.2). There were 25 replicates of 3 incomplete blocks and each block contained 36 trees in a 6 by 6 grid. Block size was 19.2 by 19.2 m, tree spacing was 3.2 by 3.2 m and there were trees missing due to an operational thinning in the surrounding stand which was also applied to the trial. A total of 2196 trees remained of the 2700 trees established in the trial (75 blocks times 36 trees).

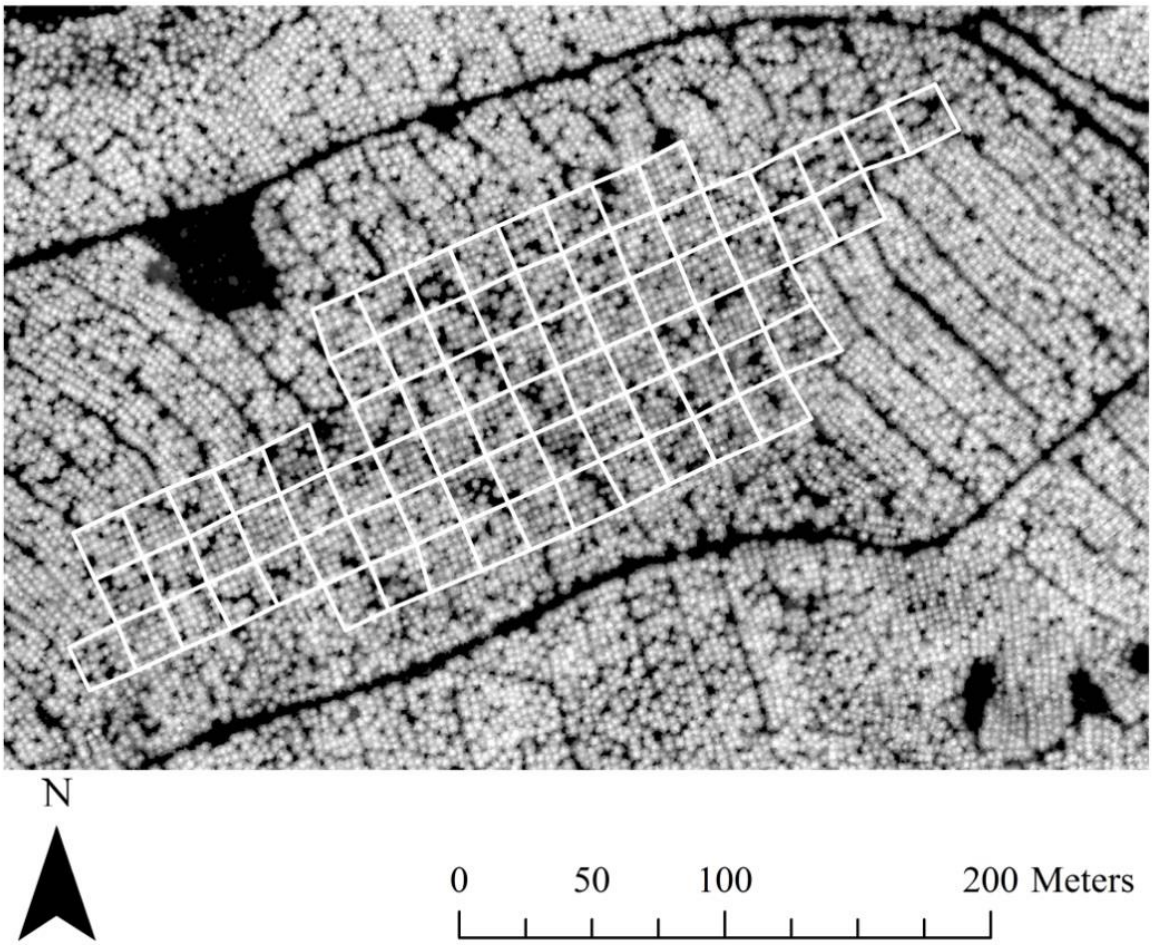

Figure 2.2. Trial layout with blocks outlined in white on the CHM image used for tree detection.

2.3 Airborne laser scanning data

The discrete return aerial LiDAR data were collected in early 2014 using an Optech Pegasus scanner with a pulse rate of 100 kHz, a maximum scan angle of 12°, a 25% swath overlap, and a 0.25 m footprint size. The data were georeferenced to the NZGD2000 NZTM coordinate system and all returns were classified as ground (using Terrascan TerraSolid software) and above ground. The point density over the trial area was 17 returns per m^2 and 7 last returns per m^2.

2.4 Canopy height model creation

The ALS data was processed to generate a CHM image with a 0.2 m pixel size for the area of interest (Figure 2.2) using methods outlined here and described by Pont et al. (2015b). The CHM image was created using the *CanopyModel* tool from the *Fusion* software (McGaughey and Carson 2003). Image defects referred to as pits were removed using the standard image processing method *closing* (Ronse and Heijmans 1991) rather than a more complex approach recently proposed in the literature (Khosravipour et al. 2013; Khosravipour et al. 2014). The simpler approach used to remove pits was found adequate for tree detection purposes, was easier to implement, and faster to process. Either method removes isolated low points, visible as dark pixels on a CHM, and replaces them with points nearer to the surrounding points. It was not thought the method for removing pits would have a significant effect on crown metrics derived for estimating tree attributes and the simpler method was chosen. A height threshold was applied to the CHM to avoid false detection of understory shrubs and other non-crop features. The histogram of LiDAR point heights for the area of interest over the trial was used to determine a height threshold of 1.5 m, corresponding to the first minima detected below the canopy (Figure 2.3).

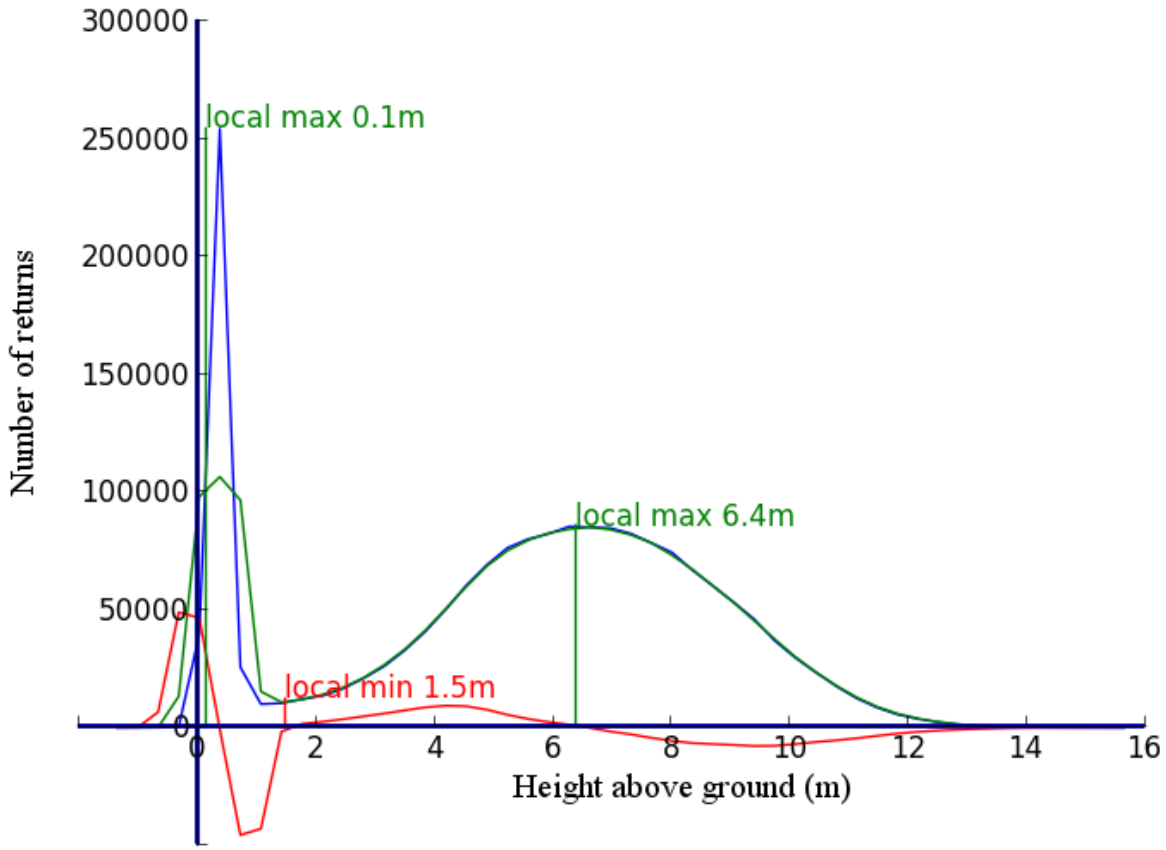

Figure 2.3. Height histogram for the LiDAR returns used to determine the height threshold for the CHM image. The histogram (blue curve) was smoothed (green curve) and zero crossings of the first derivative (red curve) used to determine minima (red line) and maxima (green line).

2.5 Tree detection

The Calibrated-ITC (CITC) tree detection process, as described by Pont et al. (2015b), was applied to the CHM image to obtain individual tree crown segments (Figure 2.4). Calibration of the tree detection process was carried out using manual calibration with eight virtual plots located on the image on a grid with random location and orientation. The overall accuracy from the initial automated tree detection was 89.82%, consistent with the accuracy of the image calibration CITC method reported by Pont et al. (2015b). Manual correction of the segmentation (described below) was then carried out, improving overall tree detection to 98.34%. These processes produced two tree segmentation results, allowing comparisons of automated and manual detection and delineation in subsequent analyses.

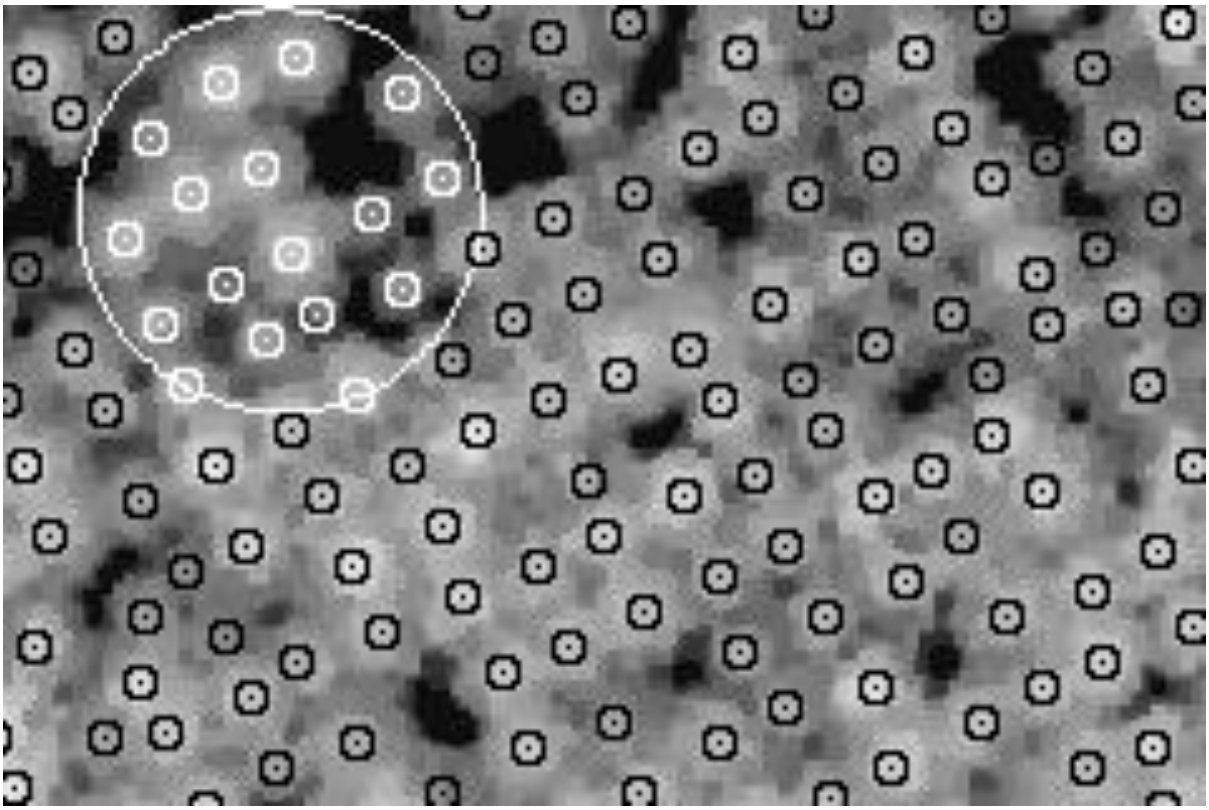

Figure 2.4. Tree detection result for part of the trial. Markers are shown on detected tree tops in the trial (black) and within a virtual calibration plot (white). The image spans a distance of 48 m in the horizontal direction.

2.6 Matching detected and ground measured trees

Results in Appendix A showed GNSS error under forest canopy, of the order of +- 2.7 m, to be 2 to 5 times too high to allow reliable identification of individual trees within the trial. In addition, the registration of tree top locations with ground locations, usually stem centre at breast height, cannot be exact. Positional error from GNSS locations can result in a different set of trees, as detected in ALS, being associated with the ground plot (Figure 2.5). Tree lean results in differences between tree top and ground measured tree locations, as illustrated in Figure 2.5 (Flewelling 2006; Mikita et al. 2013). An additional source of error is due to omission and commission errors from tree detection in the ALS.

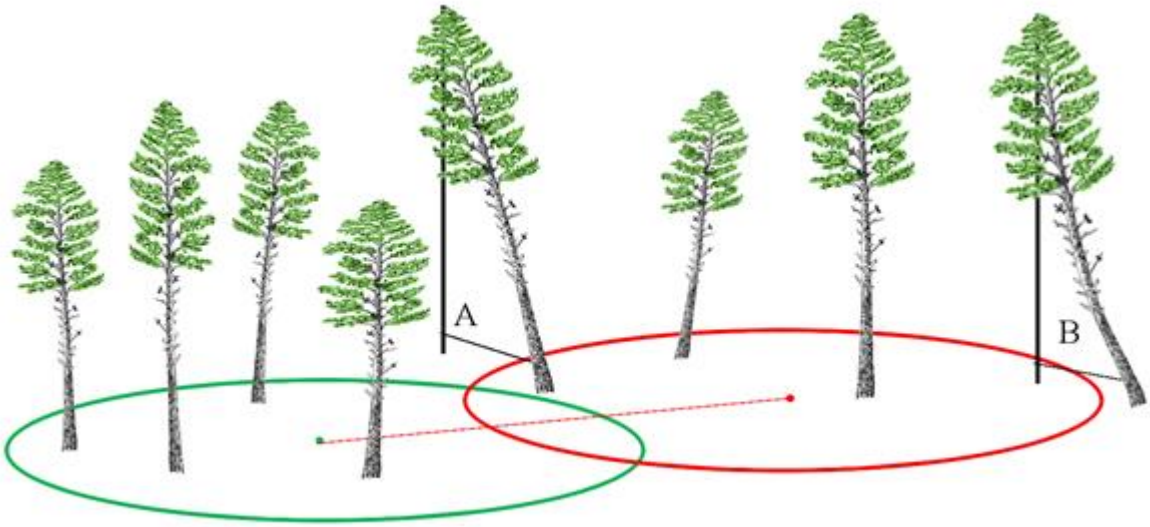

Figure 2.5. Errors in matching trees detected from ALS can result from GNSS error in plot location and from tree lean. Error in GNSS position can cause the actual ground plot location (green) to be shifted to an incorrect position (red) and therefore include a different set of trees in the ALS. Tree positions are determined at tree tops in ALS and at breast height on the ground. Tree lean can result in trees detected in ALS being falsely excluded (A) or included (B) in plots.

Least squares or similar approaches can be used to simultaneously minimise misalignment due to global GPS error, individual tree lean and missing or falsely detected trees. For example, automated least-squares matching process have been used to match ground truth data with trees detected in remotely sensed data in a number of studies (Hauglin et al. 2014a; Hauglin et al. 2014b; La et al. 2015). Residual problems of dealing with plots where registration fails completely and missing or falsely detected trees within plots, are commonly dealt with by excluding trees without a match (Chen et al. 2007; Lo and Lin 2013).

In order to address the issues noted, the matching of trees detected in the CHM with trees within the trial required a combination of initial GNSS locations for pegs, refined by operator image interpretation, and an automated least-squares matching process for trees within each block, described in more detail here. The initial segmentation of the CHM image was used to create a list of detected trees with coordinates for each tree top. In this study a least-squares matching process implemented in Python code (version 2.6.2) (van Rossum 1995), was used to

associate each detected tree with the nearest tree measured on the ground. Ground locations for trees were determined by assuming trees were located on a uniformly spaced six-by-six grid between the four corner pegs for each block. Corner peg locations were manually digitised on the CHM image, with reference to GNSS locations for a subset of pegs surveyed on the trial boundary. The least squares matching process used the estimated tree ground locations and the detected tree top locations from the CHM. The process used an iterative process to determine a rotational and translational transformation that minimised the distances between nearest ground and detected tree locations. That process required a good approximate initial starting point, provided by the manually digitised block corner peg locations.

2.7 Manual correction of segmentation

The accuracy of tree detection and delineation will strongly affect any derived crown metrics (Paris and Bruzzone 2014; Vega et al. 2014). For example, omission errors (undetected trees) can result in overestimation of crown sizes, and commission errors (falsely subdivided crowns) can result in underestimation of crown sizes (Zhang et al. 2012). Manual correction of detected tree boundaries was carried out to achieve two goals. Firstly a corrected segmentation provided the best possible basis for the determination of crown metrics and subsequent characterisation of tree attributes. Secondly it allowed comparison of results from the fully automated and semi-automated (manually corrected) methods of delineating crowns and deriving crown metrics, used as key research objectives of the study. Manual correction of crown delineations has been used in comparisons with automated delineation in a number of international studies. In two studies, manual correction was shown to significantly improve estimates of tree total volume and biomass compared to automated delineation (Kankare et al. 2013; Vastaranta et al. 2012). In another study, manual correction of the crown base height was found to improve the accuracy of DBH estimates compared to the automated crown segmentation (Korhonen et al. 2013). In that same study, manual correction of the horizontal crown boundaries was used as the sole basis of all analyses, without any comparison to an automated delineation. Manual delineation of crowns was also used as the basis of all analysis in a study into the effects of pulse density on estimates of tree DBH using crown metrics (Vauhkonen et al. 2008), and in a

study into the estimation of branch biomass (Hauglin et al. 2013a). Manually delineated crown boundaries and visual comparisons are also widely used to assess accuracies in the evaluation of tree-based methods (Brandtberg et al. 2003; González-Ferreiro et al. 2013; Jakubowski et al. 2013b; Ke et al. 2010; Lu et al. 2014; Paris et al. 2016; Vega et al. 2014; Wu et al. 2016; Zhao et al. 2014; Zhen et al. 2016). In this study tree-based analysis was carried out for a genetics trial. Because all trial trees were measured on the ground, automatic tree delineation could be readily compared against the tree map produced by ground measurements. This allowed visual inspection of all trees affected by omission and commission errors on the ground and in the CHM image, and subsequent manual correction of the segmentation. Therefore the manual component of this process was only for a subset of trees, and was guided by detailed information to enable more accurate crown delineation.

Manual correction of an automated delineation is supported by several international studies, and provides the benefit of allowing comparisons with a fully automated delineation. Such comparisons provide insight into the effects of delineation errors, but it can be argued that manual corrections cannot be used operationally on large areas. However in this study the area of interest was a research trial, and manual correction was limited to a small number of readily identified trees. Therefore the use of manual correction not only provided a useful comparison with automated methods, but it could provide a viable procedure to obtain the best possible data in operational collection of phenotyping data from research trials.

The manually corrected errors in segmentation were of two kinds, omissions and commissions. Omission trees were not initially detected, and were found to be smaller crowns merged into adjacent crowns. The effect of omissions was therefore a lack of smaller trees in the set of crown metrics, and an overestimation of crown sizes for the adjacent trees with which they were merged. The other source of segmentation error was commission errors of two distinct types. A number of commission errors resulted from large branches within tree crowns being segmented as though they were separate trees. These commission errors caused underestimation of crown size before they were corrected. The other form of commission error was the segmentation of various tree fern and shrub species growing within the trial. These

segments were counted as commissions in calculation of tree detection error, because they represented falsely detected trees. However they were not matched with ground trees, and did not contribute crown metrics to the analysis data set. In fact the detection and segmentation of these non-crop crowns is important as it ensured correct delineation of the crowns for the trees in the trial. Manual correction of omissions therefore reduced overestimated crown sizes and included missing smaller trees, and correction of commissions increased underestimated crown sizes.

2.8 Crown boundary determination

The tree detection process outlined above and described by Pont et al. (2015b) provided the starting point for new crown segmentation processes developed as part of this thesis. The initial image segmentation result comprised a set of segments, one per detected tree, which completely tiled the image into non-overlapping and completely abutting segments. These segments were then processed to determine the crown boundary for each tree by excluding any pixels within the original segment which lay below the threshold height determined earlier. This produced a crown boundary which followed the perimeter of the crown as seen from above and excluded any gaps between crowns (Figure 2.6).

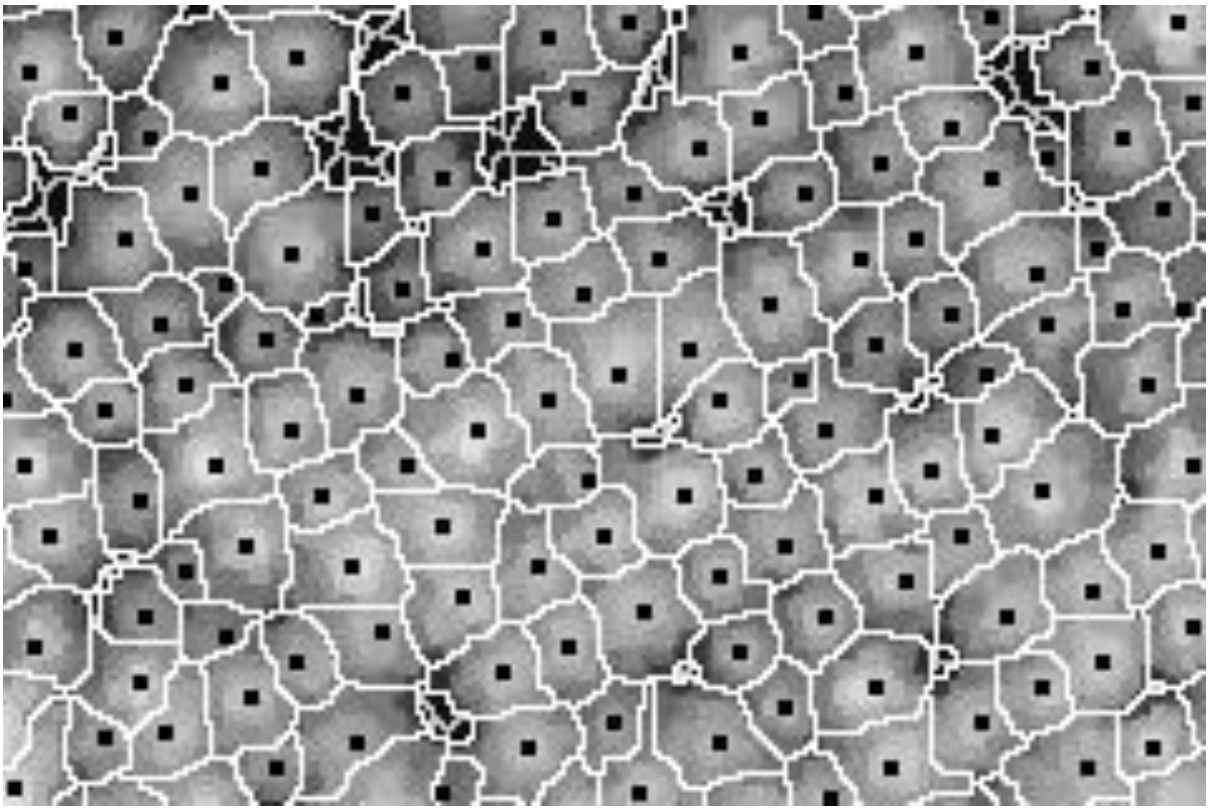

Figure 2.6. Result of crown boundary determination. Detected tree tops are indicated with a black dot. Fragments of the initial segmentation boundaries are visible as dark grey lines on a black background in the upper left of the image. Crown boundaries are shown in white. The image spans a distance of 48 m in the horizontal direction.

2.9 Derivation of crown metrics

Review of the literature in section 1.3.4 showed that a raster-based approach to analysis of ALS data was more robust, and parsimonious than more complex methods such as point-based analysis (Hadaś and Estornell 2016; Wallace et al. 2014b). The utility of crown metrics representing crown morphology for estimating tree attributes was illustrated in a study where hundreds of crown metrics were evaluated (Vauhkonen et al. 2010). In this thesis research crown metrics were derived from the CHM image, using the individual tree crown boundaries. The pixel values within each crown boundary represented heights above the ground, providing a three dimensional description of the upper crown surface (Figure 2.7). The crown surface representation was used to derive a set of crown morphological metrics quantifying crown size and shape.

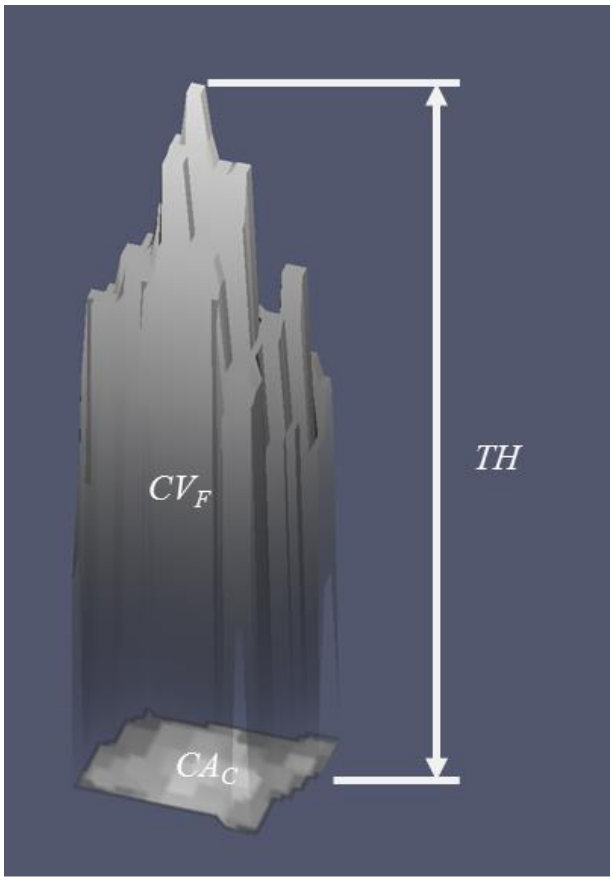

Figure 2.7. Derivation of crown metrics from a CHM image. The pixels belonging to a single tree crown are shown at the bottom. The pixel grayscale values represent heights above ground, allowing creation of a three-dimensional crown representation, and calculation of crown metrics such as the projected crown area (CA_C), maximum height above ground (TH), and the enclosed volume between the crown upper surface and the ground (CV_F).

The full set of 36 crown metrics used in this study are introduced in general groups. Metrics representing one-dimensional measures of crown size included tree and crown height (*TH*, *CH*), crown length and radii (*CL*, *CR*, CR_{av}). Basic statistical properties (mean and variance) of crown surface points provided measures derived from crown surface heights and crown radii (CH_{av}, CH_{var}, CB_{var}, CR_{var}). Several metrics quantified two-dimensional measures of crown and gap sizes, in the form of projected areas (CA_C, GA_C, CA_P, GA_P) and perimeters (C_P, G_P). Three-dimensional measures of crown size were represented by crown surface areas (CS_C, CS_T) and volumes (CV_F, CV_P). A number of metrics represented derivations from the base metrics. Measures of crown foliage distribution (*DF*, *WF*) and functions of those (*fDG* and $f\rho$) were

defined in a study relating tree crown structure with stem size and wood properties (Pont 2003). Three measures of crown slenderness were derived (*CHR*, *CRH*, *SHV*), recognizing that stem slenderness has been correlated with wood stiffness (Watt and Zoric 2010). A number of metrics quantified the regularity of crown and growing space shapes (*RU*, *C2*, $C3_P$, $C3_F$, CAR_{xy}, GAR_{xy}, CAR_R). Two measures compared crown and tree size (CV_{PF}, *CLH*), and one measure compared crown size and growing space (A_{CG}). Derivations and descriptive statistics for the set of metrics used in this study are given in Table 2.1.

Table 2.1. Individual tree crown metrics used in this study. The table includes descriptive statistics: minimum (Min.), mean, maximum (Max.), standard deviation (SD), and coefficient of variation (COV) for each crown metric.

Abbreviation / Equation	Description	Units	Min.	Mean	Max.	SD	COV
CH_{av}	Mean of heights from CHM for the crown.	m	2.410	6.145	8.898	1.015	0.165
CH_{var}	Variance of heights from CHM for the crown.	m	0.141	3.490	9.331	1.606	46.019
$CS_C = \pi CR\sqrt{CL^2 + CR^2}$	Crown surface area derived from crown radius and crown length using formula for surface area of a cone.	m^2	2.8	29.5	140.2	12.1	0.4
CR_{av}	Average of crown radii from tree top location to points on perimeter of crown boundary.	m	0.867	2.011	8.668	0.398	0.198
CA_{C}	Two-dimensional ground area of crown determined by number of pixels.	m^2	1.40	10.38	29.00	4.01	0.39
CV_{F}	The volume between the crown upper surface and the ground (Chen et al. 2007).	m^3	9.6	76.7	208.5	31.3	0.4
CH	Average height of crown boundary points.	m	0.137	4.831	7.991	1.224	0.253
CB_{var}	Variance of heights of crown boundary points.	m	0.12	3.50	11.74	2.17	61.96
CR_{var}	Variance of radii to crown boundary points.	m	0.01	0.25	18.30	0.44	173.17
$CL = H - CH$	Crown length.	m	0.692	4.279	8.597	1.201	0.281
CV_{P}	The volume between the crown upper surface and the base of the crown.	m^3	0.4	21.2	131.3	12.9	0.6
DF	Average of x + y coordinates, x relative to tree top, across all crown surface pixels. Represents mean hydraulic distance to foliage.	m	3.44	7.47	10.66	1.17	15.65
WF	Sum of volumes of crown surface voxels. A simplified representation of foliage mass.	m^3	4.1	45.6	151.8	18.7	41.0
fDG	*WF*/*DF*.		29.7	170.6	410.2	51.5	30.2
$f\rho$	*DF*/*WF*.		329.3	375.7	482.1	18.5	4.9
CP	Perimeter of crown boundary.	m	6.40	16.79	69.60	3.81	0.23
CA_{P}	Two-dimensional ground area of crown determined from polygon.	m^2	2.0	12.1	128.8	5.1	0.4

$CR = \sqrt{\frac{CA_P}{\pi}}$	Crown radius derived from crown polygon area.	m	0.806	1.926	6.403	0.375	0.194
CS_T	Surface area of triangulated crown CHM heights.	m^2	4.1	45.7	152.1	18.8	0.4
GP	Perimeter of crown growing space.	m	6.40	17.42	69.60	4.09	0.23
GA_P	Two-dimensional ground area of crown growing space determined from polygon.	m^2	2.0	12.8	131.2	5.6	0.4
TH	Height of the highest point within the tree segment from the CHM image.	m	4.82	9.11	12.73	1.29	0.14
GA_C	Two-dimensional ground area of crown growing space determined by number of pixels.	m^2	1.40	11.00	34.32	4.54	0.41
$A_{CG} = \frac{CA_P}{GA_P}$	Ratio of crown and growing space areas.	-	0.496	0.955	1.000	0.074	0.078
$CV_{PF} = \frac{CV_P}{CV_F}$	A ratio of crown size to tree size. The ratio of crown partial and full volumes.	-	0.0206	0.2731	0.9483	0.1157	0.4235
$CHR = \frac{TH}{CR}$	A measure of crown slenderness, tree height over crown radius.	-	1.22	4.83	10.82	0.77	0.16
$CLH = \frac{CL}{TH}$	A measure of crown size comparing crown length to tree height.	-	0.0983	0.4696	0.9733	0.1183	0.2519
$CRH = \frac{CR}{TH}$	A measure of crown slenderness, crown radius over tree height. Inverse of CHR.	-	0.0924	0.2124	0.8209	0.0366	0.1722
$SHV = \frac{TH}{\sqrt[3]{CV_F}}$	A measure of crown slenderness.	-	1.494	2.201	3.692	0.206	0.093
$RU = \frac{CA_S}{CA_P}$	A measure of crown surface complexity. Ratio of crown surface area and crown projected area (Bogaert et al. 2000; Kane et al. 2010).	-	0.179	3.787	7.136	0.713	0.188
$C2 = \frac{CP^2}{4\pi CA_P}$	Two dimensional compactness. Ratio of crown perimeter to two dimensional area (Bribiesca 2008; Liu et al. 2010).	-	1.324	1.919	4.119	0.261	13.609

$C3_P = \frac{{CS_T}^3}{36\pi CV_P^2}$	Three dimensional compactness. Ratio of crown surface area (CS_T) to partial crown volume (CV_P) (Bribiesca 2008).	-	0.877	2.357	337.648	7.229	3.0671
$C3_F = \frac{{CS_T}^3}{36\pi CV_F^2}$	Three dimensional compactness. Ratio of crown surface area (CS_T) to full crown volume (CV_F) (Bribiesca 2008).	-	0.003	0.190	1.993	0.182	0.9581
$CAR_{xy} = \frac{\min(R(x), R(y))}{\max(R(x), R(y))}$	Crown aspect ratio from x and y. Ratio of shorter over longer x, y dimension (Suárez 2010). The function *R()* indicates the range of *x* or *y*.	-	0.314	0.846	1.000	0.110	12.961
$GAR_{xy} = \frac{\min(R(x), R(y))}{\max(R(x), R(y))}$	Growing space aspect ratio from x and y. Ratio of shorter over longer x, y dimension. The function *R()* indicates the range of *x* or *y*.	-	0.282	0.827	1.000	0.119	14.389
$CAR_R = \frac{\min(radius)}{\max(radius)}$	Crown aspect ratio from radius. Ratio of minimum over maximum radius.	-	0.043	0.389	0.693	0.112	28.731

2.10 Field measurements of trees

A ground based assessment of the trial was carried out in July 2014 when the trees were aged 7 years, following standard tree breeding measurement methodologies (Jayawickrama 2001). Measurements of tree diameter at breast height (*DBH*), height (*H*), stem straightness score (*S*), branch cluster frequency score (*B*), malformation score (*M*), outerwood stress wave velocity (*A*), and collection of breast height cores for subsequent determination of basic density (ρ) were carried out by T. Stovold, M. Miller and K. Fleet of the Forest Genetics group at Scion, Rotorua.

Tree *DBH* was measured using a fibreglass girth tape having diameter gradations at millimetre intervals (Friedrich Richter Messwerkzeuge GmbH & Co., Speichersdorf, Germany). Tree *H* was measured using a Vertex IV (*Haglof, Sweden AB*). Total stem volume (*V*) was estimated for each tree using the standard volume equation V182, defined in Equation 4.1 (Goulding 1986).

$$V = D^{a}\left(\frac{H^{2}}{H-1.}\right)^{b} e^{c} \qquad 2.1$$

where a=1.79068, b=1.07473, c=-10.03201, and e is Euler's number.

Visual assessment was made by experienced field staff to determine *S*, *B*, and *M* scores for all trees. The assessment guides, developed by the Forest Genetics group at Scion, are presented in Figure 2.8, Figure 2.9, and Figure 2.10.

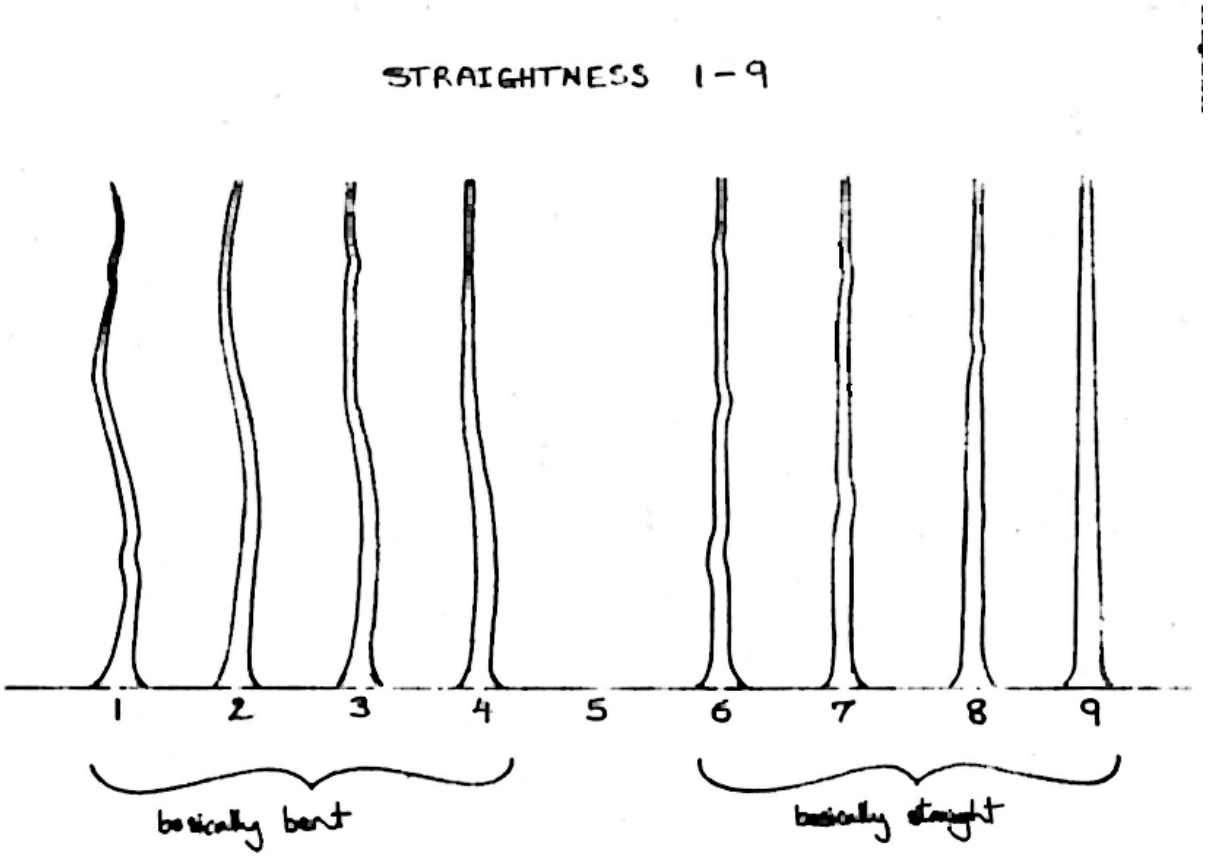

Figure 2.8. Scoring guide for visual assessment of stem straightness. Higher values represent increasing straightness. The value of 5 is not used in scoring, values from 1 to 4 represent basically bent trees, and values from 6 to 9 represent basically straight trees.

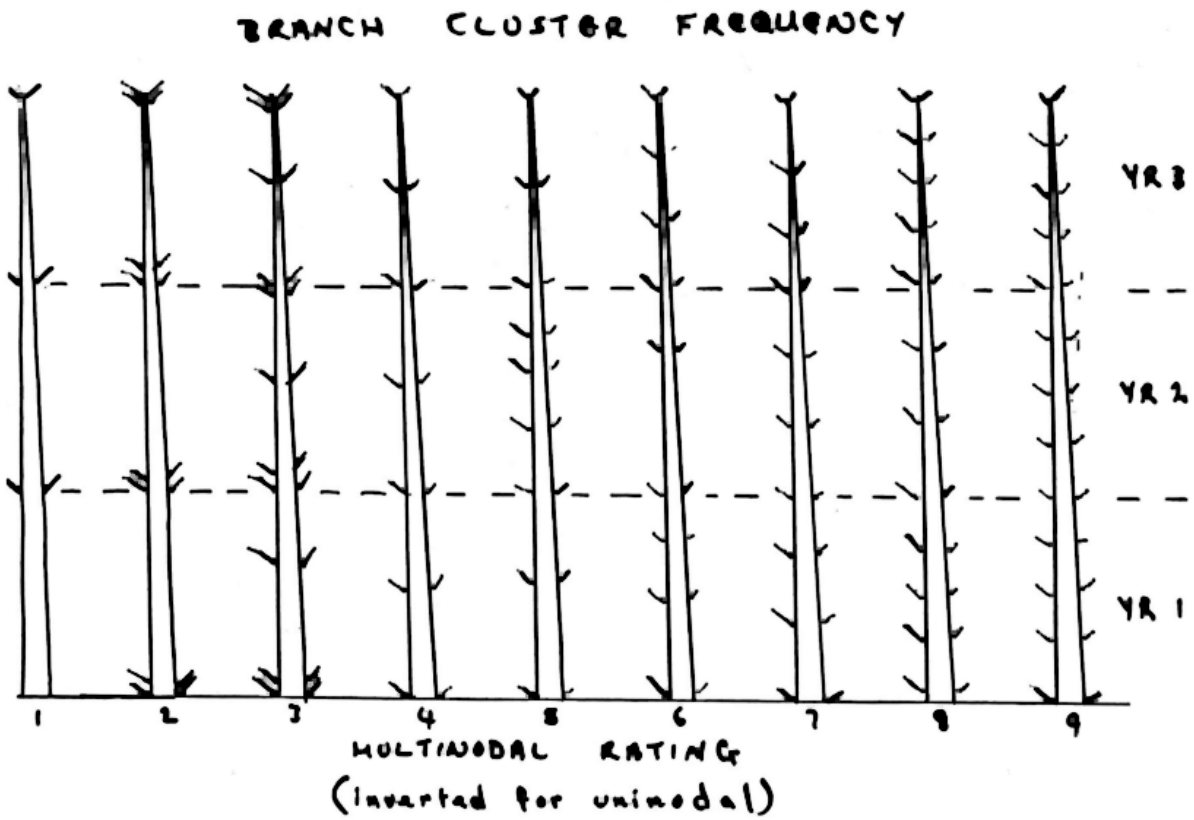

Figure 2.9. Scoring guide for visual assessment of stem branch cluster frequency. Scores from 1 to 9 represent a multinodal rating, higher values having more internodes per annual growth shoot (3 annual shoots are indicated with dotted horizontal lines). The scoring values may be inverted from 1 to 9 to be from 9 to 1 for scoring uninodal breeds, which was not necessary in this study.

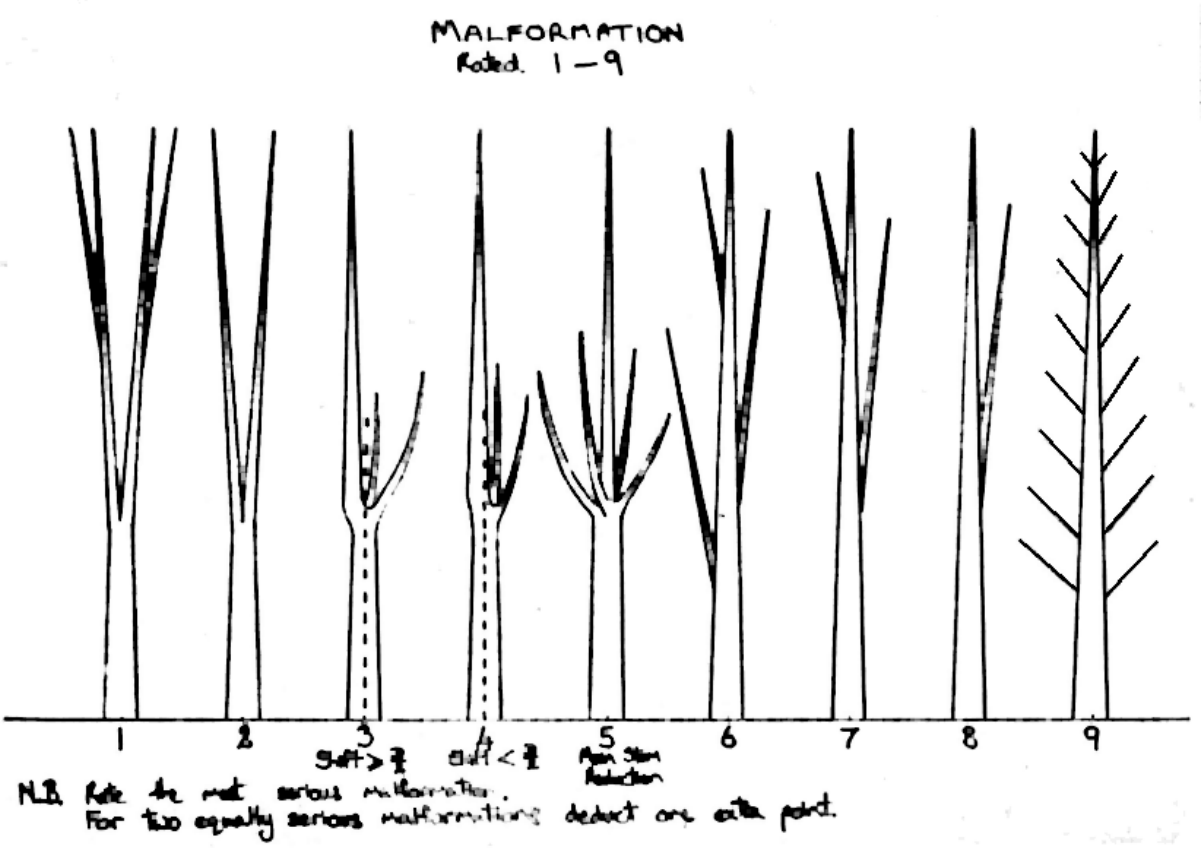

Figure 2.10. Scoring guide for visual assessment of malformation. Scores 1 and 2 represent forked trees, 3 and 4 represent leader replacements with a lateral shift > D/2 and < D/2 respectively where D is stem diameter immediately below, 5 is a main stem reduction, 6, 7, and 8 represent ramicorns (large branches), and 9 represents a tree without malformation. Notes below the figure state: rate the most serious malformation and for two equally serious malformations deduct one extra point.

Outerwood acoutic velocity (*A*) was measured using a HITMAN ST300 (fibre-gen Ltd, Christchurch, New Zealand) with the probes placed 1 m apart, avoiding knots and defects that could affect readings. Breast height bark to bark (diametral) cores were taken from each tree with a 5.1 mm Mattson (United Kingdom) increment borer. Cores were divided at the pith centre, the half with the least defects was selected, and basic density (ρ) was determined for the sample using the maximum moisture content method without resin extraction (Smith 1954).

Degree of infection by Dothistroma needle blight (*Dothistroma septosporum* (Dorog.) M. Morelet) was assessed by M. Miller and K. Fleet of the Forest Genetics group, Scion, at age 24

months (D_{24}) and by J. Wharekura of Radiata Pine Breeding Co-operative (RPBC), Rotorua, at age 38 months (D_{38}). The Dothistroma measurement data was provided by the RPBC. Degree of infection was recorded as a percentage of needles infected or lost, measured in 5 percent increments (van der Pas et al. 1984). The assessments of Dothistroma infection were made at 5 and 4 years prior to the ALS measurement, but Dothistroma needle blight is a slowly progressive disease which continues to spread within the crown over several years. It was therefore expected that effects of Dothistroma needle blight would be apparent in the crown metrics derived from the ALS data collected some years after assessment of infection.

2.11 Models for quantifying genetic variation

A brief outline follows of how underlying components of total observed (phenotypic) variation in tree attributes were estimated using established methods. For more comprehensive description of the concepts and methods the reader is referred to forest genetics texts (Fins et al. 1992; White et al. 2007). An observed phenotypic value *(P)* for a trait of interest can be expressed as the sum of genotype *(G)* and environment *(E)*:

$$P = G + E \qquad 2.2$$

Likewise the observed variance of a phenotype can be expressed as the sum of genotypic and environmental variances (White et al. 2007) :

$$Var(P) = Var(G) + Var(E) \qquad 2.3$$

Heritability is then defined as the proportion of phenotypic variance that can be attributed to genetic origin:

$$Heritability\ (broad\ sense) = H^2 = \frac{Var(G)}{Var(P)} \qquad 2.4$$

Broad sense heritability includes various genetic contributions to the variance in the phenotype, including additive and non-additive effects. It should be noted such heritability estimates are specific to the observed population and environment. The genetic variance can be partitioned into additive effects ($Var(A)$, termed breeding values), dominance effects ($Var(D)$, interactions between alleles at the same locus), and epistatic ($Var(I)$, interactions between alleles at different loci):

$$Var(G) = Var(A) + Var(D) + Var(I) \quad 2.5$$

Additive variance represents the variance due to parent-offspring resemblance and is therefore important for selection in breeding (hence the term breeding values). In practice, narrow sense heritability is estimated in terms of an observed response (change in variance) resulting from selection, requiring knowledge of the phenotypic values for parents and selected offspring. Narrow (or strict) sense heritability is defined as the proportion of phenotypic variation attributed to additive origin:

$$Heritability\ (narrow\ sense) = \ h^2 = \frac{Var(A)}{Var(P)} \quad 2.6$$

Environmental variance ($Var(E)$), might be assumed to consist of environmental variance common to groups such as siblings ($Var(CE)$), and non-genetic variance from repeat measures of individuals ($Var(PE)$), with the remainder attributed to random error variance and measurement error ($Var(RE)$):

$$VAR(E) = \ VAR(CE) + VAR(PE) + VAR(RE) \quad 2.7$$

In the simplest formulation, no specific environmental factors are identified and environmental variance remains as an unexplained component of the residual $VAR(E) = VAR(RE)$. However that approach is focussed on carefully partitioning variance according to genetic factors, and environmental variation is treated with relatively simple assumptions. Figure 2.11 illustrates a

simple conceptual model of the partitioning of both genetic and environmental variance components.

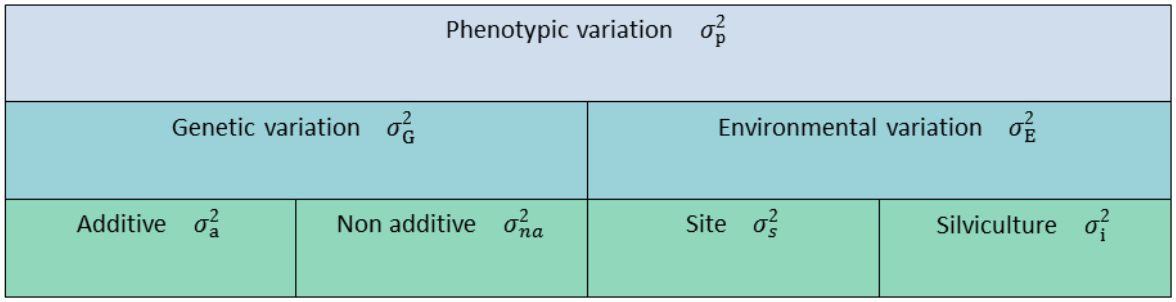

Figure 2.11. A conceptual model for the partitioning of total phenotypic variation. Total variation can be subdivided into genetic and environmental components, which can each be further separated into underlying components.

Both genetic and environmental variance can be analysed by taking account of fixed and random effects. Note that for this trial, replicate and control were specified as fixed effects, while replicate within block and pedigree were specified as the random effects, the latter used to estimate additive genetic variance (σ^2_a). The additive genetic variance was then used to estimate genetic correlations (r_g), narrow sense heritabilities h^2 and breeding values used for ranking and selection. The genetic correlations were also used to carry out clustering using the R *hclust* method with the default *complete linkage* method (Kaufman and Rousseeuw 2008; R Core Team 2014). Clustering was carried out to reveal groups of variables with closer genetic associations. Such associations are important when ranking and selecting superior trees on the basis of a single trait because they indicate other traits which will also be effectively selected.

Chapter 3 Correlations between Crown Metrics and Ground Measures of Tree Attributes

3.1 Introduction

The ability to estimate the key attributes of individual trees from remotely sensed data would provide valuable information for precision forestry at an unprecedented level of detail. The aim of this study was to evaluate individual tree crown metrics derived from ALS data for their utility to estimate tree size, quality and disease expression for precision forestry. The tree attributes of interest were tree height, diameter at breast height (DBH), total stem volume, stem straightness, malformation, branching, wood stiffness, basic density, and level of Dothistroma infection. The ability to estimate these variables from ALS would offer potential cost savings for operational forest inventory and management, and for trial measurement. Additionally, conventional forest inventory is based on the measurement of trees within sample plots. The ability to accurately identify all trees in an area and accurately estimate their sizes could be used to replace ground measurement of plots, or it could lead to development of alternative, more accurate, methods of forest inventory through assessment of all trees in an area of interest.

There is extensive literature concerning the use of area-based analysis of ALS to estimate mean tree attributes such as top height, basal area and stem volume, to support forest inventory (Bouvier et al. 2015; Vauhkonen et al. 2014; White et al. 2013). Some literature has indicated the potential to use ALS data to estimate measures of wood quality (Van Leeuwen et al. 2011) and some promising results using area-based methods have been reported recently (Luther et al. 2014). A review of literature focused on estimation of individual tree-level metrics from ALS was made. Although some researchers have suggested the potential use of ALS data to estimate individual tree attributes, there are few actual studies to date, generally limited to estimation of tree size attributes. In this study the ability to estimate a broader set of operationally relevant tree attributes is evaluated, encompassing measures of tree size, form, wood quality and disease, for trees in New Zealand radiata pine plantations.

3.1.1 Estimating tree size

A number of other researchers have used prototype tree identification methods to demonstrate estimation of various measures of tree size. Canopy geometric volume was used to estimate tree basal area and stem volume with R^2=0.77 and 0.79 respectively, but the results were reliant on accurate tree segmentation (Chen et al. 2007). In another example a new tree algorithm for tree segmentation was presented and it was noted that TBA had utility for estimating variables of interest such as biomass and forest growth, but this area of research was still regarded as an open problem (Tang et al. 2013). A new segmentation method was applied to ALS to estimate tree height, crown diameter and crown base height (Solberg et al. 2006a). Watershed segmentation was applied to identify individual trees from ALS and estimate individual tree heights with an RMSE of 0.42 m compared with ground measurements (Chen and Zhu 2012). The tree heights were then used to estimate predominant stand height as a measure of site quality for *Pinus radiata* stands in Australia.

Tree-based analysis was used to estimate tree DBH and biomass (Kim et al. 2012). Tree-based analysis of a CHM was used to estimate tree DBH and volume from the following tree metrics: position, height, crown radius and competition index (Lo and Lin 2013). A combination of ALS and optical imagery have also been used to detect individual trees and estimate tree height (R^2=0.99) and DBH (R^2=0.87) (Prieditis et al. 2012). A simple tree identification process applied to ALS data was used to estimate tree DBH from LiDAR height, and significant potential benefits described for harvest planning from having an accurate map of tree locations and sizes (Heinimann and Breschan 2012). However the authors also noted this potential cannot be realised until reliable tree identification methods are available and pointed out smoothing of the canopy model is a critical step requiring further research.

In a series of papers, Swedish researchers used ITC methods in combination with other ALS analysis methods to derive tree lists: DBH and height; and to estimate stand volume (Lindberg et al. 2008; Lindberg et al. 2010, 2013). In a study of boreal forest in eastern Finland the use of ITC methods showed improvements in estimation of diameter distributions compared with use

of ABA methods alone (Xu et al. 2014). In recognition of the inability to reliably identify all trees in boreal forest conditions researchers were developing statistical methods to estimate realistic distributions of tree size (Vauhkonen and Mehtätalo 2015). New Zealand radiata pine forests represent a more regular forest type, being even aged and single species and such approaches may not be necessary.

Review of the literature has shown there is good potential to estimate tree size in New Zealand plantation forest conditions using tree-based analysis of ALS data. The problem of accurate tree detection, noted by researchers dealing with more complex forest types, could be less of a barrier in New Zealand conditions and the potential for development of ITC methods to characterise individual trees is therefore greater.

3.1.2 Estimating tree form

Few research papers specifically related to estimation of tree or log quality from ALS were found, and most used area-based methods (Hilker et al. 2013; Luther 2013; Watt and Watt 2013). Tree-based analysis of ALS data was applied to estimate tree branch biomass with higher accuracy than estimates derived from ground measurements (Hauglin et al. 2013a; Hauglin et al. 2013b), and to estimate pruned height using extremely high laser pulse density over a Eucalyptus globulus plantation (Wallace et al. 2014b). The combined use of ABA and ITC methods showed improvements in estimation of timber assortments in a study of boreal forest in eastern Finland (Xu et al. 2014). In a study in Canadian boreal forest, tree maximum branch diameters were estimated with an RMSE of 0.32 cm using tree and stand attributes that the authors noted might be estimated from remotely sensed data, such as ALS, in the future (Groot and Schneider 2011).

The following three studies used a combination of ALS data with more direct measures of stem quality for boreal forests in Finland and Sweden. Stem attributes were estimated from ALS and terrestrial laser scanning (TLS), by using attributes detected from the ALS to lookup stems with TLS data in a library (Lindberg et al. 2012). ALS based estimates of DBH, height and volume

had RMSE of 15.4%, 3.7% and 34.0% respectively, as compared with values from the TLS. In a related approach ALS and harvester measurements were combined to estimate stem attributes for forested areas (Holmgren et al. 2012). Estimates were made of mean tree height, mean stem diameter, stem volume and stem density, with an RMSE of 8%, 12%, 11% and 19% respectively. The authors noted this approach was useful to estimate log assortments for planned areas. Tree TLS scans were used with ALS to estimate yields of sawlog and pulp logs and estimates of sawlog volumes had RMSE of 16.8%.

3.1.3 Estimating wood quality

Examples of research on estimation of wood properties from ALS are also limited, although the potential to do so has been raised. In a review paper the potential for the use of ALS to estimate various wood quality variables for forest management purposes was discussed (Van Leeuwen et al. 2011). In one study moderate success was achieved in estimating wood properties in individual trees (measured with Silviscan) in Canadian boreal forest from ground measured crown variables: tree height, crown dimensions, number and diameters of branches in selected whorls (Lenz et al. 2012). The authors suggested the possibility of using remote sensing such as ALS to do this in the future. This research approach was also described in another article, with the authors also concluding remote sensing could be used in the future (Groot et al. 2015).

In a study using ABA metrics describing canopy height, canopy depth and canopy light zones, about half of the observed variance was explained for six wood fibre attributes measured at the plot level using Silviscan: wood density, cell perimeter, cell coarseness, mature fibre length, microfibril angle, and modulus of elasticity (Hilker et al. 2013). In a Canadian study of boreal forest a mixture of ABA and analysis of the CHM were used to estimate a number of wood properties, measured using Silviscan, at the plot level (Luther et al. 2012). Moderate success was achieved, for black spruce R^2 ranged from 0.42 for wood density to 0.57 for modulus of elasticity. In subsequent research using the same database, canopy structure and tree

competition metrics derived from TLS data were used to estimate plot means of wood properties, with R^2 from 0.63 to 0.72 for black spruce (Blanchette et al. 2015).

In a pilot study on a pre-harvest area of radiata pine in New Zealand crown metrics derived using TBA were used to estimate standing tree acoustic velocity (STAV) (Pont et al. 2012b). STAV is highly correlated with modulus of elasticity (stiffness), a key wood property for structural log and timber grades. A model using metrics from ABA had an R^2 of 0.27. Addition of crown metrics from TBA to the model improved the R^2 to 0.69. The international literature indicates strong interest in, and potential for, estimating wood quality attributes using remote sensing (Luther et al. 2012; Van Leeuwen et al. 2011), but the use of tree-based analysis has so far been limited to a few studies at the plot level.

3.1.4 Estimating needle blight

New Zealand tree breeders have identified Dothistroma (*Dothistroma septosporum* (Dorog.) M. Morelet) as a disease that significantly affects profitability, and have an objective to develop breeds with improved Dothistroma resistance (Jayawickrama and Carson 2000). Dothistroma is a needle blight which progressively results in needle discoloration, death and early defoliation (Gadgil 1967). Although complete needle loss and tree death are rare, the disease can significantly reduce tree growth (van der Pas 1981; Watt et al. 2011; Woollons and Hayward 1984).

There is some limited research into the use of ALS to determine the effects of needle loss in trees. In a study of the effects of mountain pine beetle infestation in British Columbia, discrete return ALS density metrics were found to correlate well with plot-level observations of the degree of needle loss (R^2 = 0.76) (Coops et al. 2014). In a study of defoliation in Scots pine stands by pine sawfly in southern Finland, a combination of aerial spectral and ALS data were used to classify individual trees as healthy or infected with an accuracy of up to 88.1% (Kantola et al. 2010). Subsequent research by the same researchers using ALS data only showed classification accuracies for individual trees from 82.8% to 83.7% dependant on ALS pulse

density which ranged from 20 to 2 pulses m^{-2} (Kantola et al. 2013). In further associated research using the same data, 84.3 % accuracy was achieved estimating needle loss classification at the plot level using an area-based approach (Vastaranta et al. 2013).

3.1.5 Research objectives

International research has demonstrated the use of crown metrics from ALS data to estimate tree size attributes, and has indicated potential to estimate stem form, wood quality and disease attributes. A set of 36 crown metrics were derived from analysis of a LiDAR CHM in section 2.9 to meet the first objective: *"Derive a set of individual crown metrics from raster-based analysis of ALS data in which individual trees have been detected"*. Those crown metrics were then utilised to meet the second objective: *"Quantify correlations between LiDAR crown metrics and ground-based measures of tree size, form, wood quality, and disease expression"*. The effects of manual correction of the tree segmentation were evaluated to meet the third objective: *"Evaluate the effect of errors in tree detection and delineation by comparing estimates of correlations from automatic and manual segmentation of individual trees"*. This study represented the first known example of using ALS data to estimate a comprehensive set of tree size, form, wood quality and diseases attributes together at the individual tree level. Results were used to evaluate the ability to answer the research question: "**Can methods be developed to estimate key attributes of individual trees using airborne laser scanning data?**".

3.2 Materials and methods

Refer to Chapter 2 for a detailed description of the materials and methods used to measure tree attributes in a breeding trial, and to derive crown metrics from ALS data collected above the trial. In this section only a brief outline will be given of the data to be used. A complete description will be given of the methods used to examine correlations between the ground measured attributes and crown metrics from the ALS data.

3.2.1 Tree attributes measured on the ground

Variables available for all trees were diameter at breast height (*DBH*), height (*H*), total stem volume (*V*), straightness (*S*), branching (*B*), malformation (*M*), outerwood stress wave velocity (*A*), basic density (ρ), degree of Dothistroma infection at ages 24 and 38 months (D_{24} and D_{38} respectively). Variables were placed into four groups for analyses: tree size (*H*, *DBH*, and *V*), stem form (*S*, *B*, and *M*), wood quality (*A* and ρ) and disease resistance (D_{24} and D_{38}).

3.2.2 Individual tree crown metrics

A CHM created from remotely sensed ALS data of the tree breeding trial was processed using the CITC methodology, with the image calibration method, to segment individual trees on the CHM image (Pont et al. 2015b). The initial automated tree detection rate was 89.82%, consistent with the accuracy of the image calibration method reported by Pont et al. (2015b). Manual correction of the automated segmentation was carried out, improving tree detection to 98.34%. Refer to section 2.7 for a more detailed description of the manual corrections carried out and the effects on tree crown segments. Tree top locations and tree crown boundaries were then determined from the image segment for each tree and 36 morphological crown metrics derived, representing measures of crown size and shape.

3.2.3 Analysis of correlations

Statistical analyses and model fitting were carried out using R (R Core Team 2014). Correlations between ground measures and crown metrics were examined using Pearson's product-moment correlation (*r*). Further analysis of correlations was carried out among ground measured attributes and crown metrics by deriving a dissimilarity measure (*DM*) from the Pearson's *r*:

$$DM = 1 - abs(r) \qquad 3.1$$

Taking the absolute value of *r* allowed either positive or negative correlations to be treated as similar levels. The dissimilarity measure was used to carry out clustering to identify groups of

crown metrics, using the R *hclust* method with the default *complete linkage* method for determining clusters (Kaufman and Rousseeuw 2008; Legendre and Legendre 2012). Clustering provided insights into fundamental relationships among the range of variables being investigated by grouping variables that were more closely correlated, irrespective of the sign of the correlation.

3.2.4 Fitting univariate linear models

Univariate linear models were fitted to quantify the predictive ability of the best correlated crown metric for each tree attribute. Each model was fitted twice, using crown metric values derived before and after manual correction of the crown segmentation was undertaken. The manually corrected segmentation was used as the reference segmentation, allowing evaluation of the effects of errors in segmentation on correlations. The model fitting process followed a general approach used for development of models for forestry applications (Watt et al. 2013c; Watt and Watt 2013). Models were created for each of the ground measures using the single best correlated crown metric, entered as a second order polynomial term. Polynomial terms were evaluated because they can accommodate variables which have curvilinear, as well as strictly linear, responses within models, resulting in better model fit (Kleinbaum et al. 2013). Additional variables were not added to the models as the focus was on determination of the main relationships between crown metrics and tree attributes. Only significant quadratic and linear coefficients ($p<0.05$) were retained in each final model.

Model bias and heteroscedasticity were evaluated by examining plots of residual values against predicted values and the independent variables in the model. Residuals should show random distribution, while patterns indicate model bias. The precision of the models was quantified using the coefficient of determination (R^2), the root mean square error (RMSE) and the RMSE normalised by the mean of the measured values (CV(RMSE)). The R^2 is the proportion of the response variable variation explained by the model. The RMSE provides an absolute measure of the goodness of fit, being the square root of the variance in the residuals, in the units of the

response variable. The derived value CV(RMSE) expresses RMSE as a value relative to the mean, to allow comparisons across models. Model RMSE was determined as:

$$RMSE = \sqrt{\sum_{i=1}^{n} \frac{(\bar{Y}_i - Y_i)^2}{n}} \qquad 3.2$$

where $\bar{Y}_i$ and Y_i represent predicted and actual values respectively.

3.3 Results

3.3.1 Descriptive statistics for measured attributes

The descriptive statistics of the ground measured attributes are given in Table 3.1. The measured attributes generally showed a wide range of variation (see coefficient of variation in Table 3.1). Tree height and the wood quality variables (*H*, *A*, and ρ) were the least variable, with COVs of 13%, 14%, and 6% respectively. Diameter and two of the form variables (*DBH*, *S*, and *B*) were of intermediate variability, with COVs of 21%, 27%, and 28% respectively. Measures of volume, malformation, and Dothistroma infection (*V*, *M*, D_{24}, and D_{38}) exhibited the highest levels of variability with COVs of 0.42, 0.49, 0.33, and 0.32 respectively.

Table 3.1. Descriptive statistics of tree attributes measured from the ground in the trial. (n=2188).

Variable	Units	Minimum	Mean	Maximum	Standard deviation	Coefficient of variation
H	m	4.30	11.34	16.30	1.44	0.13
DBH	mm	13.00	181.18	285.00	37.48	0.21
V	m^3	0.00	0.13	0.35	0.06	0.42
S	1 to 9	1.00	5.96	9.00	1.62	0.27
B	1 to 9	1.00	5.90	9.00	1.65	0.28
M	1 to 9	1.00	6.21	9.00	3.06	0.49
A	$km.s^{-1}$	1.91	2.86	4.17	0.39	0.14
ρ	$kg.m^{-3}$	264.00	327.01	410.00	19.57	0.06
D_{24}	%	5.00	33.86	90.00	11.31	0.33

Correlations

D_{38}	%	5.00	35.65	90.00	11.33	0.32

3.3.2 Correlations among ground measured variables

There were a few high correlations (r >0.7) observed among the measured attributes (Table 3.2). The high correlations for *V* with *D* (r=0.974) and *H* (r=0.826) were expected as total stem volume (*V*) was estimated from *D* and *H*. The next highest correlation was between *H* and *D* (r=0.750), and a moderate correlation (r=0.558) between the degree of Dothistroma infection assessed at ages 24 and 38 months (D_{24} and D_{38} resp.).

Moderate correlation values with D_{24} (r<-0.37) and D_{38} (r<-0.48) were observed for the tree size attributes *DBH*, *V* and *H*. The strongest correlations with Dothistroma infection were with *DBH* (r=-0.590) and *V* (r=-0.569) when assessed at the later age (D_{38}). There were some weak correlations (0.3<r<0.4) among the tree form attributes *S*, *B*, and *M*.

Table 3.2. Pearson's product-moment correlation coefficients (*r*) among the ground measured attributes.

	H	*DBH*	*V*	*S*	*B*	*M*	*A*	ρ	D_{24}	D_{38}
H	1.000	**0.750**	**0.826**	0.293	0.220	0.241	0.144	0.018	-0.371	-0.470
DBH	**0.750**	1.000	**0.974**	0.219	0.219	0.127	-0.140	-0.106	-0.492	**-0.590**
V	**0.826**	**0.974**	1.000	0.243	0.232	0.160	-0.092	-0.084	-0.467	**-0.569**
S	0.293	0.219	0.243	1.000	0.392	0.286	0.151	-0.002	-0.101	-0.168
B	0.220	0.219	0.232	0.392	1.000	0.263	0.029	-0.006	-0.122	-0.166
M	0.241	0.127	0.160	0.286	0.263	1.000	0.036	-0.015	-0.009	-0.063
A	0.144	-0.140	-0.092	0.151	0.029	0.036	1.000	0.157	0.110	0.109
P	0.018	-0.106	-0.084	-0.002	-0.006	-0.015	0.157	1.000	-0.030	-0.025
D_{24}	-0.371	-0.492	-0.467	-0.101	-0.122	-0.009	0.110	-0.030	1.000	**0.558**
D_{38}	-0.470	**-0.590**	**-0.569**	-0.168	-0.166	-0.063	0.109	-0.025	**0.558**	1.000

Note: Pearson's r with absolute values greater than 0.5 are shown in bold.

3.3.3 Correlations between crown metrics and ground measured attributes.

Several crown metrics showed correlations over 0.5 (Table 3.3) with the ground measured tree size attributes (*H*, *DBH*, and *V*). The best correlations were between *TH* and *H* (r=0.904) and between CV_F and *DBH* and *V* (r=0.824 and r=0.844 resp.). The crown metric *TH* was also the most strongly correlated metric for *S* (r=0.261), *B* (r=0.173), *M* (r=0.204) and D_{24} (r=-0.390). The crown metric CV_F provided the strongest correlation with D_{38} (r=-0.499), and with *DBH* and *V*. The crown metrics *RU* and *SHV* had the strongest correlations with the wood quality attributes ρ (r=0.080) and *A* (r=0.219) respectively.

Table 3.3. Pearson's correlation coefficients (*r*) between the measured attributes and the crown metrics derived from the segmented CHM after manual correction.

	H	*DBH*	*V*	*S*	*B*	*M*	*A*	ρ	D_{24}	D_{38}
GP	0.420	**0.587**	**0.573**	0.149	0.099	0.098	-0.095	0.026	-0.282	-0.367
GA_C	0.432	**0.619**	**0.603**	0.145	0.105	0.112	-0.128	0.011	-0.284	-0.369
GA_P	0.367	**0.518**	**0.511**	0.138	0.091	0.084	-0.089	0.038	-0.246	-0.323
GAR_{xy}	0.078	0.073	0.079	0.035	0.050	-0.015	0.054	0.011	-0.041	-0.030
CA_C	**0.535**	**0.704**	**0.697**	0.179	0.121	0.130	-0.101	0.005	-0.321	-0.425
CA_P	0.443	**0.573**	**0.574**	0.164	0.101	0.094	-0.061	0.035	-0.270	-0.362
CAR_{xy}	0.038	0.047	0.050	0.022	0.051	-0.008	0.052	0.035	-0.040	0.017
CAR_R	0.210	0.137	0.148	0.094	0.108	0.100	0.054	0.044	-0.055	-0.048
TH	**0.904**	**0.772**	**0.821**	0.261	0.173	0.204	0.146	0.003	-0.390	-0.485
CH	0.486	0.385	0.412	0.097	0.046	0.053	0.133	-0.053	-0.202	-0.275
CL	0.476	0.437	0.462	0.181	0.139	0.165	0.020	0.057	-0.213	-0.241
CR_{av}	0.492	**0.636**	**0.628**	0.168	0.104	0.100	-0.068	0.024	-0.301	-0.404
CR	**0.535**	**0.679**	**0.670**	0.186	0.122	0.121	-0.068	0.023	-0.319	-0.420
CS_C	**0.519**	**0.584**	**0.598**	0.191	0.130	0.144	-0.041	0.046	-0.276	-0.347
CS_T	0.478	**0.568**	**0.574**	0.175	0.122	0.136	-0.050	0.041	-0.259	-0.324
WF	0.479	**0.569**	**0.575**	0.175	0.122	0.136	-0.050	0.041	-0.259	-0.324
DF	**0.759**	**0.688**	**0.718**	0.190	0.118	0.126	0.126	-0.036	-0.338	-0.456
fDG	0.410	**0.503**	**0.502**	0.160	0.117	0.128	-0.054	0.047	-0.228	-0.280
$f\rho$	-0.244	-0.331	-0.322	-0.120	-0.103	-0.110	0.045	-0.057	0.144	0.163
CP	**0.504**	**0.647**	**0.639**	0.176	0.106	0.105	-0.066	0.016	-0.306	-0.411
CV_F	**0.718**	**0.824**	**0.844**	0.221	0.149	0.159	-0.019	-0.013	-0.384	-0.499
CV_P	0.417	**0.541**	**0.541**	0.166	0.118	0.121	-0.074	0.032	-0.256	-0.310
A_{CG}	0.297	0.187	0.207	0.089	0.017	0.014	0.104	-0.022	-0.089	-0.157
C2	0.183	0.252	0.242	0.054	0.007	0.007	-0.029	-0.020	-0.131	-0.189
$C3_P$	0.004	-0.032	-0.010	-0.023	-0.045	-0.028	0.001	0.036	0.057	0.012

Correlations

$C3_F$	-0.124	-0.081	-0.081	-0.005	0.011	0.017	-0.054	0.062	0.062	0.109
CLH	0.011	0.044	0.045	0.052	0.064	0.073	-0.053	0.066	-0.011	0.018
CV_{PF}	-0.115	-0.046	-0.056	0.020	0.045	0.035	-0.055	0.059	0.031	0.083
CRH	-0.157	0.122	0.070	-0.014	-0.007	-0.039	-0.198	0.029	-0.032	-0.067
CHR	0.118	-0.175	-0.119	0.006	-0.002	0.018	0.201	-0.014	0.055	0.085
RU	0.005	-0.140	-0.104	0.046	0.063	0.073	0.118	0.080	0.076	0.145
CB_{var}	0.111	0.150	0.146	0.097	0.072	0.076	0.002	0.025	-0.115	-0.070
CR_{var}	0.004	0.033	0.038	0.018	-0.017	-0.042	0.003	0.046	-0.033	-0.063
CH_{av}	**0.720**	**0.614**	**0.648**	0.183	0.116	0.119	0.167	-0.035	-0.316	-0.400
CH_{var}	0.290	0.258	0.274	0.153	0.118	0.116	0.050	0.053	-0.140	-0.130
SHV	0.179	-0.163	-0.092	0.038	0.020	0.056	0.219	0.015	0.047	0.082

Note: Pearson's *r* with absolute values of at least 0.5 are shown in bold. The highest correlation for the ground variable in each column is underlined.

3.3.4 Clustering of variables

Clustering is a data exploration technique used to determine groups of variables that are more similar to each other than those in other groups. This is a useful way to screen correlations among a large number of variables such as the set of crown metrics and ground measured attributes available in this study, and to aid identification of relationships among the variables. Tabular and graphical presentation of correlations among a large set of variables, such as the 36 crown metrics employed in this study, is not feasible. Clustering is a useful technique in this situation, as it allows examination of correlations among the variables in a structured and compact representation. Clustering effectively filters out the clutter of numerous weak correlations, revealing stronger associations and groupings among variables. A dissimilarity measure, determined from the correlation values in Table 3.3 (using Equation 3.1), was used to apply a clustering algorithm to the 36 crown metrics and the 10 ground variables evaluated in this study. Examination of the clustering results indicated a set of six main clusters. In the dendrogram produced from the clustering results (Figure 3.1), vertical lines joining groups of one or more variables indicate the dissimilarity measure of those two groups. Therefore vertical lines on the left of the dendrogram join groups with higher dissimilarity and vertical lines on the right join groups with high similarity.

Six clusters ranging in size from 2 to 16 variables were segregated from the data. The second largest cluster (black labels in Figure 3.1) contained 11 variables including the tree size and disease attributes (*H*, *DBH*, *V*, D_{24} and D_{38}), representing 5 of the 10 ground measured attributes. Those attributes were already seen to have moderate to high correlations with each other in Table 3.2. This cluster also included the two crown metrics *TH* and CV_F, which were the best correlated metrics for 8 of the 10 ground measured attributes (see Equations 3.4 to 3.13). The tree form attributes (*B*, *S*, and *M*) and the wood quality attributes (*A* and ρ) formed two isolated clusters (red and blue labels resp. in Figure 3.1), indicating poor correlations with all of the crown metrics. Three clusters containing only crown metrics comprised the remainder of the variables, those groups containing 16, 8, and 6 crown metrics (green, purple and brown labels resp. in Figure 3.1). This result indicated those metrics did not have significant correlations with any of the ground measured attributes.

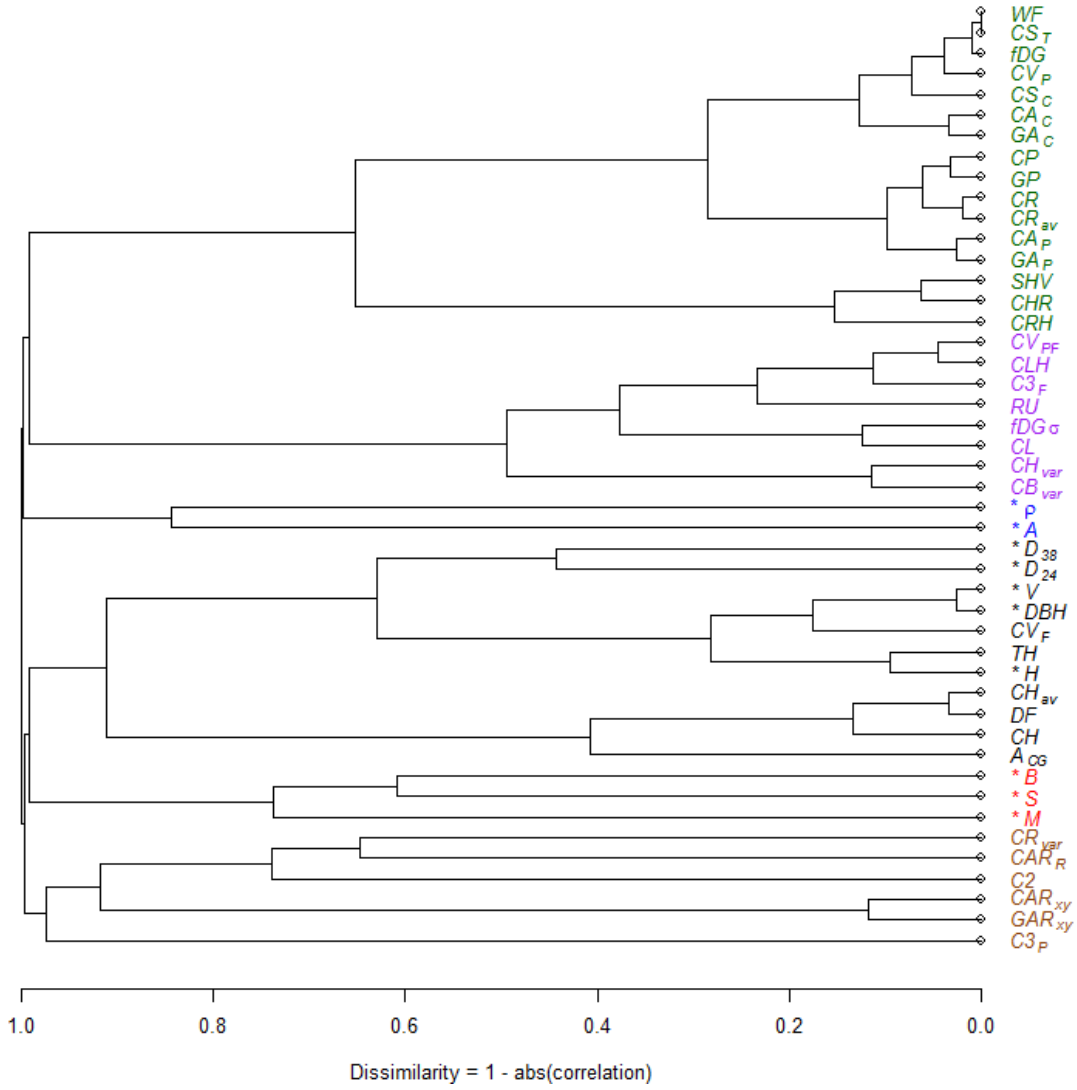

Figure 3.1. Similarities among measured attributes and crown metrics. Dendrogram plot of ground measured attributes (prefixed with asterisk) and crown metrics showing dissimilarity of variables. Clustering was used to define six groups which are indicated by different coloured labels.

3.3.5 Linear models relating tree attributes and crown metrics

Linear univariate models were fitted to define the basic mathematical nature of the relationships between crown metrics and the corresponding ground measured attributes. One model was fitted for each of the ten ground measured attributes. Estimation of tree height from diameter

can be useful because tree height and diameter are typically strongly related, and diameter is significantly easier to measure than height. An additional model was therefore fitted to estimate *H* from *DBH*, for comparison with the model fitted to estimate *H* from a crown metric.

Models were fitted to crown metrics derived before and after correction of the crown segmentation. Coefficients obtained from re-fitting with crown metrics from the uncorrected segmentation were generally only slightly changed. The coefficients presented below for each model are from fitting to the crown metrics derived from the manually corrected segmentation.

$$H = 4.17 + 0.056\,DBH - 0.000067\,DBH^2 \quad 3.3$$

$$H = 1.36 + 1.31\,TH - 0.0219\,TH^2 \quad 3.4$$

$$DBH = 85.2 + 1.71\,CV_F - 0.00483\,{CV_F}^2 \quad 3.5$$

$$V = 0.00139 + 0.00208\,CV_F - 0.00000402\,{CV_F}^2 \quad 3.6$$

$$S = 3.03 + 0.325\,TH \quad 3.7$$

$$B = 3.94 + 0.219\,TH \quad 3.8$$

$$M = 1.84 + 0.482\,TH \quad 3.9$$

$$A = 1.94 + 0.416\,SHV \quad 3.10$$

$$\rho = 319 + 2.19\,RU \quad 3.11$$

$$D_{24} = 93.9 - 10.5\,TH + 0.410\,TH^2 \quad 3.12$$

$$D_{38} = 55.6 - 0.376\;CV_F + 0.00124\;{CV_F}^2 \quad 3.13$$

Results for accuracies of the fitted models are given in Table 3.4. The first model (Equation 3.3) estimates tree height (*H*) from *DBH*. The subsequent models (Equations 3.4 to 3.13) estimate each of the ground measured attributes. There are two sets of results for each model in

Table 3.4. Results from models fitted after manual correction of the segmentation are indicated by the entry A in the Model fit column. Results for using metrics obtained before correction are indicated with B.

The model to estimate *H* from *DBH* has an R^2 of 0.57 and an RMSE of 0.87 m (7.6%). The model to estimate *H* from the crown metric *TH* has an R^2 of 0.82 and an RMSE of 0.56 m (4.9%). Models to estimate *DBH* and *V* from the crown metric CV_F had similar R^2 values of 0.71 and 0.72 respectively. Normalised RMSE values of 10.2% from the model for *DBH* model and 20.8% from the model for *V* showed there is double the variability in residuals for the latter model.

Quadratic terms were not significant in the models to estimate the tree form and wood quality variables (*S*, *B*, *M*, *A*, and ρ) and were dropped. The resulting linear models had extremely low R^2, explaining less than 7% of the variation in the response variables. Quadratic terms were significant in models to estimate level of Dothistroma infection at ages 24 and 38 months, and the models explained 16% and 27% of the variation respectively.

There was an increase in R^2 for all models fitted using crown metrics derived after manual correction of the image segmentation (model fit A in Table 3.4) compared with metrics from before correction (model fit B). The improvement in R^2 due to manual correction was 2% for *H*, 9% for *DBH*, 8% for *V* and 15% for D_{38}.

Table 3.4. Accuracy of model prediction estimates for the ground measured attributes.

Trait	Units	Equation	Model fit	Adjusted R^2	RMSE	CV(RMSE) %
H	m	3.3	A	0.57	0.87	7.56
			B	0.57	0.85	7.40
H	m	3.4	A	0.82	0.56	4.93
			B	0.80	0.57	5.00
DBH	mm	3.5	A	0.71	18.75	10.23
			B	0.65	20.05	10.88
V	m^3	3.6	A	0.72	0.03	20.81
			B	0.67	0.03	22.19
S	1 to 9	3.7	A	0.07	1.55	25.91
			B	0.06	1.55	25.90
B	1 to 9	3.8	A	0.03	1.61	27.12
			B	0.03	1.62	27.22
M	1 to 9	3.9	A	0.04	2.99	47.88
			B	0.04	2.99	47.93
A	km s^{-1}	3.10	A	0.05	0.38	13.33
			B	0.04	0.38	13.45
ρ	kg m^{-3}	3.11	A	0.01	19.43	5.94
			B	0.01	19.40	5.93
D_{24}	1 to 100	3.12	A	0.16	9.85	29.51
			B	0.15	9.81	29.39
D_{38}	1 to 100	3.13	A	0.27	9.23	26.22
			B	0.23	9.37	26.75

Note: Model fit values of A and B represent the model fitted to values After and Before (resp.) manual correction of the CHM segmentation. RMSE values are in the units of the variable being estimated. CV (RMSE)% values are the RMSE normalised by dividing by the mean value for the corresponding variable and expressed as a percentage to allow comparison among models.

3.4 Discussion

This is the first known example of a study to investigate correlations with a combination of individual tree size, form, quality and disease attributes using metrics derived from ALS data. Analysis has shown that key individual tree size attributes were strongly correlated with crown metrics derived from the ALS data. Moderate correlations between crown metrics and a

measure of Dothistroma infection were also demonstrated, while correlations with tree form and wood quality attributes were poor.

3.4.1 Correlations with tree size

Tree height and diameter are basic measures of tree size widely used in forest inventory and research measurement. Tree height is more difficult to measure on the ground than diameter and is therefore usually measured on a sub-sample in forest inventory and may not always be measured in research trials. Stem volume is a measure of tree size that is operationally and ecologically relevant and is usually estimated from tree height and diameter because direct measurement is prohibitively challenging. Correlations among the three size attributes were relatively high ($0.75<r<0.97$), as expected, and they also had high correlations with a number of the crown metrics being evaluated. These strong correlative relationships were further evidenced by cluster analysis which grouped the three tree size attributes (*H*, *DBH*, and *V*) together with two crown metrics (*TH* and CV_F). Tree height *H* had a strong correlation (r=0.90) with the crown metric *TH* and the fitted model had an R^2 of 0.82. In comparison, a model fitted to estimate *H* from *DBH* had a substantially lower R^2 of 0.57. The normalised RMSEs from models fitted to *H*, *DBH* and *V* (CV(RMSE) = 5%, 10%, and 21% resp.) compared favourably with values reported in the limited existing literature estimating individual tree size attributes. For example Vauhkonen et al. (2010) reported similar errors for *H*, *DBH*, and *V* (CV(RMSE) = 3%, 13%, and 31% resp.), as did Lindberg et al. (2012) (CV(RMSE) = 4%, 15%, and 34% resp.).

It is worth noting that for area-based analysis of ALS, R^2s over 0.9 are routinely obtained for height (Maltamo et al. 2014), but this is for the mean height of trees in a patch, typically of the order of 0.5 ha in size. The lower R^2 obtained for height in this study, using tree-based analysis, is due to the attempt to estimate the heights of individual trees, which are inherently more variable, and subject to more measurement error. The crown metric *TH* represents the maximum height from the CHM segment for the tree. This is effectively the height to the top of the tree, as represented by the CHM (see Figure 2.7). Incident laser pulses may not exactly

intercept the very top of every tree, and each pulse must encounter sufficient material for the reflected energy to trigger registration of a discrete return. Also, the highest discrete return in any CHM pixel may come from a second or subsequent return, dependant on pulse density. The combination of these three factors means that a CHM derived from discrete return ALS data is a raster representation of a surface which lies some distance below the actual upper surface of the canopy at any given location (Khosravipour et al. 2014; Liu and Dong 2014). Notwithstanding this bias, the inherent spatial accuracy of ALS data means a CHM provides useful information about canopy heights. With an accurate delineation of individual trees, a CHM could also provide a useful measure of tree height. Results in this study demonstrated a high correlation between individual tree heights and a CHM crown height metric. A simple univariate model fitted to the crown metric *TH* estimated 82% of the variance in individual tree heights.

The remaining two tree size attributes *DBH* and *V* were highly correlated with each other and were both highly correlated with the crown metric CV_F. Linear models using CV_F predicted just over 70% of the variation in *DBH* and *V*, although normalised RMSE of 21% for *V* was double the value of 10% for *DBH*. Model RMSE and R^2 values for *DBH* and *V* also compared favourably with international results estimating individual tree size attributes (Chen and Zhu 2012; Lindberg et al. 2012; Lo and Lin 2013; Vauhkonen et al. 2010). For example Vauhkonen et al. (2010) fitted models for *V* and *DBH* having CV(RMSE) values of 31% and 13% respectively, while Lindberg et al. (2012) had corresponding values of 34% and 16%.

In the past researchers have found measures of crown size, such as crown diameter and projected area, to be strongly correlated with tree diameter and stem volume (Balenović et al. 2015; Filipescu et al. 2012; Gonzalez-Benecke et al. 2014; Groot et al. 2015; Leech 1984; Madgwick 1994). Such relationships effectively link current crown size with past cumulative stem growth, although Filipescu et al. (2012) has suggested crown size might integrate the effects of past growth conditions. In this study crown metrics representing crown radius (*CR*) and crown area (CA_C) had strong correlations with *DBH* and *V* (*r* values near 0.7) but the strongest correlations were with the crown metric CV_F (*r* values over 0.8). The crown metric

CV_F quantified the enclosed volume between the upper surface of the tree crown and the ground (see Figure 2.7). This metric quantifying crown volume was derived relatively easily from the CHM but would be difficult to estimate from ground measurements, which would explain why relationships with measures of crown volume are not as widely reported as for the more easily measured crown diameter. The crown metric CV_F effectively incorporates crown diameter, accounting for relative tree size, and a measure of tree height, accounting for age-related growth. The crown volume metric was therefore interpreted as including useful additional explanatory information about past growth compared with more widely reported measures of crown size used to estimate tree size.

Relationships between measures of crown and tree size have been found to be stand specific, modified by factors such as species, site, stand age, tree genetics and silviculture (Balenović et al. 2015; Madgwick 1994; Watt and Kirschbaum 2011). One limitation of crown diameter in accounting for tree size is that after canopy closure, crown diameter will remain static, while stem diameter and volume will increase. This could explain the lack of generality of the relationship between crown diameter and stem size at different ages. In this study the crown volume metric CV_F has been shown to explain a large proportion of variation in tree size due to genetics because the trial included a range of genetic material. It will be interesting to test the generality of the crown volume metric over a range of stand conditions.

3.4.2 Correlations with tree form

The tree form attributes *S*, *B* and *M* were most highly correlated with each other, and correlations with crown metrics were low, the highest being r=0.26 for *S*. This was clearly illustrated by cluster analysis which showed these three attributes grouped together in an isolated cluster. The lack of useful correlations with crown metrics was also demonstrated in the inability to fit quadratic terms in the models, and the very low R^2s of the final models. The crown metric *TH*, representing tree height, was the best correlated crown metric for all three form attributes. This correlation indicates that within this trial there was a slight trend for taller trees to have better stem straightness, more branch clusters and a lower incidence of stem

malformations. Those correlations between height and tree form are to be expected, resulting from the long-term focus on tree growth and form in the radiata pine breeding programme (Mead 2013).

3.4.3 Correlations with wood quality

The two wood quality attributes, standing tree acoustic velocity (*A*) and wood basic density (ρ), were most highly correlated with each other, although the correlation was low (r=0.16) and they were also grouped together in an isolated cluster by cluster analysis (Figure 3.1). Tree *A* was most highly correlated with the crown metric *SHV*. Although the correlation was low (r=0.2) it is interesting to note this crown metric is derived as the ratio between *TH* and the cube root of CV_F, effectively a measure of slenderness (height/diameter), which was a key variable in a site level model estimating modulus of elasticity (Watt and Zoric 2010). Despite the appearance of this plausible crown metric, a linear model incorporating *SHV* explained less than 5% of the variation in *A*. Correlations between ρ and crown metrics were even lower than for *A*. The finding that crown metrics were not highly correlated with tree basic density or stiffness also agrees with observations made by Groot et al. (2015), finding no evidence in the international literature of reliable correlations between crown structure and wood density. Rather, they concluded wood density may be determined by mechanical and water conduction requirements.

3.4.4 Correlations with level of needle blight

The degree of Dothistroma infection, expressed as a percentage, was assessed at two prior ages, 24 and 38 months, (D_{24} and D_{38} respectively). There was a moderate correlation between D_{24} and D_{38} (r=0.6), which was expected as Dothistroma infection is known to persist for several years (van der Pas et al. 1984). Cluster analysis confirmed this association and also illustrated moderate negative correlations (r from -0.5 to -0.6) with the tree size attributes *DBH* and *V*. Correlations with tree size and crown metrics were higher for D_{38} than D_{24}. This was interpreted as evidence of a stronger effect of Dothistroma infection on tree size at the later age and further discussion will be limited to D_{38}.

The best correlated crown metric for D_{38} was CV_F (r=-0.5) which was already found to correlate highly with the tree size measures *DBH* and *V*. This is further evidence of the observed negative correlation between D_{38} and tree size. Defoliation due to Dothistroma damage is well known to reduce tree growth (van der Pas et al. 1984) and therefore the negative correlation between CV_F and D_{38} is interpreted as representing reduced tree growth associated with higher levels of Dothistroma infection. A linear model using CV_F explained 27% of the variation in D_{38}. At this early stage of evaluating crown metrics it is not clear to what degree the crown size metric CV_F includes some measure of the effect of defoliation or to what degree the apparent correlation between D_{38} and CV_F is due to the co-variance of *DBH* (or *V*) and D_{38}.

3.4.5 Improvements from manual correction of segmentation

Correlations between crown metrics and tree attributes after manual correction (See Table 3.3) were compared with correlations before correction (not presented). Correlations were found to be improved by manual correction of the image segmentation. For the tree size attributes (with r>0.5) the degree of improvement in r was 1% for *H*, 4% for *DBH* and *V*. Manual correction was found to result in improved correlations for all attributes although the effect was small. This was an important finding, showing only slight benefit from the extra effort of manual correction.

The numbers and locations of trees were known from the trial layout and ground measurement data. Automated matching of trees assessed on the ground and detected in the automated segmentation allowed identification of individual omissions and commissions within the trial. The interpretation of the segmented CHM image needed to correct erroneous crown segments was not onerous and the process largely became a matter of investing the time needed to carry out the corrections. In an experimental application, such as measurement of a trial, the extra time required could be warranted in order to obtain data for all trees and to obtain the best possible crown metrics. For operational forest inventory applications the small improvements demonstrated in this study might not be practical, or worthwhile. However application of the automated methodology in forest stands is likely to experience greater variations in crown

sizes, and the effects of this on detection errors, crown metrics, and correlations requires further study.

3.4.6 Morphological crown metrics

Two principal approaches to creating crown metrics were identified during review of the literature. In the first approach various statistics of the point cloud belonging to each tree are used, similar to the metrics widely used in area-based analysis of ALS data. The second approach identified was the use of measures of crown size and shape, such as crown diameter and volume. The term morphological metrics was applied to geometric measures of the tree crown and it is the use of these metrics that was applied in this study.

The metrics *TH* and CV_F, representing tree height and crown volume respectively, were identified as key morphological crown metrics, suitable for evaluation in future studies. The lack of correlations between wood quality attributes and crown metrics could be considered as evidence against the theories of Larson (1969) relating crown structure to wood quality. The results presented are from a limited study and further research could be applied to develop and evaluate additional metrics which might lead to better correlations with tree form, wood quality and disease attributes.

3.5 Conclusions

A set of crown metrics were derived from ALS data, representing measures of crown morphology, meeting the first objective for this section of the thesis: *"Derive a set of individual crown metrics from raster-based analysis of ALS data in which individual trees have been detected"*. Those metrics were evaluated for correlations with key individual tree attributes, meeting the second objective: *"Quantify correlations between LiDAR crown metrics and ground-based measures of tree size, form, wood quality, and disease expression"*. Results showed high correlations between crown metrics representing tree height (*TH*) and crown volume (CV_F) and the important tree size attributes: *H* (r=0.904), *DBH* (r=0.824), and *V* (r=0.844). Moderate correlations were found between crown metrics and measures of

Dothistroma infection (D_{24} r=-0.390 and D_{38} r=-0.499). Correlations between crown metrics and the tree form and wood quality attributes were very weak (r<0.27).

Investigations were carried out to determine the effect of manual correction on correlations, meeting the third objective: *"Evaluate the effect of errors in tree detection and delineation by comparing estimates of correlations from automatic and manual segmentation of individual trees"*. Results showed that manual correction of the initial segmentation did not substantially increase the strength of correlations.

Demonstration of strong correlations for the height, diameter, and stem volume of individual trees from remotely sensed ALS data is a significant result, providing an affirmative response to the research question "**Can methods be developed to estimate key attributes of individual trees using airborne laser scanning data**". Future effort should be directed to look for opportunities to estimate stem form and wood quality attributes from ALS data, by evaluating a wider range of stand conditions and by development of additional crown metrics.

Chapter 4 Quantifying Sources of Variation in Tree Growth

4.1 Introduction

Observed attributes of trees can be viewed as the expression of the intrinsic genetic program modified by environmental influences. This viewpoint establishes a useful basis for analysis and partitioning of the different factors driving tree size and quality attributes. Knowledge about the key drivers of growth in forest trees can then be integrated into models and decision support tools for use in forest management to grow trees fit for purpose (Dungey et al. 2013; Scion 2014; Telfer et al. 2015). Tree-based analysis of remotely sensed ALS data provides an opportunity to do this at an unprecedented level of detail, creating novel methods supporting the development of precision forestry for the New Zealand forestry sector.

4.1.1 Statistical quantification of sources of variation

Geneticists view variability in tree attributes as being the result of genetic and environmental factors and phenotyping can be described as separating genetic effects from environmental effects and experimental error (Cobb et al. 2013) This is echoed in the analytical approach they take to quantifying variation. Models are constructed to partition variance in observed traits from measurements taken in carefully constructed trials, which can be designed to quantify genetic, within and between site, and silvicultural factors (Burdon et al. 1992; Cullis et al. 2014; Gilmour et al. 1995; Liu et al. 2014). Recently developed methods can apply the considerable computing power necessary to fully take into account the complex incomplete block trial designs, and pedigree information, such as found in the trial to be used in this study (Butler et al. 2009).

The base analytical model partitions phenotypic (observed) variation into genetic and environmental origins, along with unexplained residual variation. Tree breeders and growth modellers typically focus on genetic and environmental (site and silvicultural) effects, respectively (see Figure 2.11). According to trial design and research objectives, the genetic

and environmental factors can be further partitioned to more precisely quantify factors of interest.

It can be easier to measure a trait which is not of direct interest in its own right, but which is correlated with a trait of interest. This could be particularly relevant in the case of using remote sensing to assess traits. Researchers or foresters might have limited interest in metrics such as crown diameter, but this metric would be useful to them if it were to correlate with stem volume for example. From a tree breeder's perspective, selection to improve one attribute also gives improvements in other attributes having strong genetic correlations. Attributes having negative genetic correlations are also of interest, because selection for gains in one attribute will result in losses for the other attribute. Such correlations are also valuable for the insights they can give into functional relationships associated with tree growth.

4.1.2 The potential role of remote sensing

The use of remotely sensed data to phenotype trees offers a number of potential benefits for tree breeders, researchers, and forest managers. It would be useful to develop and evaluate methods to analyse remotely sensed data at the individual tree level, with the ability to separate and quantify genetic and environmental effects. Internationally, crop researchers have identified the need for development of remote sensing, image processing, and analytical methods in order to build the high-throughput, accurate phenotyping systems they desire (Cobb et al. 2013; Dhondt et al. 2013). Tree breeders identified the potential of applying such methods for forestry, and incorporated remote sensing and phenotyping as core elements underpinning a multi-year forestry research programme (Dungey et al. 2013; NZ Forest Owners Association 2012; Scion 2014; Telfer et al. 2015). The use of remotely sensed ALS data, along with methods to detect individual trees, could make it possible to estimate tree attributes, such as individual tree heights (Pont et al. 2015a; Pont et al. 2015b). This could be a useful alternative to the somewhat slow and error-prone conventional methods for height measurement. In addition to providing a tool to measure research trials, the ability to characterise individual trees could be applied in wide scale phenotyping in forest stands. The merit in this approach would

be the ability to assess large numbers of trees across varying environmental conditions. Localised patches showing correlation among traits (such as an area with taller trees) may reveal information about environmental drivers such as soil or micro-site conditions. Individual trees with notable differences to neighbours (a lone tall or disease resistant tree) may indicate a tree of interest for tree breeding. The ability to quantify distributions of key tree attributes may also provide a useful measure of variability in stands or parts of stands.

4.1.3 Using a genetics trial as a case study

A genetics trial is a useful basis for developing and evaluating methods to characterise individual trees using ALS data. Trials with single tree plots generally have a block structure for replication to manage within site variability, and have single trees within the blocks representing individual families. Replication and randomisation of tree locations within blocks are used to minimise effects of tree-to-tree interactions and local site variability. Such trials are also established with trees planted on a highly regular grid to minimise variability in competition effects (Fu 2003).

The regular structure of a trial simplifies the problem of tree detection because tree spacing and crown sizes are relatively regular compared with general forest stand conditions (Williams et al. 1999). This allows a principal focus on development and evaluation of crown metrics, rather than tree detection. The block layout of a trial also simplifies the problem of matching trees detected in the ALS data with the correct ground measurements. In 0 the issue of accurately locating trees on the ground was investigated and it was shown that available GNSS devices are inadequate to determine unambiguous tree locations. This issue was addressed by using GNSS locations of trial boundary pegs to determine initial block boundary locations which were then refined by manual interpretation of ground measurement records and the CHM image for the trial area. Matching of trees was then able to be completed using an automated process.

Use of a genetics trial as a case study has another significant benefit: the trees have known genetic parentage. This provides a controlled basis for partitioning variance using the powerful

methods developed by geneticists (Butler et al. 2009; Gilmour et al. 1995). A genetics trial therefore provides a tightly controlled environment within which to develop and evaluate methods to characterise trees using ALS data. These methods have important application for assessment of genetics trials, by potentially supplementing ground based measurement methods and potentially improving efficiency and reducing costs of measuring genetics trials. There would also be precision forestry applications using such methods, for wide scale phenotyping, research and inventory.

4.1.4 Research objectives

Statistical methods were applied to partition variance components using individual tree crown metrics derived from ALS data, and to evaluate the utility of crown metrics in estimating a number of standard genetic parameters in a genetics trial. Models allowed determination of genetic and environmental variance components, used to estimate heritabilities, genetic correlations, breeding values and selection rankings for several key tree attributes, to meet the first objective: *"Estimate genetic parameters for measures of tree size, form, wood quality, and disease expression using crown metrics and compare these with estimates from ground measurements"*.

The genetic parameters were estimated from metrics based on automatic and from manually corrected tree delineation, in order to meet the second objective "*Evaluate the effect of errors in tree detection and delineation by comparing estimates of genetic parameters from automatic and manual segmentation of individual trees"*. Analyses were also used to gain insights into functional relationships between genetics, environment and tree growth, wood quality and disease. Results were used to address the research question: "**Can methods be developed to estimate variance components of individual trees using airborne laser scanning data to elucidate the genetic and environmental drivers of tree growth**".

4.2 Methods

The statistical tool ASReml-R (Butler et al. 2009; Gilmour et al. 2009; R Core Team 2014) was used to construct mixed-effects models to estimate variance components for a set of tree size, form, wood quality and disease attributes. Estimates were produced using tree-level ground measurements and crown metrics, before and after manual correction of the crown segmentation created by the initial tree detection process. Refer to Chapter 2 for a more detailed description of the materials and methods used, an outline is provided below for convenience.

4.2.1 Ground measurements of trees

The ground measurements of tree size comprised diameter at breast height (*DBH*) and height (*H*), used to estimate total stem volume (*V*). Tree form was assessed with straightness (*S*), malformation (*M*), and branching (*B*) scores described in the Methods chapter. Wood quality measures were represented by basic density (ρ) and standing tree acoustic velocity (*A*), the latter known to correlate strongly with wood stiffness. Tree disease measurements were Dothistroma infection scores at 24 months (D_{24}) and 38 months (D_{38}). Together, those measures represented key attributes of interest to forest managers, as well as the key traits in the current breeding programme, selected to improve wood production (Burdon 2001; Dungey et al. 2009; Jayawickrama and Carson 2000; Mead 2013).

4.2.2 Airborne laser scanning data

A canopy height model (CHM) extracted from ALS data collected over the trial was processed to detect individual trees using a method developed by Pont et al. (2015b). A set of 36 individual tree crown metrics were then derived for each detected tree, refer to section 2.9 for their definitions. The automatic segmentation of tree crowns was corrected manually to remove omission and commission errors, and the crown metrics were derived before and after correction. Correction of omission errors added small crowns that were merged with adjacent crowns, and reduced the size of the crowns they were previously merged with. Correction of commission errors increased the size of crowns where large branches, forks or multiple leaders

had been falsely segmented. Corrections therefore reduced errors in determination of crown size and shape and affected the derived crown metrics. Manual correction enabled comparison of results using metrics from automated and from manually corrected tree detection and delineation.

4.2.3 Analytical model for variance components

Analyses to estimate variance components were carried out using ASReml-R which implements efficient fitting of a general linear mixed model by residual maximum likelihood (Butler et al. 2009). The following general individual tree linear mixed model was used

$$\boldsymbol{y} = \boldsymbol{Xb} + \boldsymbol{Zu} + \boldsymbol{e} \qquad 4.1$$

where $\boldsymbol{y}$ is a vector of individual tree observations of an attribute, $\boldsymbol{b}$ is a vector of fixed effects, $\boldsymbol{u}$ is a vector of random effects, and $\boldsymbol{e}$ is a vector of random residuals. The terms $\boldsymbol{X}$ and $\boldsymbol{Z}$ correspond to design matrices relating the observations in $\boldsymbol{y}$ to the fixed and random effects in $\boldsymbol{b}$ and $\boldsymbol{u}$, respectively (Costa et al. 2004; Dungey et al. 2012).

Fixed terms in vector **b** included the overall means, a factor to represent replication, and a factor to account for control families present in every trial block. Random terms in vector **u** included the additive genetic effects of individual genotypes and the effects of replicates within incomplete blocks. Fixed, additive (random), and residual variances were obtained for further analysis. It is worth noting that single-site estimates of additive genetic variance will usually be overestimated (Cullis et al. 2014). The emphasis in this study is however not the determination of definitive values, but evaluation of the use of crown metrics to derive estimates, and the comparison of automated and corrected data for tree selection accuracy.

4.2.4 Genetic parameters

Variance components obtained from ASReml-R were used to determine a number of standard genetic parameters (Fins et al. 1992). Narrow sense heritability (h^2) was estimated as the

proportion of total phenotypic variance (σ_p^2) attributable to additive genetic effects (σ_a^2) respectively (Equation 7.2).

$$h^2 = \frac{\sigma_a^2}{\sigma_p^2} \qquad 4.2$$

where the phenotypic variance was the sum of the additive and residual variances.

In this trial, like many forest genetics trials, generally only the female parents were known, with limited information for a few of the male parents. There was also information from prior generations, largely on the female side, which altogether created a complex set of partial pedigree information. In the analysis, ASReml-R took into account all available pedigree information to give the best possible estimates of the variance components and heritabilities.

Breeding values were estimated and trees ranked for each attribute. Typical breeding selection practices are to exclude malformed trees and to retain only a single tree per family, in order to avoid inbreeding depression. Selections of the best 100, 30 and 10 trees are typically made for the respective scenarios: forward selection for a next generation; selection for a seed orchard; selection for clonal deployment. In this study, trees were not excluded on the basis of malformation, in order to permit comparable genetic gain results from ground-based selection, where malformation scores were available, and from selection using crown metrics obtained from ALS, where malformation was unknown.

As there were only 96 families in the trial, the 100 tree selection level was represented by selection of a single tree from each family, giving a selection level of 96 trees. Mean breeding values for each attribute in the three selection subpopulations (96, 30 and 10 trees) were determined. Subtraction of the population mean gave a selection differential, the improvement obtained by each selection. A measure of genetic gain (ΔG) was then determined, by expressing the selection differential as a percentage of the appropriate population mean. Genetic gain was determined for all three levels of selection, for each of the ten ground measured attributes,

using three methods of tree assessment: ground measurements, and using crown metrics, before and after correction of tree segmentation. Selections from ground measurements represented standard operational selection methods based on trial measurement. Selections from crown metrics represented the potential use of remotely sensed ALS data for trial measurement, and allowed comparison of estimates using automated and manually corrected tree segmentation.

Genetic correlations were also estimated among the set of ground variables and selected crown metrics. A genetic correlation (r_g) is the estimate of the shared additive genetic variance among two variables, computed in the same manner as Pearson's *r*, but using the additive variance components only, rather than total phenotypic variance, for a pair of attributes *x* and *y*. The additive variance components were obtained from ASReml-R, where $\hat{\sigma}^2_{a_{xy}}$ is the estimate for the additive genetic covariance between the two attributes, and $\hat{\sigma}^2_{a_x}$ and $\hat{\sigma}^2_{a_y}$ are the estimates for additive genetic variances of the two separate attributes (Equation 4.3).

$$r_g = \frac{\hat{\sigma}^2_{a_{xy}}}{\sqrt{\hat{\sigma}^2_{a_x}\hat{\sigma}^2_{a_y}}} \qquad 4.3$$

Clustering was carried out, using the R *hclust* method with the default *complete linkage* method, based on genetic correlation values. Analysis of the results of clustering was used to determine groups of attributes associated in terms of genetic variance (Kaufman and Rousseeuw 2008).

4.3 Results

4.3.1 Variance components and heritabilities

The fixed, additive genetic (random), and residual variance components estimated by ASReml-R were presented as proportions of the total observed phenotypic variance in Figure 4.1. The fixed effects were replicate and control, and the additive genetic effects were estimated from the random effects of replicate and control. The residual variance component included non-

additive genetic variance and unexplained environmental variance. Unexplained residual variance accounted for more than 50% of total variation for all but one variable (ρ). For the ground measured variables, fixed effects accounted for less than 10% of the total variation, and additive genetic variance ranged from 13% to 57%.

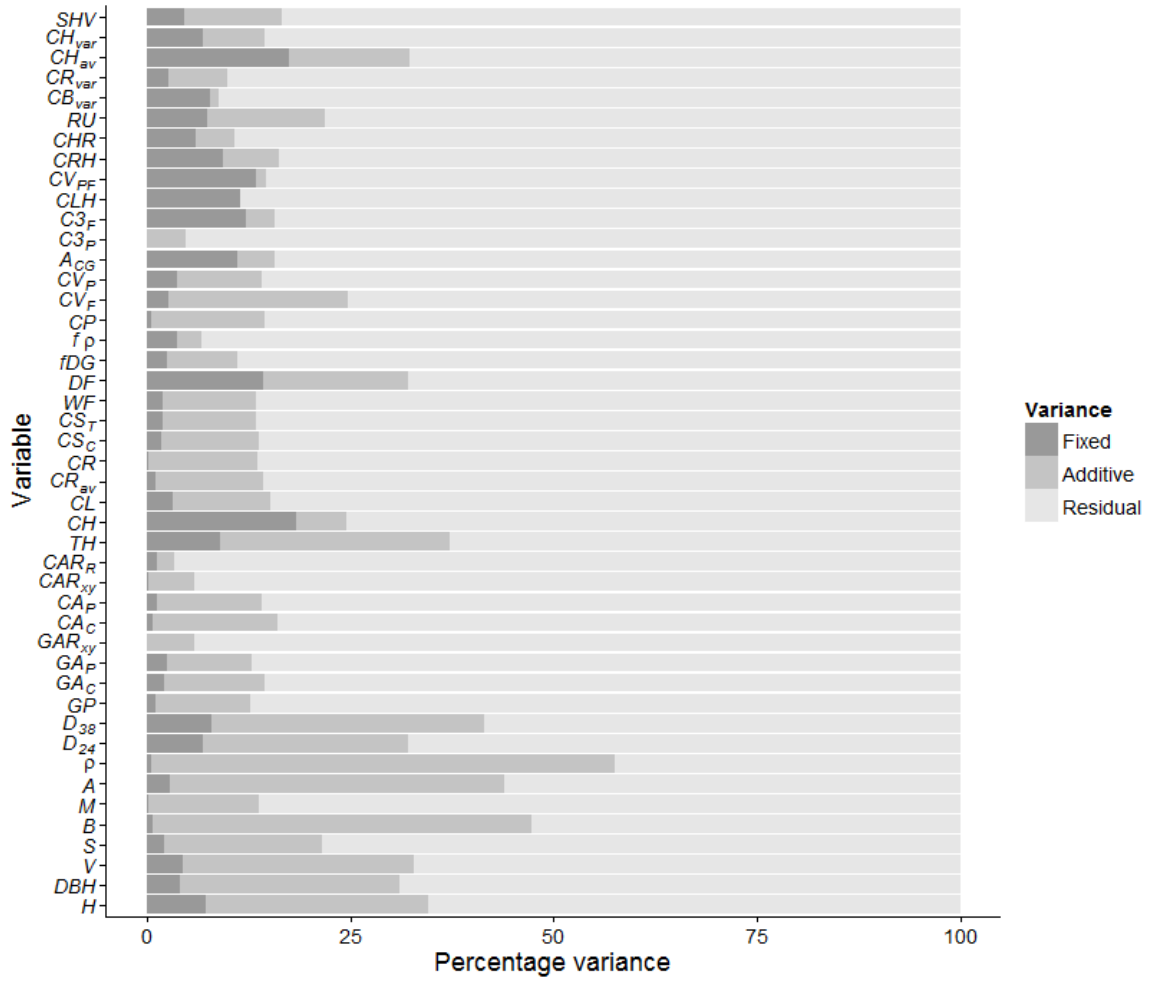

Figure 4.1. Variance components for measured attributes and crown metrics. Fixed, additive (random), and residual variance components as percentages of the total phenotypic variance for all ground measured variables (the lower set of ten items in the chart) and crown metrics (upper items in the chart).

Overall, comparing the ground measured variables and crown metrics in groups (in the lower and upper sections of Figure 4.1 respectively), there were similar levels of variation due to

fixed effects (averaging 4-5%), but variation attributed to additive genetic origin was lower for crown metrics than ground variables (averaging 10% and 30% respectively). A number of crown metrics with a relatively high fixed effects variance component (approaching 10%) and a relatively low additive genetic variance component were also apparent (top of Figure 4.1).

Results showing variance components and narrow-sense heritabilities for the ground measured attributes and selected crown metrics are presented in Table 4.1. Heritabilities for the ground measured attributes were examined and found to agree with typical values for radiata pine (Burdon and Low 1992; Carson et al. 1988; Jayawickrama 2001; Mead 2013; Wilcox 1982).

Table 4.1. Descriptive statistics and genetic parameters for measured attributes and selected crown metrics. The table includes descriptive statistics, variance components, and narrow-sense heritabilities (h^2), with associated standard error (SE), estimated using ASReml-R for ground measured attributes (Source G) and selected crown metrics after and before correction of the crown segmentation (Source A and B respectively).

						Variance					
Variable measured	Units	Source	Mean	SD	COV	Phenotypic	Fixed effects	Additive	Residual	Heritability	SE
H	m	G	11.3	1.44	12.7	1.89	0.149	0.560	1.33	0.295	0.066
DBH	mm	G	181	37.5	20.7	1320	55.8	371	949	0.281	0.064
V	m^3	G	0.131	0.055	41.7	0.003	0.001	0.001	0.002	0.297	0.064
S	1 to 9	G	5.96	1.62	27.1	2.54	0.057	0.506	2.04	0.199	0.052
B	1 to 9	G	5.90	1.65	27.9	2.73	0.019	1.28	1.45	0.470	0.080
M	1 to 9	G	6.21	3.06	49.3	9.36	0.02	1.26	8.10	0.135	0.04
A	$km.s^{-1}$	G	2.86	0.391	13.7	0.147	0.004	0.06	0.085	0.422	0.077
ρ	$kg.m^{-3}$	G	327	19.6	5.98	392	2.24	224	168	0.573	0.087
D_{24}	%	G	33.9	11.3	33.4	109	8.11	29.6	79.7	0.271	0.061
D_{38}	%	G	35.7	11.3	31.8	115	9.88	42.0	73.3	0.365	0.071
TH	m	A	9.05	1.37	15.1	1.66	0.164	0.52	1.15	0.311	0.068
		B	9.09	1.33	14.6	1.56	0.150	0.436	1.12	0.280	0.064
CV_F	m^3	A	75.3	32.1	42.6	982	27.1	222	760	0.226	0.056
		B	76.1	32.3	42.5	1000	16.9	193	810	0.193	0.052
RU	-	A	3.80	0.728	19.1	0.492	0.040	0.077	0.415	0.156	0.048
		B	3.81	0.716	18.8	0.475	0.042	0.077	0.398	0.162	0.049
SHV	-	A	2.21	0.216	9.79	0.043	0.002	0.006	0.038	0.126	0.044
		B	2.21	0.225	10.2	0.048	0.003	0.004	0.044	0.092	0.040

The tree attributes having the highest heritability were the two wood quality attributes and branching (ρ, *A*, and *B*), indicating relatively high genetic control. The attributes with the lowest heritability were the form attributes malformation and straightness (*M* and *S*), which indicated stronger environmental influences for these stem defects.

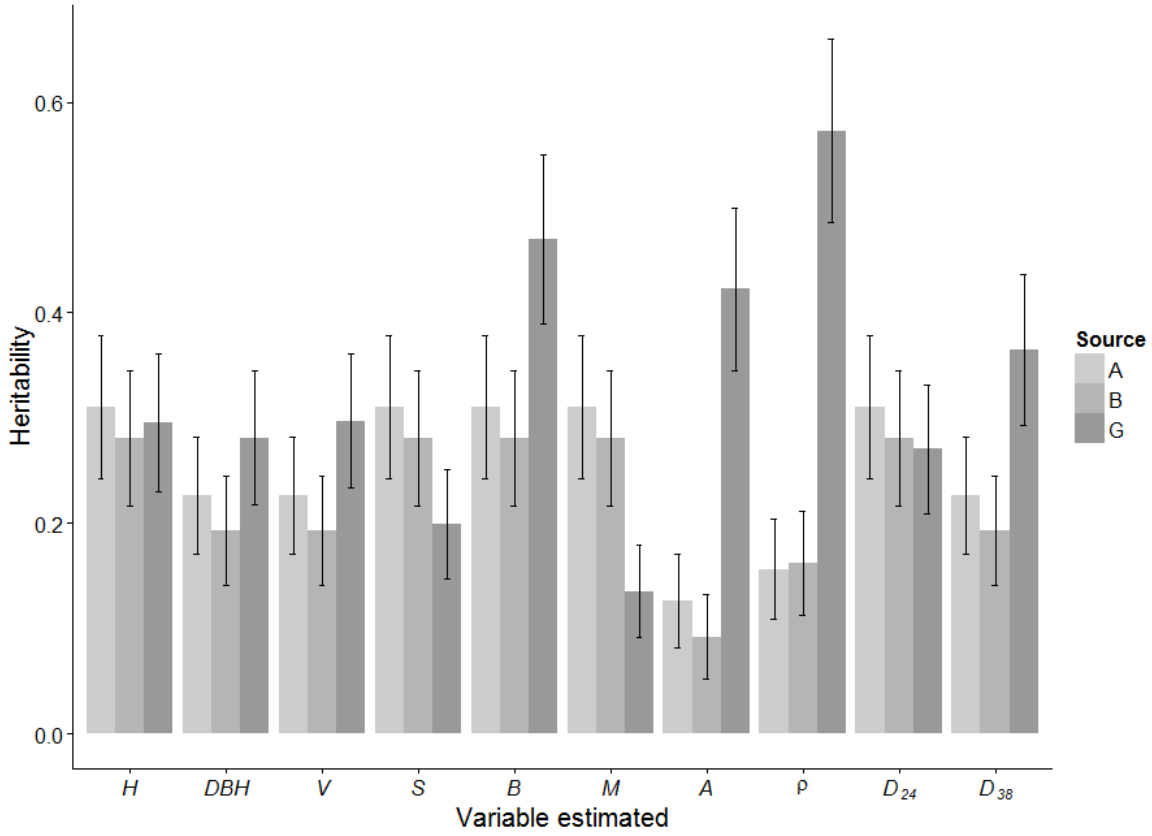

Figure 4.2. Estimated narrow-sense heritabilities (h^2) by variable. Standard errors are indicated with error bars. Estimates were derived from ground measurement (G) and using crown metrics before (B) and after (A) correction of the crown segmentation.

Estimates of h^2 obtained using the best correlated crown metrics from the ALS data, before and after correction of the segmentation, were compared against estimates from ground measurement (see Figure 4.2). Estimates of h^2 derived using crown metrics were within the standard errors of ground based estimates for *H* and D_{24}, just outside the standard errors for *DBH*, *V*, and *S*, and well outside the standard errors for all other variables. Percentage

differences of h^2 estimates from ground and crown measures were 5.0%, -19.5% and -23.9% for *H*, *DBH*, and *V* respectively. Correction of the automated segmentation made only small changes in estimates of h^2, falling well within the standard errors (refer to Figure 4.2), for all variables.

4.3.2 Genetic gains

Genetic gains (ΔG), based on breeding values, were determined for all ten ground measured attributes, using selections of the best 96, 30 and 10 trees, with a limit of one tree per family. Selections were made using ground measurement data, and using the best correlated crown metric, before and after manual correction of the crown segmentation (Figure 4.3).

For all variables and selection levels, the use of a crown metric for selection (A or B in Figure 4.3) resulted in a reduction in ΔG compared with selection based on ground measurement (G in Figure 4.3). The reductions in gain tended to increase with higher selection intensity, implying the effect is generally proportional to the total amount of gain. Reductions in ΔG resulting from use of crown metrics for ranking and selection varied across the different attributes and seemed to be related to the strength of the phenotypic correlations (quantified using Pearson's *r* in the previous chapter) between the respective ground measures and crown metrics. The Pearson's *r* between *H* and *TH* was 0.90 and the reductions in ΔG using an uncorrected segmentation were 19%, 18%, and 27% for the 96, 30, and 10 tree selection levels respectively. The lower *r* observed between *DBH* and CV_F (r=0.8) corresponded with greater reductions in ΔG, ranging from 25% to 35%. The correlation between D_{38} and CV_F was moderate (r=-0.50), and reductions in ΔG were larger, ranging from 25% to 46%. Those results indicate that a minimum Pearson's *r* of 0.8 between a crown metric and an attribute is a requirement for realising genetic gain comparable to that obtained using ground measurement. The effect of manual correction of the crown segmentation on ΔG was minor (compare A and B in Figure 4.3). This finding was consistent with the small effects observed for estimates of variance components and h^2.

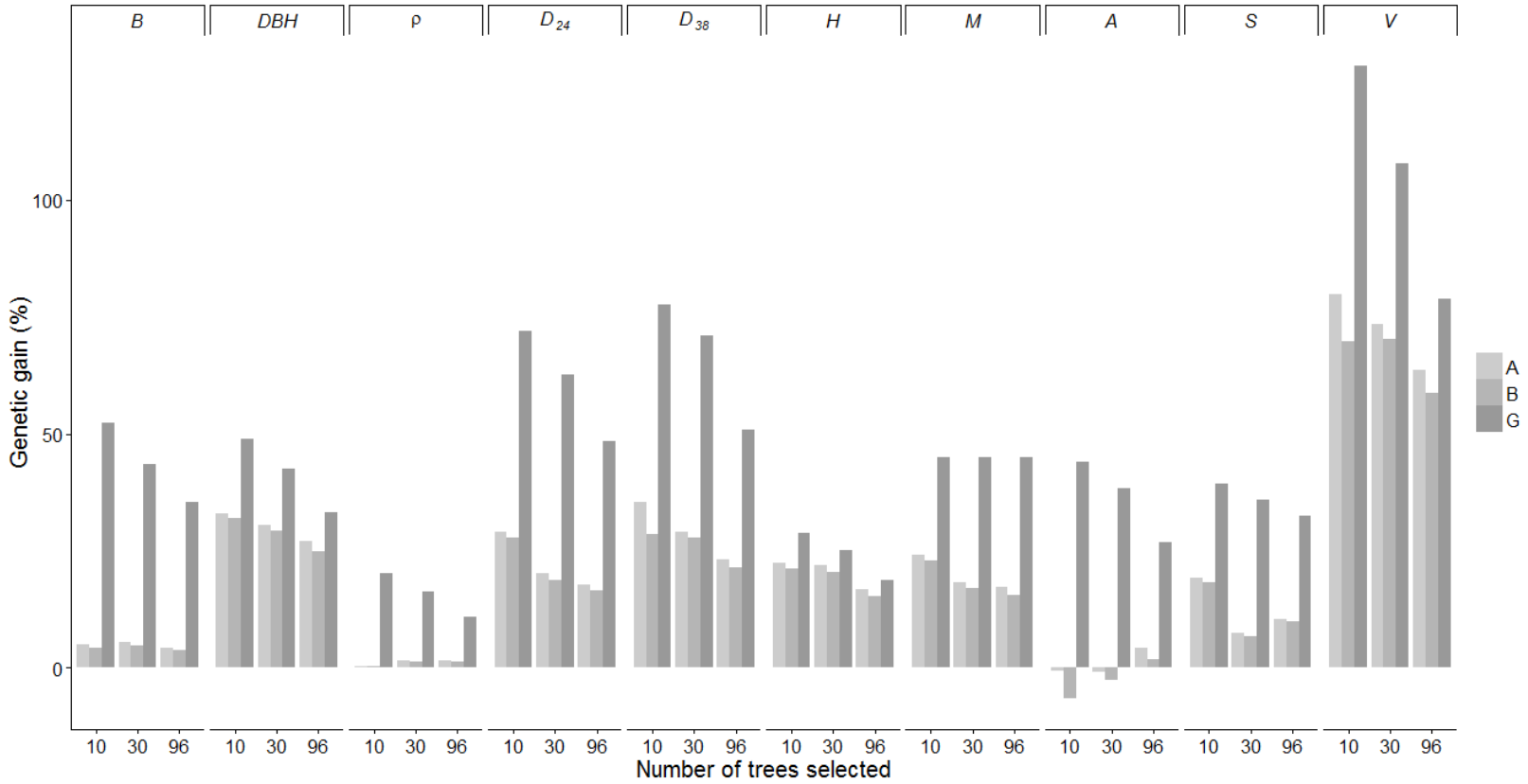
B
DBH
ρ
D24
D38
H
M
A
S
V
Genetic gain (%)
100
50
0
10 30 96
Number of trees selected
A
B
G

Figure 4.3. Percentage genetic gain by variable after selection of the best 96 (all), 30 and 10 trees (one per family). Selections were made using ground measurement (G), and crown metrics before (B) and after (A) correction of the crown segmentation. Negative gains have occurred for *A* from selections using the best crown metric (*SHV*) because of the poor correlation between *A* and *SHV*.

For tree breeders it was of interest to consider how stable tree rankings were when using crown metrics instead of ground measurements. Individual tree and family rankings for the key attributes were examined across the selections made using ground measured data and crown metrics. In general large changes in tree and family rankings were observed when crown metrics rather than ground measures were used to select trees. Changes in family rankings were moderate for *H*, attributed to the strong correlation with the crown metric *TH*. This finding supports the use of ALS to carry out assessment of tree heights for tree selection purposes.

4.3.3 Genetic correlations

Genetic correlations (r_g) among the ground measured attributes and selected crown metrics were estimated using variance and co-variance components estimated in ASReml-R (see Figure 4.4). Examination of correlation values before and after correction of the crown segmentation showed minor changes in r_g, consistent with the small changes observed in the variance components, h^2 and ΔG.

Clustering, based on genetic correlation values, revealed five groups of variables, outlined with a dark line in Figure 4.4. Selection of superior trees on the basis of one attribute would also effectively select for any other attributes having strong genetic correlations. Note that selection for one attribute will result in positive or negative gains on a correlated attribute, dependant on the sign of the correlation. The groups identified were broadly consistent with groups identified using clustering on Pearson's *r* in the previous chapter. The main group, with r_g ranging from 0.7 to 1.0, comprised the tree size variables (*H*, *DBH*, and *V*) and the crown metrics (*TH* and CV_F) they correlated most strongly with, according to Pearson's *r*. The measures of Dothistroma infection (D_{24} and D_{38}) and the tree form variables (*M* and *S*) formed another two strongly correlated groups. Moderate to strong negative correlations between Dothistroma infection and tree size measures were also evident in Figure 4.4. Those groups of variables were not merged because clustering used the signed values of r_g.

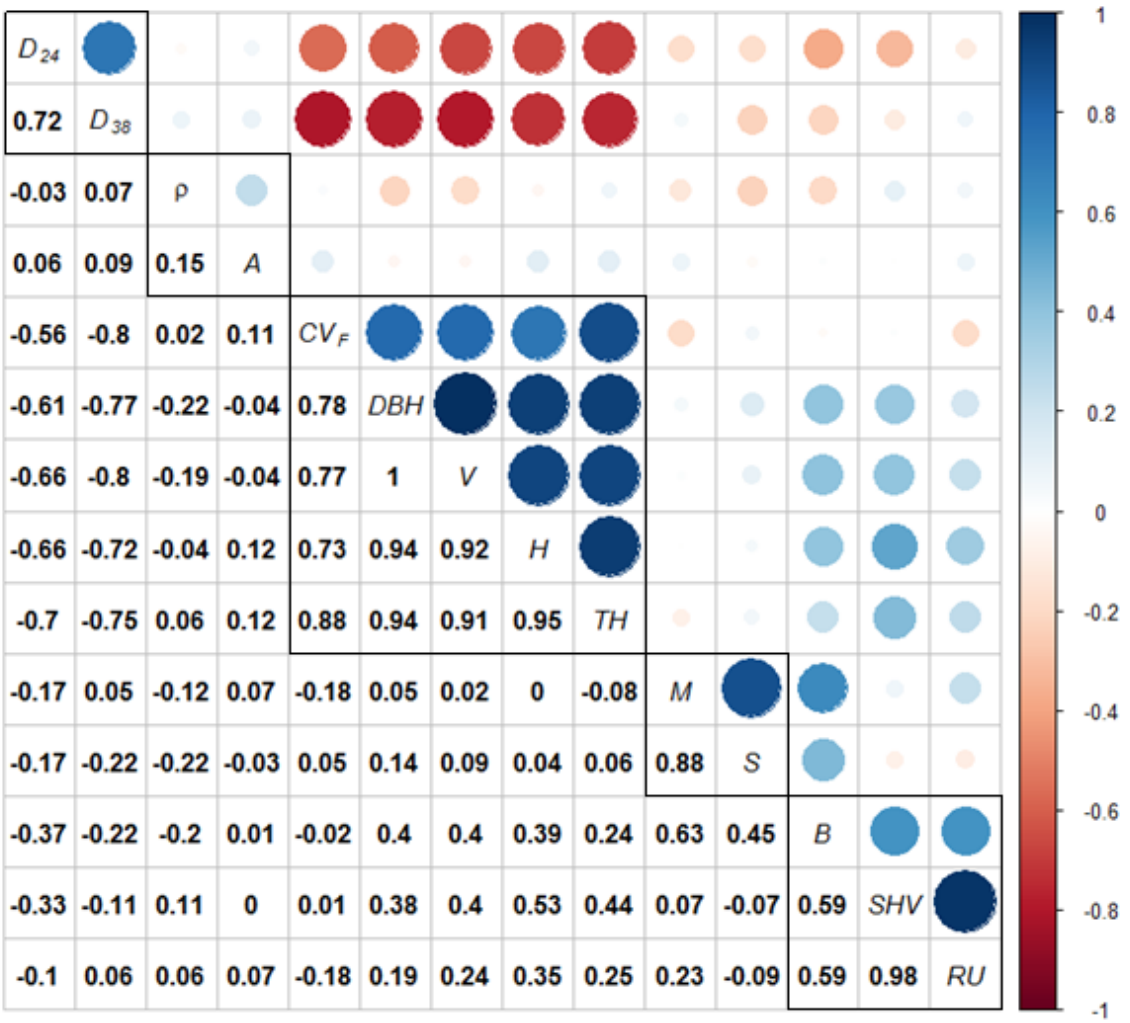

Figure 4.4. Genetic correlations (r_g) among the ground measured attributes and selected crown metrics. Correlation values are shown in the lower left, and indicated with circles in the upper right, where colour and size represent the correlation value. Variables were grouped using the R *hclust* method with the default *complete linkage* method based on the genetic correlation. The five groups from clustering are outlined with bold squares.

The strong positive r_g of 0.88 observed between malformation (*M*) and straightness (*S*) scores indicated a strong positive relationship among these two measures of stem defects. This indicates selection for one of these attributes would also realise gains in the other attribute. The moderate positive r_g of 0.59 between branching score (*B*) and crown slenderness (*SHV*), indicated a genetic correlation between slender crowns and light uniform branching. There was also evidence of moderate to weak correlations among *B*, *SHV* and tree size attributes. It is

interesting to note the Pearson's correlations between *M* and *S* and between *B* and *SHV*, 0.29 and 0.02 respectively (Chapter 3, Table 3.2 and Table 3.3), were much weaker than the genetic correlations. This indicated that stronger underlying genetic correlations are masked by environmental noise when observing overall phenotypic correlations.

The r_g values among *B* and the other two form variables (*S* and *M*) were slightly weaker than the r_g values among the two crown metrics (*SHV* and *RU*) with which it was clustered. The two wood quality attributes (ρ and *A*) were grouped into an isolated, weakly correlated group.

4.4 Discussion

In this study the utility of crown metrics for estimating variance components and genetic parameters was evaluated for measures of tree size, stem form, wood quality and disease expression, representing major attributes of interest in tree breeding and forest management. This represents the first time such methods have been used in the analysis of individual tree data from ALS. Sensitivity to the accuracy of crown segmentation was also evaluated using crown metrics produced using automated and manually corrected segmentation. The statistical software ASReml-R was used to estimate variance components and genetic parameters, from ground measurements and using crown metrics derived from remotely sensed ALS data before and after manual correction.

4.4.1 Estimation of genetic parameters

4.4.1.1 Tree size

The crown metrics *TH* and CV_F were found to have strong genetic (r_g) correlations with the tree size attributes *H*, *DBH*, and *V*, in addition to the strong phenotypic (*r*) correlations shown in the previous chapter. Those strong underlying correlations are known to have contributed to the success of the long term selection of trees for improved growth in terms of *H*, *DBH*, and *V*, over the last 60 years of tree breeding in New Zealand (Dungey et al. 2009; Kimberley et al. 2015b; Mead 2013).

Crown metrics were found to provide operationally useful estimates of heritability for *H* and D_{24} and to show potential for *DBH*, *V*, and *S*. Reduced genetic gains were realised when selecting superior trees on the basis of crown metrics. However the relatively small reductions in gains evident for *H* and *DBH* were low enough to support the use of remotely sensed crown metrics in selection of trees of superior height, and possibly for diameter growth. The ability to estimate tree size attributes from ALS crown metrics agrees with international studies (Lindberg et al. 2012; Vauhkonen et al. 2010), but this is the first study to evaluate an application in forest genetics. Tree size attributes have historically been the principal focus of tree breeding programmes in New Zealand (Dungey et al. 2009), therefore the ability to estimate these attributes and their genetic parameters from ALS data is an important outcome, with applications for tree breeding, forest research and forest management.

4.4.1.2 Tree form and wood quality

Estimates of h^2 obtained using crown metrics for tree form and wood quality attributes were poor except for straightness (*S*), which had the highest Pearson's *r* value among this set of attributes. Genetic gains in form and quality realised by selection using crown metrics instead of ground measurements were greatly reduced. This was interpreted as a result of poor correlations with the crown metrics used, and the low phenotypic variability available for selection. Tree form attributes have always been an important aspect of the radiata pine tree breeding program, and more recently wood quality attributes have also been recognised due to their importance to log and product performance (Dungey et al. 2009; Dungey et al. 2006; Jayawickrama and Carson 2000; Kennedy et al. 2014). It would be highly desirable to reliably estimate the genetic parameters for tree form and wood quality attributes from ALS data, as they are difficult and costly to assess using conventional ground-based methods. Measurements of the tree form attributes rely on subjective visual assessment, and the wood quality attributes require specialised equipment and methods. However the morphological crown metrics evaluated in this study were found to be unsuitable for estimation of these important attributes within genetics trials.

4.4.1.3 Dothistroma infection

Possible genetic gains by selection for reduced Dothistroma infection as assessed with ground measurement were found to be relatively high, ranging from 50% to 80% depending on selection level, and were slightly higher when assessed at age 38 months (D_{38}). However more than half of that gain was lost when trees were selected using correlated crown metrics, the resultant gain falling to range from 17% to 29%. Such large reductions in gains for this important attribute are unacceptable for the use of crown metrics in selecting trees from genetics trials for disease resistance. It must be noted that there was a delay of at least two years between the latest Dothistroma assessment (D_{38}) and the collection of the ALS data used to derive crown metrics. This delay may have weakened correlations and it could be useful to further evaluate the utility of crown metrics for estimating Dothistroma infection in future research.

4.4.2 The effects of segmentation accuracy

An initial automated segmentation of the tree crowns within the trial was found to have a number of omission and commission errors. Manual correction of those errors resulted in changes to the size and shape of the segmented crowns, affecting crown metrics for the corrected crowns. Corrections added small crowns (omissions), reduced the size of some large crowns (omissions), and increased the size of some large crowns (commissions). It was thought tree detection errors could affect the relationships between crown metrics and measured attributes and therefore affect estimates of genetic parameters. Because these changes occurred at the extremes of crown size they were also thought likely to affect selection of superior trees for genetic gains (Fins et al. 1992). Results have shown correction of the crown segmentation has had negligible effect on estimates of the key genetic parameters: h^2, r_g and ΔG. It is therefore concluded that in applications of the methodology, the extra effort of carrying out manual correction of the initial automated segmentation would not be warranted, unless the resulting small gains in estimates were critical.

4.4.3 Understanding the drivers of tree growth

This study represented a novel approach to the investigation of individual tree crown (ITC) methods for forestry applications, and a novel application to genetic analyses. The use of data from a genetics trial, coupled with the use of analytical techniques to segregate environmental and genetic variance components, provided useful insights into the drivers of tree growth. Partitioning of variance using an individual tree mixed effects model has allowed quantification of fixed effects (in the trial design), additive genetic, and residual variance components (Costa et al. 2004; Fu 2003; Gilmour et al. 1997). This approach revealed that the crown metrics evaluated in this study, which were predominantly measures of crown morphology (such as height, diameter, volume, and slenderness), accounted for less additive genetic variance than was observed from ground measurement of the attributes of interest. This could be attributed to error in the ability to estimate tree attributes using crown metrics, supported by the observation that the best estimates of genetic parameters were obtained using crown metrics having stronger correlations with the attributes. However some of the error in the relationships is likely to have come from variation due to environmental influences. Spatial variation can occur within the trial due to localised changes in site conditions such as soils, topography and competition effects among trees (Gilmour et al. 1997; Liu et al. 2014; Zas 2006). Such variation could be investigated in future work by including spatial terms in the REML models.

4.4.3.1 Tree size

An important finding of this study was the identification of strong relationships between crown size metrics and ground measurements of tree size. Other researchers have found useful relationships between measures of crown size and tree size, but usually in inventory or forest settings rather than research trials (Chen et al. 2007; Chen and Zhu 2012; Lindberg et al. 2012; Lo and Lin 2013). Several researchers also evaluated additional, non-morphological, crown metrics with less success in estimating tree size (Chen et al. 2007; Lindberg et al. 2013; Yu et al. 2011). The results of this study, when considered in the context of the earlier work by others, supports the conclusion that morphological crown metrics provide useful correlations

with tree size attributes, due to underlying allometric relationships (Filipescu et al. 2012; Groot et al. 2015; Madgwick 1994). Such relationships can have important applications in assessment of research trials, for tree growth and breeding, and in assessment of forest stands for management applications. This potential to use remote sensing could offer considerable cost savings and open up opportunities for new approaches to phenotyping forest trees.

4.4.3.2 Dothistroma infection

The moderate to strong negative correlations observed between crown size metrics and the measures of Dothistroma infection at a young age (r = -0.8 at 38 months) were noted earlier (Chapter 3) and agree with findings of Kennedy et al. (2014). Results from the current chapter re-confirm the interpretation that these correlations are the result of reduced tree growth due to Dothistroma infection (van der Pas et al. 1984; Watt et al. 2011; Wilcox 1982). The implication is that the reduced tree growth, evident in tree *DBH* and *V*, is echoed in reduced crown volume (CV_F). This is the first known observation of this effect through the use of crown metrics derived from remote sensing.

While the correlation between crown volume and Dothistroma infection is not strong enough for operational use in tree selection for breeding, there may be utility in being able to quantify the effects of Dothistroma and other diseases on tree growth, through the use of crown metrics. Growth losses due to the effects of disease are an important issue in New Zealand, and internationally, and remote sensing can play an important role in detection and quantification of loss (Coops et al. 2014; Dungey et al. 2009; Kantola et al. 2013; Mead 2013). Reduction in growth could be evaluated through differences in crown metrics between areas with and without the disease, and candidate areas affected by disease might be detected by observing reduced growth (van der Pas 1981; Watt et al. 2011). Spatial analysis of areas with known levels of infection could also be used to identify site conditions prone to Dothistroma, such as moist areas in gullies, (Watt et al. 2011; Wilcox 1982). Such an approach could be developed in genetics trials or in general forest stands, using crown metrics from ALS as a tool to map and characterise areas related to Dothistroma infection. This methodology might even be extended

to characterise susceptible areas for other diseases of economic importance (Coops et al. 2014; Kantola et al. 2013; Wallace et al. 2012; Watt et al. 2011).

4.4.3.3 Wood quality

Partitioning of variance from ground measurements showed the wood quality variables to have high additive genetic variance components, high heritabilities, and low overall variability. These attributes therefore appeared to be under relatively stronger genetic control. Correlations, both r and r_g, were notably absent between the wood quality variables and crown metrics. It was already noted the crown metrics evaluated in this study represent crown morphology. The lack of correlation between the wood quality attributes and crown metrics indicated that wood quality is not related to crown morphology at the level of individual trees, a finding also made by Lenz et al. (2012). This finding was evidence against the theories of Larson which suggested that crown morphology (specifically crown size and proximity to crown) determined stem wood basic density and ring width (Groot 2014; Larson 1962, 1963, 1969; Pont 2003). The crown metric most strongly correlated with tree stiffness (*A)* was a measure of crown slenderness, a relationship that has been observed in other research and interpreted as possibly representing a mechanical influence on wood stiffness (Dean 2004; Dean et al. 2013; Groot et al. 2015; Waghorn et al. 2007; Watt and Zoric 2010). However the correlation observed between *A* and crown slenderness in this study was weak. This study was restricted to a single genetics trial, where the environmental effects were minimised and the range of crown morphology was small. In a pilot study in radiata pine stands crown area was found to be strongly negatively correlated with stiffness (*A*), reflecting variations in stand density within and among stands (Pont et al. 2012b). In recent studies for radiata pine in New Zealand it was shown that both stand density and seedlot affected *A*, microfibril angle, modulus of elasticity, and wood density (Carson et al. 2014; Moore et al. 2015). Another recent study of New Zealand radiata pine showed ring width, attributable to stand and tree-level competition effects, and site had a significant negative correlation with wood density (Kimberley et al. 2015a). Further studies with a wider range of crown morphology, as examined by other researchers, are suggested to look for evidence of relationships between crown morphology and wood

properties for forest management applications (Dean et al. 2013; Fournier et al. 2013; Lenz et al. 2012; Swetnam and Falk 2014).

4.4.3.4 Tree form

Strong genetic correlations were observed among the form attributes, indicating a tendency for trees to exhibit multiple form defects. The branching frequency score (*B*) was found to have a strong additive genetic variance component, interpreted as stronger genetic control of this attribute, at a level comparable to the wood quality attributes. Tree form measures were poorly correlated with crown morphology, and there was little evidence in the literature on the use of ALS data for estimating tree form. In a study of Canadian conifer species, measures of crown size obtained from the ground were used with stand metrics to estimate maximum branch size, and the potential use of ALS data to derive crown metrics was noted (Groot and Schneider 2011). However in the New Zealand tree breeding program the desired branching characteristic is uniform light branching and maximum branch size is not a useful indicator for this (Dungey et al. 2009). In a study of boreal forest in Sweden, individual tree metrics from ALS were combined with harvester data in models to successfully estimate log products, but not to explicitly estimate stem form characteristics (Barth et al. 2014). As a result it is concluded that ground-based measurements which more directly observe stem and branching characteristics are required to characterise tree form, particularly in the valuable lower logs. LiDAR could still play an important role, in the form of vehicle-mounted or hand-held scanners that can measure stem shape and branching (Kaartinen et al. 2015; Kankare et al. 2014; Pont and Lorraine 2015).

4.4.3.5 Correlations among crown metrics and measured tree attributes

A number of tree attributes were most strongly correlated with the *TH* and *CVF* crown metrics (see Chapter 3, Table 3.3) supporting widely recognised allometric relationships among tree size, crown configuration, stand density and site characteristics for forest trees (Allouis et al. 2013; Enquist et al. 2009; Filipescu et al. 2012; Groot et al. 2015; Groot and Schneider 2011; Kempes et al. 2011). An implication of the observed correlations was that selection of trees of

superior size using either of these crown metrics would result in concomitant improvements in the other correlated attributes. Selection at the 96 tree level on the crown metric *TH*, using an uncorrected segmentation, gave ΔG of 15% in *H* and also gave associated gains for *S* (10%), *B* (4%), *M* (16%) and D_{24} (17%). Selection under the same conditions using the crown metric *CVF* gave ΔG of 25% for *DBH*, with associated gains in *V* (59%), and D_{38} (21%). This was an important finding for tree breeders, as it confirmed that general genetic correlations they would expect from ground based selection will also be realised using crown metrics from ALS data (Dungey et al. 2009; Kennedy et al. 2013; Kennedy et al. 2014). This observation lends confidence in the use of remotely sensed data for phenotyping applications such as tree breeding and forest management (Scion 2014).

4.5 Conclusions

This is the first known study to utilise individual tree crown metrics from remotely sensed ALS data to quantify variance components in order to better understand genetic and environmental factors affecting tree growth. The tree measures studied covered the range of attributes important to forest managers and tree breeders, comprising: growth, form, wood quality and disease expression, thereby meeting the first objective *"Estimate genetic parameters for measures of tree size, form, wood quality, and disease expression using crown metrics and compare these with estimates from ground measurements"*. The first known evaluation of the effects of tree segmentation accuracy on estimates of tree attributes from crown metrics in a genetics trial was also carried out, meeting the second objective *"Evaluate the effect of errors in tree detection and delineation by comparing estimates of genetic parameters from automatic and manual segmentation of individual trees"*.

Results showed the ability to accurately estimate genetic parameters for the tree size attributes *H*, *DBH*, and marginally for *V*. Estimates of genetic parameters for the tree form, wood quality, and disease expression attributes were generally poor, the best estimates, with moderate error, were for the tree form measure *S*.

The considerable investments in establishing and maintaining trials, in propagation of selected superior trees, and the long rotation of forest trees before gains are realised make every ounce of genetic gain precious (Dungey et al. 2009; Mead 2013). Results showed the losses in genetic gain incurred when selecting superior trees using crown metrics are acceptable to tree breeders in operational tree selection applications for the tree size attributes only.

Genetic parameters estimated from metrics based on manually corrected tree delineation showed negligible improvement over those from an automated delineation. This is seen as an important finding for operational uses of the methodology, because the extra effort of manual correction could be avoided. This study demonstrated that, for the methodology evaluated, the main determinant of accuracy in estimates of genetic parameters was the strength of correlations between crown metrics and tree attributes, rather than the accuracy of tree detection. A minimum Pearson's r of 0.8 between crown metrics and tree attributes was indicated as a threshold for obtaining operationally useful estimates of genetic gain, which provides a benchmark for future development of crown metrics.

Opportunities for future research were identified. Strong correlations between crown metrics and the tree size attributes were interpreted as having a sound allometric basis, with potential for general applications in forest trial and stand conditions that should be further evaluated. Correlations were also observed among tree size, crown size and disease expression which could offer opportunities for detection, and quantification of disease expression, and for identifying disease prone site conditions. Genetic and phenotypic correlations among branching, crown slenderness and tree size were also observed, indication potential for better understanding relationships between environment and genetic effects on tree growth. Given the importance of tree form, wood quality and disease expression to researchers, tree breeders and forest managers, further research into crown metrics to estimate these attributes will be worthwhile.

This study has established a novel and useful methodological approach to the tree-based analysis of remotely sensed ALS data. It has revealed useful insights into relationships between

genetics, environment, and tree growth and supports an affirmative answer to the research question: "**Can methods be developed to estimate variance components of individual trees using airborne laser scanning data to elucidate the genetic and environmental drivers of tree growth**". The methods developed can provide useful tools for precision forestry, with broad applicability in analysis of research trials and management of forest stands, and warrant future development.

Chapter 5 The Effects of Laser Pulse Density on Tree-based Analyses of ALS

5.1 Introduction

Analysis of discrete return LiDAR is now being widely used to characterise forests for management purposes around the world (Maltamo et al. 2014; Næsset 2004; Næsset et al. 2004). This is due to the ability to accurately and cost effectively estimate important forest measures such as mean height, volume, biomass and basal area. Pulse density is an important measure of the resolution of LiDAR data and the cost of obtaining increased pulse density must be balanced against the accuracy and precision desired.

5.1.1 Measures of LiDAR resolution

Factors affecting pulse density are scanner pulse rate, altitude, and aircraft speed (Gatziolis and Andersen 2008; Wehr and Lohr 1999). Pulse rate and altitude affect the spacing of pulses within each scan line, while aircraft speed principally affects spacing of pulses along the flight line. Discrete return LiDAR scanners in current use for forestry applications typically provide up to four returns (points) per outgoing pulse (Gatziolis and Andersen 2008; Wulder et al. 2012). The number of returns observed largely depends on the nature of the target. Paved surfaces, buildings and flat ground will provide one return, while vegetation can be penetrated by the laser pulse to record multiple returns, depending on the depth and density of vegetation, and number of returns supported by the hardware system. Point density, the number of points (or returns) per unit ground area, is therefore a more variable measure of resolution than pulse density, and is highly dependent on the nature of the target. Both pulse and point density are terms seen in the literature, and it is important to distinguish which is being referred to. While it is the points that are analysed, pulse density is a useful measure as it allows comparisons across vegetation types and can be used in specifications for LiDAR capture (Ferraz et al. 2015).

Another measure of LiDAR resolution is pulse spacing (*S*), derived as the inverse square root of pulse density (*D*):

$$S = \frac{1}{\sqrt{D}} \qquad 5.1$$

Pulse spacing expresses the mean spacing between pulses on the ground plane, following the inverse-square law formulated by Sir Isaac Newton, which describes the dilution of energy in three-dimensional space, stated as: "the intensity of radiation emitted by a point source is inversely proportional to the square of the distance from that source" (Waff 1976). By considering only last (or first if only one return) returns, pulse spacing can be determined from LiDAR point data, providing a measure that is independent of vegetation characteristics, like pulse density.

5.1.2 Area-based analysis of LiDAR

A number of researchers have investigated the effect of pulse density on estimates of forest variables obtained from area-based analyses of LiDAR (Gobakken and Næsset 2008; Hansen et al. 2015; Jakubowski et al. 2013a; Magnusson et al. 2007; Watt et al. 2013a). In a mixed conifer forest, accuracies of estimates for a number of commonly assessed forest variables, including height, diameter and basal area, were relatively unaffected above pulse densities of 1 $Pu.m^{-2}$ (Jakubowski et al. 2013a). In a study on the effects of reduced pulse density on precision of total stem volume estimates from area-based analysis of LiDAR for New Zealand planted forests (94% *Pinus radiata*), it was found there was little effect of thinning pulse densities down to 1 $Pu.m^{-2}$, but a significant decline in precision following pulse density below 0.1 $Pu.m^{-2}$ (Watt et al. 2013a). In a study of high density Douglas-fir stands in New Zealand, precision declined rapidly at pulse densities below 1 $Pu.m^{-2}$ (Watt et al. 2014). It was also noted that the number of pulses per plot integrated the effects of plot size and pulse density, with precision falling markedly below a threshold value of 100 pulses per plot. In a study of tropical forest, reliable estimates of common metrics were found at pulse densities above 0.5 $Pu.m^{-2}$, with a plot size of 0.7 ha, indicating a threshold of 350 pulses per plot for this more complex forest

type (Hansen et al. 2015). These results from a range of forest types indicate reliable estimates from area-based analyses generally require pulse densities greater than 0.1 to 1 $Pu.m^{-2}$.

5.1.3 Tree-based analysis of LiDAR

Tree-based analysis of LiDAR is a widely researched approach to the assessment of forest trees (Hyyppä and Inkinen 2002; Kaartinen et al. 2012; Larsen et al. 2011; Persson et al. 2002). Tree-based analysis of LiDAR requires accurate detection, delineation and characterisation of individual trees (Holmgren and Lindberg 2014; Ke et al. 2010; Wang et al. 2016; Zhen et al. 2015). There is general agreement that tree-based analysis of LiDAR requires higher density LiDAR compared to area-based analysis, with a minimum of 4 returns m^{-2} being stated by Gatziolis and Andersen (2008), and a minimum of 5 $Pu.m^{-2}$ mentioned by Vauhkonen et al. (2008).

There have been few studies that have investigated the effects of pulse density on tree-based analyses of LiDAR. In a study of different forest types in southern Sweden using ALS data at two pulse densities (approximately 5 and 2.5 $Pu.m^{-2}$), and at range of beam footprint sizes (from 0.26 to 3.68 m), tree detection and estimates of tree height, diameter and volume were evaluated (Persson et al. 2002). Better tree detection was observed for the forest type with more trees per unit area, and a smaller laser footprint size, but estimates of tree height and crown diameter were not strongly affected by footprint size or the two evaluated pulse densities.

In a study on boreal forest, the effects of reducing point density on a number of crown metrics were examined, although this was based on tree detection carried out with the highest point density (Vauhkonen et al. 2008). Crown metrics based on alpha shapes were much more sensitive to reductions in point density than metrics based on maximum height, crown area, height and intensity distributions, and CHM texture. It was concluded 3 $Pu.m^{-2}$ were required to obtain reliable species classification and estimation of tree DBH.

In a recent study, a comparison was made of five tree detection methods in forest types including sub-dominant and suppressed trees (Wang et al. 2016). Detection methods were described as raster-based, point-based, and hybrid (utilising raster and point analysis). The two point-based methods were found to detect a much greater proportion of sub-dominant trees. The two point-based methods were evaluated at three point densities (8, 4, and 2 points m^{-2}). It was concluded that 2 points m^{-2} could be adequate for detecting dominant trees only, while at 8 points m^{-2} approximately one third of supressed trees were detected by the best method.

Another recent study estimated crown dimensions of olive trees from LiDAR at three point densities (0.5, 3.5, and 9 points m^{-2}) using raster and point-based approaches (Hadaś and Estornell 2016). Results showed improved accuracies at higher density, and the point-based approach performed slightly better at the higher density, while the raster-based approach was insensitive to point density.

Prior research has evaluated the sensitivity of area-based analysis to LiDAR resolution and has indicated pulse densities in the range of 1 to 0.1 $Pu.m^{-2}$ to ensure reliable estimates of mean height, volume and basal area. There is a lack of corresponding research into the effects of pulse density on tree-based analysis of LiDAR. The limited research to date has evaluated only a narrow range of LiDAR resolutions and has not evaluated tree detection and subsequent derivation of crown metrics together, for forest trees.

5.1.4 Research objectives

In this chapter the effects of reducing LiDAR resolution on tree detection, correlations between crown metrics and ground measures, and estimation of heritabilities and genetic gains were evaluated. The approach used was to artificially thin LiDAR data to simulate data capture at a range of lower pulse densities and to evaluate the effects on results of subsequent processing and analysis of the LiDAR. Investigations into the effects of pulse thinning were aimed to meet three objectives: *"Quantify the effect of reducing pulse densities on the accuracy of tree detection"*, "*Quantify the effect of reducing pulse densities on correlations between crown*

metrics and ground measurements of key tree attributes", and *"Quantify the effect of reducing pulse densities on estimates of heritabilities and genetic gains"*. Results can be used to inform decisions about pulse densities specified for LiDAR data capture to be used for tree-based analyses, addressing the overall research question "**What is the effect of varying pulse density on the accuracy of estimates obtained from the analysis of discrete return LiDAR?"**.

5.2 Methods

5.2.1 Pulse thinning

In order to evaluate the effects of reduced LiDAR resolution, LiDAR point clouds at a range of pulse densities were created by artificially thinning the initial data set. There are a number of approaches to artificially reducing the resolution of discrete return LiDAR. None of these approaches produce point clouds exactly equivalent to those that would be obtained by collecting data at the equivalent pulse density (Jakubowski et al. 2013a; Vauhkonen et al. 2008). The removal of selected pulses, with all of their associated returns, is preferable to removing individual points as this more closely mimics real world conditions.

In this study, pulse thinning was carried out so as to leave pulses at regular time intervals. The first step was to sort the LiDAR file by the GPS time field using the *LAStools* (version 160329 rapidlasso GmbH, http://rapidlasso.com/LAStools) tool *lassort* to ensure returns occur in the file in acquisition order. Next the median time separation of returns in the original LiDAR file was determined by examining the output of the *LAStools* tool *las2txt* with the *–parse rnt#* option, which outputs return number (*r*), number of returns for the pulse (*n*), timestamp (*t*), and time difference from the prior return (*#*). The median time separation between returns in the original LiDAR file was 6.0 µs. The average pulse and point densities were 6.09 $Pu.m^{-2}$ and 15.68 points m^{-2} respectively, determined using *LAStools lasinfo*.

Pulse thinning was then carried out using the *LAStools* tool *las2las* with the *-thin_with_time* option, which retained the first occurrence of a particular time stamp within a user-specified

time interval. LiDAR files, thinned to different time separations, were created to cover a range of pulse densities. A set of 2 µs time steps were used to cover the range from 6 to 2 $Pu.m^{-2}$, and below this, steps doubling the prior time separation were used to extend the range down to 0.3 $Pu.m^{-2}$. Characteristics of the 11 LiDAR files created are presented in Table 5.1.

Table 5.1. Resolution characteristics of the thinned LiDAR data.

Test	Subsample µs	Pulse density ($Pu.m^{-2}$)	Pulse spacing (m)	Point density (Points m^{-2})	Point spacing (m)
1	6*	6.09	0.41	15.68	0.25
2	8	4.35	0.48	11.19	0.30
3	10	3.48	0.54	8.96	0.33
4	12	2.90	0.59	7.48	0.37
5	14	2.49	0.63	6.41	0.39
6	16	2.18	0.68	5.61	0.42
7	18	1.94	0.72	5.00	0.45
8	20	1.74	0.76	4.50	0.47
9	40	0.88	1.07	2.27	0.66
10	80	0.47	1.46	1.22	0.91
11	160	0.31	1.81	0.80	1.12

* Unthinned data, having a measured median time spacing of 6.0 µs.

5.2.2 Tree detection

Canopy Height Model (CHM) images were created from the series of LiDAR files using the methodology described earlier (section 2.4 Canopy height model creation). A pixel size of 0.2 m was used for all images so as to accommodate the minimum average point spacing of 0.25 m in the unthinned LiDAR. At the lower pulse densities there was an increase in the number of image pixels having no LiDAR returns, referred to as pits. The image processing method used (*closing*) removed the majority of pits at all pulse densities. Tree detection was then carried out according to the approach documented earlier (2.5 Tree detection) using a manual calibration determined on the original CHM image. Tree detection accuracy was quantified using omission error, commission error and overall accuracy measures, calculated using a conventional method of error matrix assessment as shown by Equations 5.2-5.4 (Girard 2003; Zhang et al. 2014).

$$CE = \frac{N_{det-}N_{cor}}{N_{det}} \quad 5.2$$

$$OE = \frac{N_{ref-}N_{cor}}{N_{ref}} \quad 5.3$$

$$OA = \frac{N_{cor}}{N_{cor} + (N_{det} - N_{cor}) + \left(N_{ref} - N_{cor}\right)} \quad 5.4$$

Where *CE* is commission error (falsely detected trees), OE is omission error (trees not detected), *OA* is overall accuracy taking omissions and commissions into account, N_{cor} is the number of correctly detected (and matched) trees, N_{det} is the total number of trees detected by the algorithm within the trial, and N_{ref} is the number of reference trees counted on the ground.

The error values defined above were then used to derive additional measures of error. User's and producer's accuracy (*UA* and *PA* respectively) are terms also used to quantify detection error, derived from commission and omission errors respectively (Equations 5.5 and 5.6).

$$UA = 1 - CE \quad 5.5$$

$$PA = 1 - OE \quad 5.6$$

All tree detection error measures (Equations 5.2 to 5.6) were multiplied by 100 to be expressed as percentages. In this study the value for N_{ref} , the total number of trees in the trial, was 2196.

5.2.3 Quantifying the effects of pulse density

For each of the eleven LiDAR data sets the derived crown metrics for individual trees were analysed to determine correlations with ground measures, estimates of heritabilities, and genetic gains. Detected trees were matched to trees measured on the ground and crown metrics were derived for each detected tree using the methods described earlier (refer to sections 2.5 2.8 and 2.9). Next, correlations (Pearson's *r*) between crown metrics and all ground measurements were determined using the approach described in section 3.2.3 Analysis of correlations. Then,

narrow sense heritabilities (h^2), were determined for tree height and diameter, according to the methods described in section 4.2.4 Genetic parameters. Finally genetic gains were estimated at three operational selection levels for height and diameter using the methods described in section 4.2.4 Genetic parameters. To support comparisons across different pulse densities the genetic gains were expressed as a proportion (from 0 to 1) of the gain estimated using ground measurements, and referred to as realised gain.

Results for tree detection accuracies, correlations, narrow sense heritabilities and genetic gains were used to establish simple regression models with pulse spacing. The fitted linear models were then used to predict the pulse spacing, and corresponding pulse density, at which 5% and 10% of initial estimates (tree detection, correlations, and genetic parameters) at the full 6 $Pu.m^{-2}$ were lost due to increased pulse thinning.

5.3 Results

5.3.1 Tree detection

The results of tree detection carried out on CHM images derived from the thinned LiDAR data sets are presented in Table 5.2. Commissions occurred at over double the rate of omissions across the range of pulse densities, although their occurrence was more variable. Both commission and omission error rates (*CE* and *OE* respectively) increased with decreasing pulse density. The increases in errors were moderate from 6 to 4 $Pu.m^{-2}$, and more marked below 2 $Pu.m^{-2}$.

Table 5.2. Tree detection results from thinned LiDAR. The total number of trees in the trial (N_{ref}) is 2196.

Test	Pulse density Pu.m^{-2}	Total detected (N_{det})	Correctly detected (N_{cor})	Commissions	Omissions	Commission error (*CE*) %	Omission error (*OE*) %
1	6.09	2317	2132	121	64	7.98	2.91
2	4.35	2416	2117	220	79	12.38	3.60
3	3.48	2471	2117	275	79	14.33	3.60
4	2.90	2388	2106	192	90	11.81	4.10
5	2.49	2537	2097	341	99	17.34	4.51
6	2.18	2508	2098	312	98	16.35	4.46
7	1.94	2571	2087	375	109	18.83	4.96
8	1.74	2483	2056	287	140	17.20	6.38
9	0.88	2616	1974	420	222	24.54	10.11
10	0.47	2804	1932	608	264	31.10	12.02
11	0.31	2904	1851	708	345	36.26	15.71

Producer's, user's, and overall accuracy measures are presented in Figure 5.1. Producer's accuracy, derived from omission error, was higher than user's accuracy, derived from commission error. Both those measures of accuracy were higher than overall accuracy, which takes into account both omission and commission errors. Overall accuracy was similar to user's accuracy because the commission error component was much greater than the omission error component. Overall accuracy ranged from 90% at 6 Pu.m^{-2} down to 57% at 0.3 Pu.m^{-2}. The producer's, user's, and overall accuracy measures reflected the trends noted for the underlying omission and commission measures they are derived from, with a moderate, linear, decrease in accuracies from 6 to 4 Pu.m^{-2}, and a higher, exponential, decrease in accuracies below 2 Pu.m^{-2} (Figure 5.1). When tree detection accuracies were plotted against pulse spacing, linear trends of declining accuracy with increasing pulse spacing were evident across the range of thinning tests (Figure 5.2).

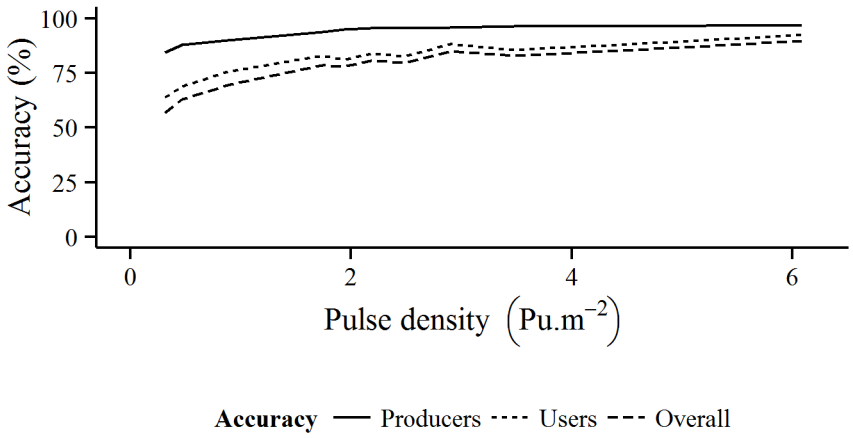

Figure 5.1. Producer's, user's and overall tree detection accuracies plotted against thinned pulse density.

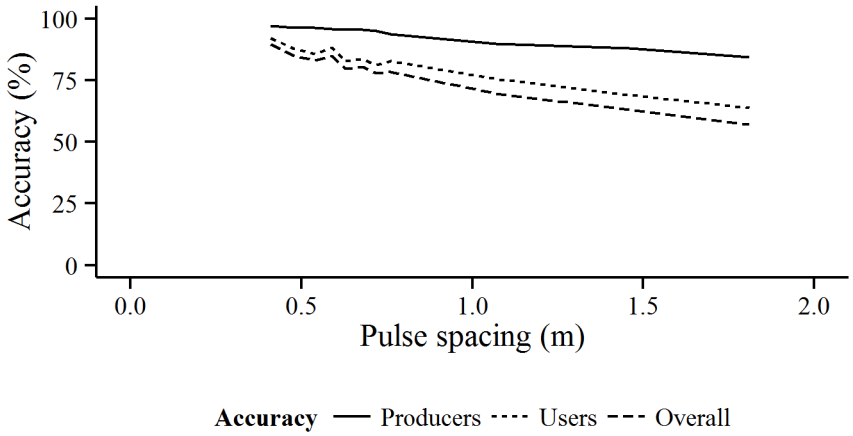

Figure 5.2. Producer's, user's and overall tree detection accuracies plotted against thinned pulse spacing.

5.3.2 Correlations

In section 3.3.3 the best correlated crown metric was determined for each of the ten ground measured tree attributes. The strength of those correlations was re-evaluated using crown metrics derived from detection and delineation carried out with each of the thinned LiDAR data

sets. For each ground measured attribute the best correlated crown metric determined earlier with the full pulse density data set was retained for comparison.

Estimated Pearson's correlation coefficients (*r*) for each of the ground measured attributes were plotted against pulse density (

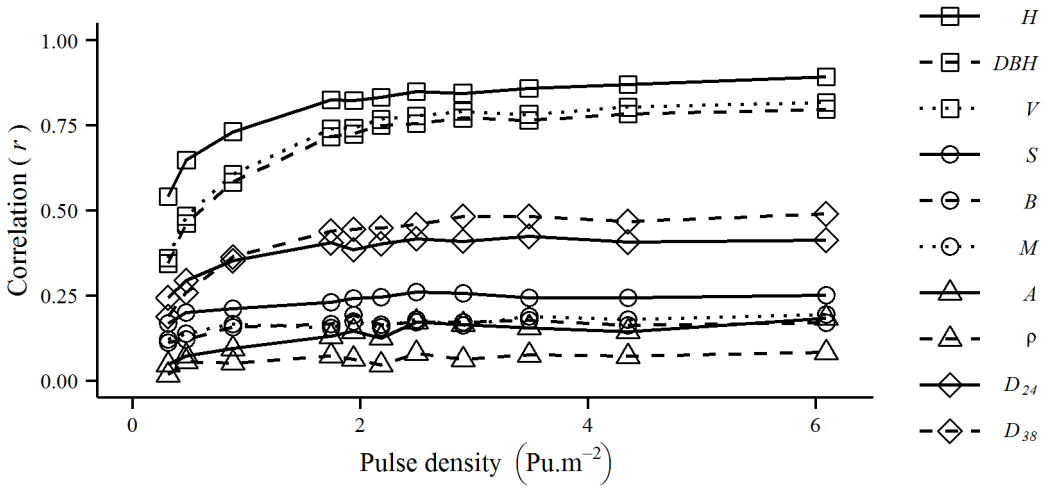

Figure 5.3). Absolute values of *r* were plotted to aid comparisons across all attributes. Correlations declined with reducing pulse density for all tree attributes. At the higher pulse density (6 Pu.m^{-2}) correlations for *H*, *DBH* and *V* were relatively high (*r*= 0.89, 0.80, and 0.82 resp.) and were moderate for D_{24} and D_{38} (*r*= -0.41 and -0.49 resp.). For those attributes the fall in *r* was moderate and linear from 6 Pu.m^{-2} down to 2 Pu.m^{-2}, and a more exponential decrease was evident below 1 Pu.m^{-2}. For the remaining tree attributes correlations were initially low (*r*<0.25) and the decrease in *r* with reduced pulse density was slight. Plotting Pearson's *r* against pulse spacing showed a trend for a linear decline in correlations as spacing increased with lower pulse densities (

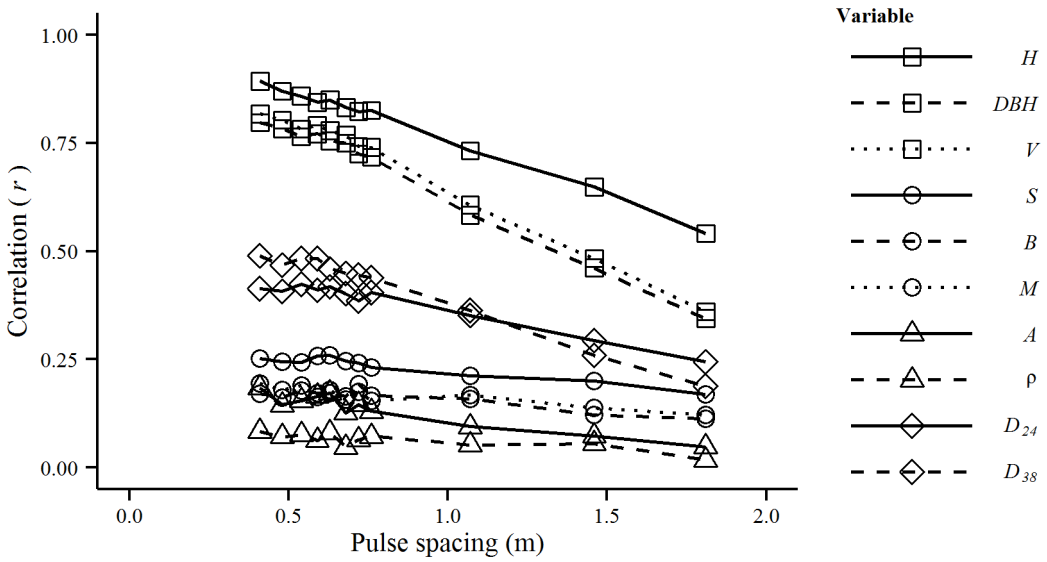

Figure 5.4).

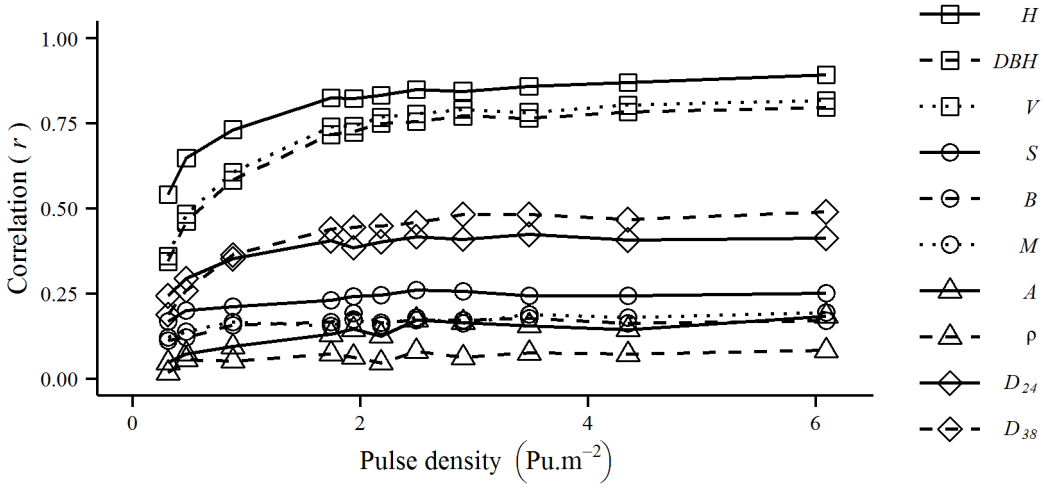

Figure 5.3. Pearson's correlation coefficients (*r*) from the best correlated crown metrics for each of the ground measured variables plotted against thinned pulse density. Note that absolute values of the negative correlations for D_{24} and D_{38} are plotted for ease of comparison with the other correlations. Variables are indicated with shapes: squares for size, circles for form, triangles for wood quality, and diamonds for disease.

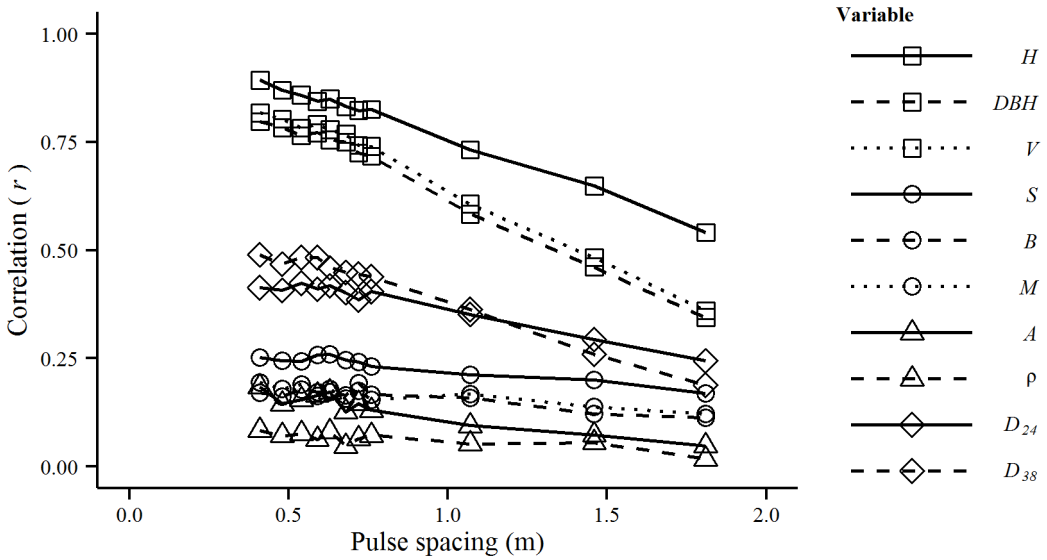

Figure 5.4. Pearson's correlation coefficients (*r*) from the best correlated crown metrics for each of the ground measured variables plotted against thinned pulse spacing. Note that absolute values of the negative correlations for D_{24} and D_{38} are plotted for ease of comparison with the other correlations. Variables are indicated with shapes: squares for size, circles for form, triangles for wood quality, and diamonds for disease.

5.3.3 Heritabilities and genetic gains

In section 4.3 the narrow sense heritabilities and genetic gains were estimated for the ground measured attributes. Results showed that estimated genetic gains, and the underlying heritabilities, were considered of acceptable accuracy for operational use for the tree attributes *H* and *DBH*. The effects of reducing pulse densities on heritabilities and genetic gains were investigated for those two tree attributes. Estimated heritabilities for *H* and *DBH*, as well as the respective best correlated crown metrics (*TH* and CV_F), were plotted against pulse densities in

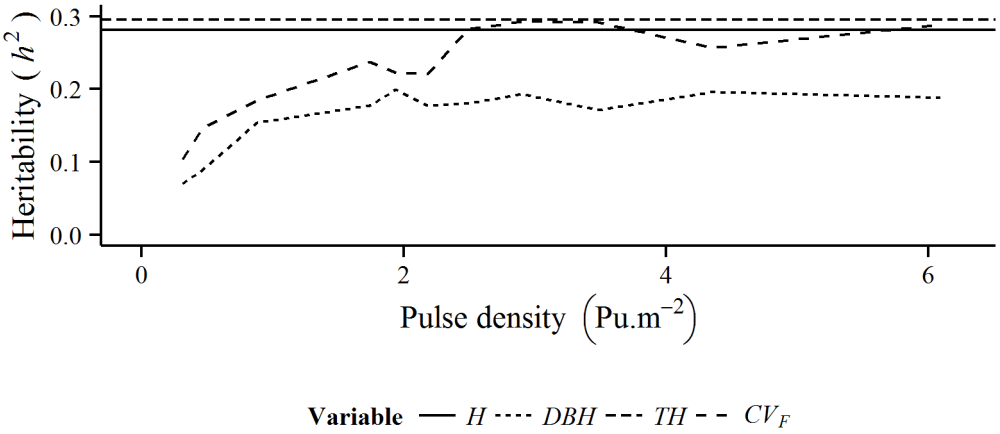

Figure 5.5, and against pulse spacing in

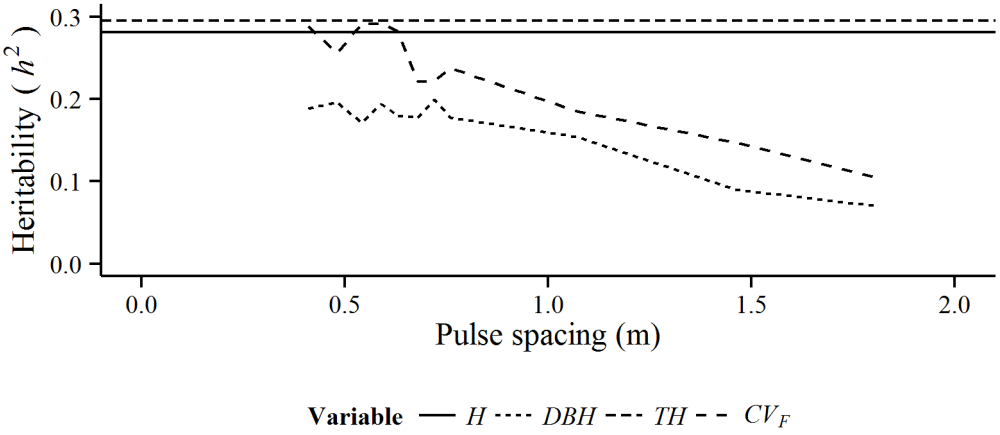

Figure 5.6.

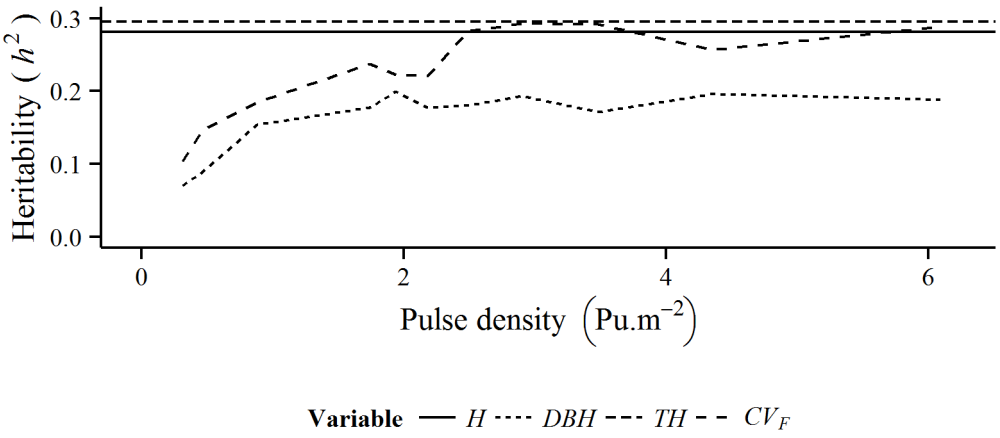

Figure 5.5. Estimated narrow sense heritabilities (h^2) plotted against thinned pulse density. Horizontal lines indicate the h^2 values for *H* and *DBH* estimated using conventional ground measurements. Curves show h^2 values estimated using the best correlated crown metrics for *H* and *DBH* (*TH* and CV_F respectively) plotted against thinned pulse density.

The estimated heritability (h^2) for *H* using the best correlated crown metric (*TH*) was similar to that from ground measurement for pulse densities from 6 down to 2.5 Pu.m^{-2} (

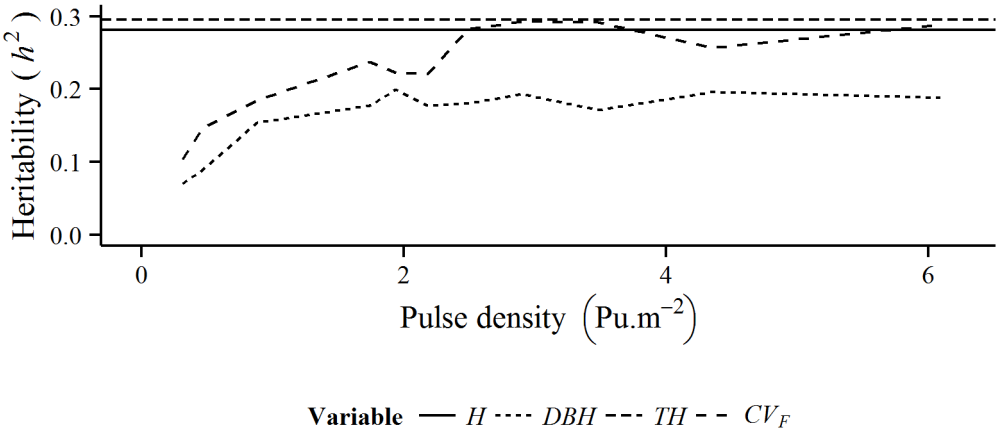

Figure 5.5). Below 2.5 Pu.m^{-2} heritability was increasingly under-estimated. The estimated heritability for CV_F was lower than that for *D*, but was stable down to 2 Pu.m^{-2}, below which it declined sharply. When heritability estimates were plotted against pulse spacing they appeared

variable at lower spacing, corresponding to the higher pulse densities, and then exhibited a steady linear decline with increasing pulse spacing below 0.6 m.

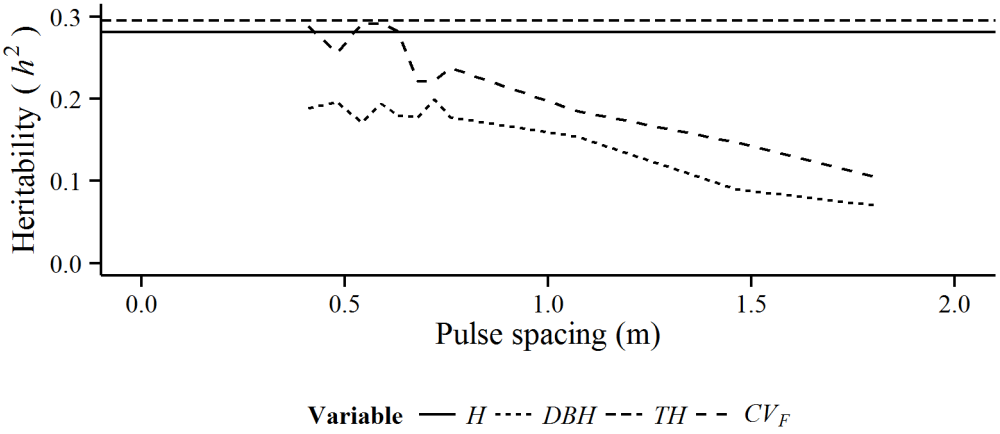

Figure 5.6. Estimated narrow sense heritabilities (h^2) plotted against thinned pulse spacing. Horizontal lines indicate the h^2 values for *H* and *DBH* estimated using conventional ground measurements. Curves show h^2 values estimated using the best correlated crown metrics for *H* and *DBH* (*TH* and CV_F respectively) plotted against thinned pulse spacing.

Genetic gains for *H* and *DBH* were estimated using the respective best correlated crown metrics *TH* and CV_F. Gains were estimated at three selection levels (best 10, 30 and 96 trees), using each thinned LiDAR dataset. Realised genetic gains were derived by comparing the gain obtained when using the appropriate best correlated crown metric, with the gain obtained when using the ground measurements for selection. Realised gains were plotted against pulse Laser Pulse densities (

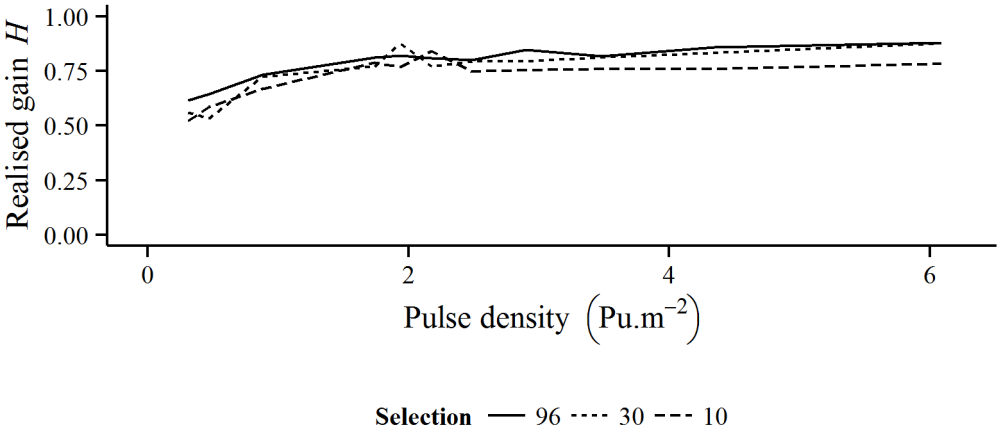

Figure 5.7 and

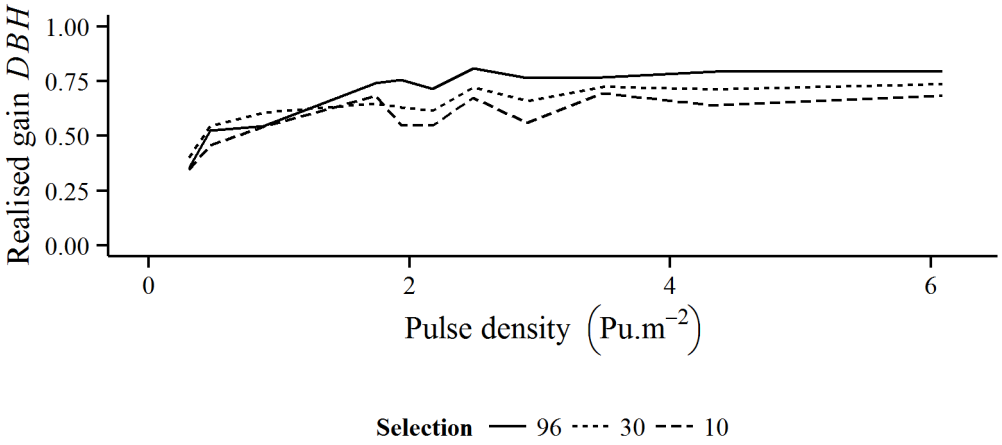

Figure 5.9) and against pulse spacing (

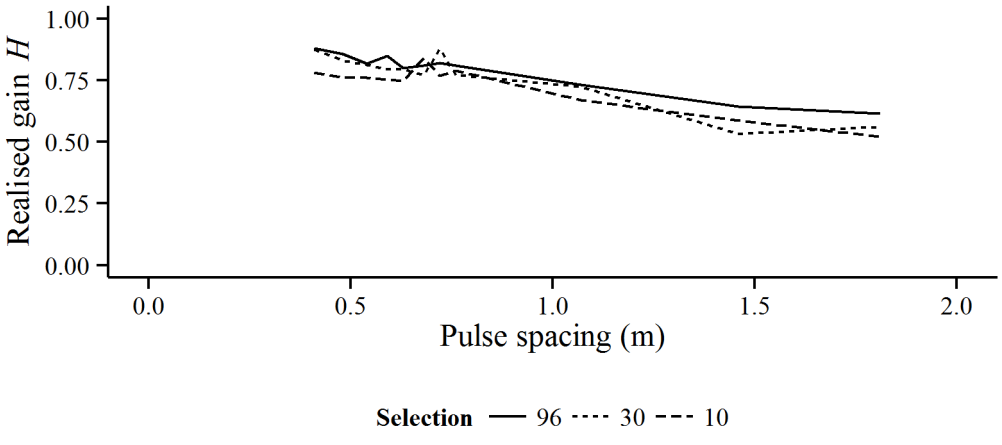

Figure 5.8 and

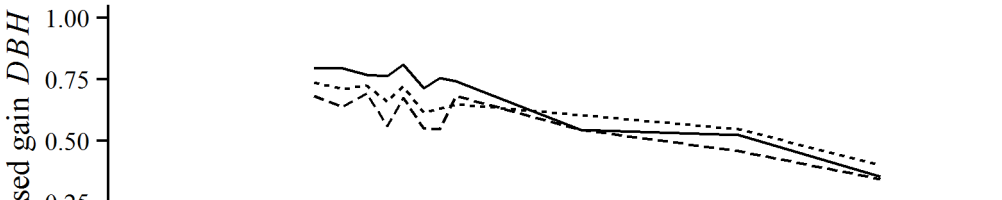

Figure 5.10).

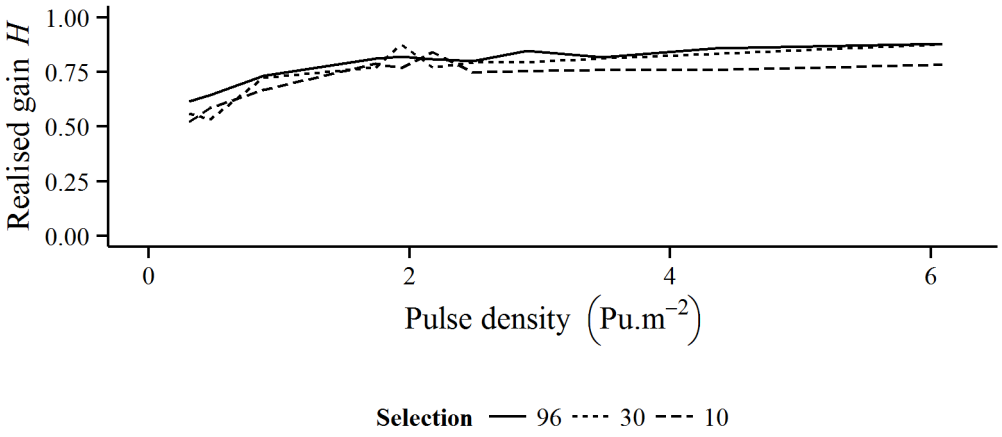

Figure 5.7. Proportion of genetic gain realised for *H* when selecting using the best correlated crown metric *TH* for three selection levels (best 10, 30 and 96 trees) plotted against thinned pulse density.

For tree height (*H*), selection of the best trees using the *TH* crown metric derived from LiDAR data at a density of 6 Pu.m^{-2} realised 80 to 90% of the gain obtained when selecting using ground measured heights (

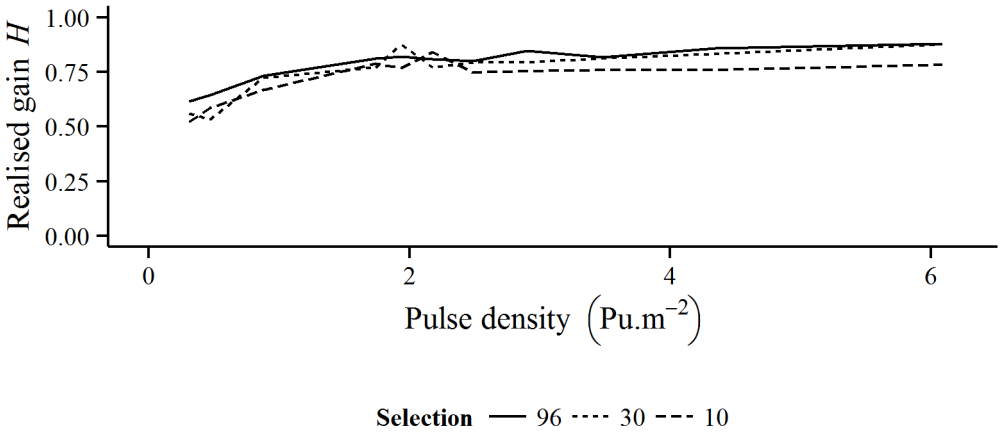

Figure 5.7). Realised gain for *H* was quite stable as pulse density decreased to 2 Pu.m^{-2}, and then dropped markedly below that pulse density. Gains realised for *DBH* when using the CV_F crown metric for selection, derived at 6 Pu.m^{-2}, ranged from 70 to 80% of the gain obtained using ground measurements of diameters (

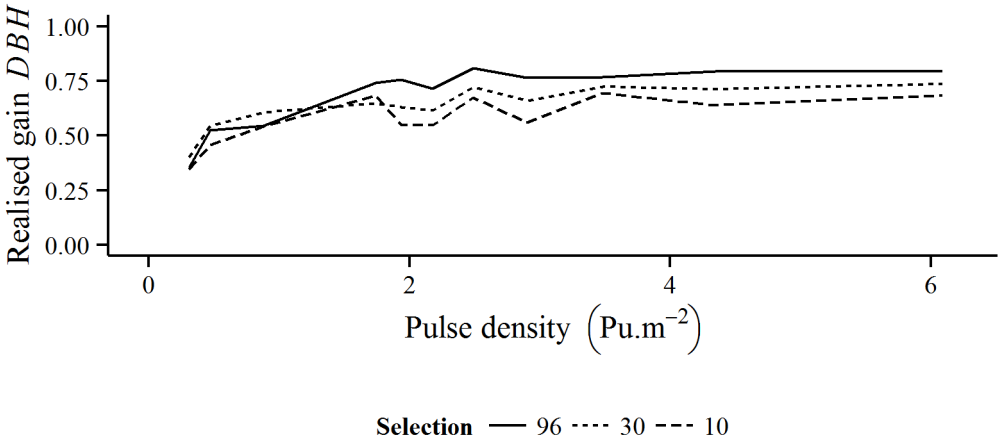

Figure 5.9).

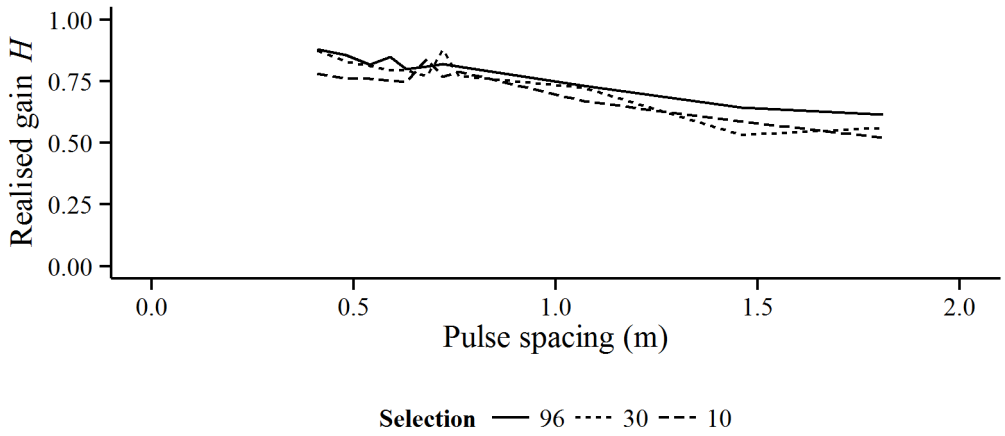

Figure 5.8. Proportion of genetic gain realised for *H* when selecting using the best correlated crown metric *TH*. Realised gain is shown for three selection levels (best 10, 30 and 96 trees) plotted against pulse spacing.

Similar to the trends observed for *H*, realised gain for *DBH* declined only slightly as pulse density reduced to 2 Pu.m^{-2}, below which it dropped quite rapidly. When realised gains were plotted against pulse spacing very similar patterns were observed for *H* and *DBH*, with realised gains declining quite linearly with increased pulse spacing (

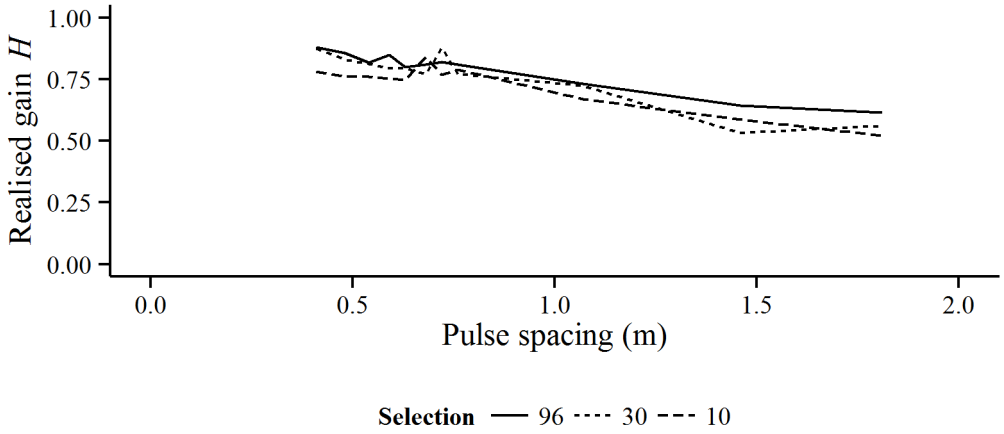

Figure 5.8 and

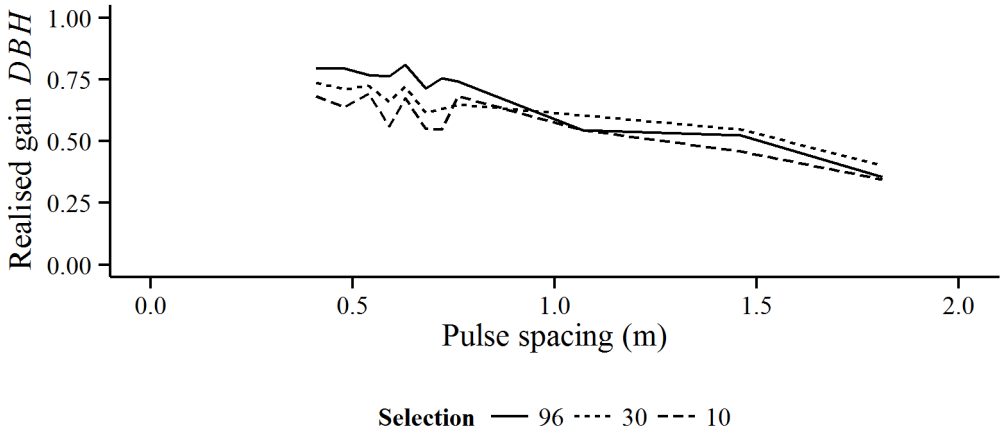

Figure 5.10).

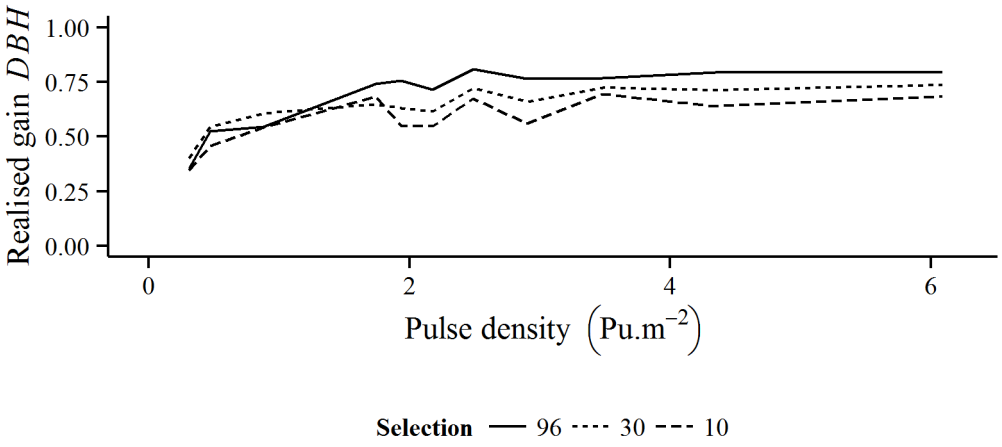

Figure 5.9. Proportion of genetic gain realised for *DBH* when selecting using the best correlated crown metric CV_F. Realised gain is shown for three selection levels (best 10, 30 and 96 trees) plotted against thinned pulse density.

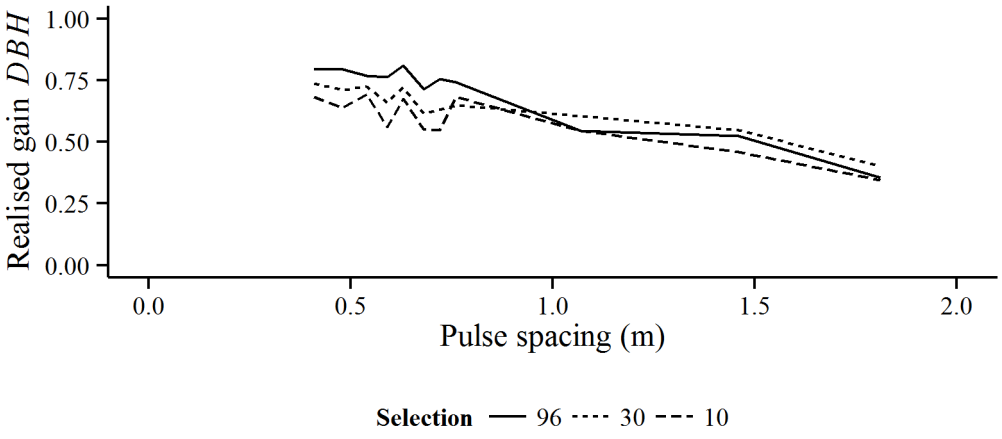

Figure 5.10. Proportion of genetic gain realised for *DBH* when selecting using the best correlated crown metric CV_F. Realised gain is shown for three selection levels (best 10, 30 and 96 trees) plotted against pulse spacing.

Regressions fitted to results were used the estimate the pulse densities at which 5% and 10% reductions in initial estimates occurred. Estimated pulse densities for correlations, heritability

and realised gain were made for tree height (*H*) only, selected because it yielded the most significant results amongst the ground measured variables. Realised genetic gain for *H* was estimated at the 96 tree selection level. Estimates showed that pulse densities of 3 to 5 $Pu.m^{-2}$ were required to maintain estimates within 5% of the initial values and a 10% reduction in estimates occurred at pulse densities of 2 to 3 $Pu.m^{-2}$ (Table 5.3).

Table 5.3. Pulse densities at which 5% and 10% reductions in initial estimates from full pulse density (6.1 $Pu.m^{-2}$) are predicted for the various quantities examined in this study.

Estimated quantity	Estimate at 6.1 $Pu.m^{-2}$	Pulse density for 5% reduction $Pu.m^{-2}$	Pulse density for 10% reduction $Pu.m^{-2}$
Tree detection overall accuracy	89.54%	4.4	2.2
Pearson's correlation coefficient*	0.89	2.7	1.6
Narrow sense heritability*	0.29	3.9	2.7
Realised genetic gain (selection of 96 trees)*	0.88	3.1	1.6

* These estimates are for tree height (H)

5.4 Discussion

5.4.1 Accuracy of tree detection

Relatively few omission errors occurred, by failing to identify trees with smaller crowns, while commission errors occurred more than twice as often, and were found to result from two causes: falsely subdivided large branches, and segmented shrubs or ferns. The use of a height threshold derived from the LiDAR point cloud to create CHM images, as applied in this study, reduced segmentation of understory vegetation and any other sub-canopy features, and therefore reduced commission errors due to detection of non-target objects. However some errors of this type still occurred, where non-target shrubs and ferns exceeded the threshold height. Those errors contributed to the commission and user's error measures, but did not negatively affect crown metrics. In fact segmentation of those non-target objects is important to ensure accuracy of crown segmentation and derived crown metrics for the target trees.

This study has shown clear effects of pulse density on tree-based analyses of ALS data. Tree detection accuracy declined with reducing pulse density and overall accuracy dropped from 89.54% to 84.85% when pulse density decreased from 6.1 to 4.4 $Pu.m^{-2}$. The observed accuracy at 6.1 $Pu.m^{-2}$ for the genetics trial used in this study is in general agreement with the documented accuracies for operational stands in earlier work using the same tree detection methods (Pont et al. 2015b). Analyses have considered a range of pulse densities, and results have quantified trade-offs between pulse density and accuracy of detection, and have showed a linear decline in the accuracy of tree detection when compared to pulse spacing, rather than density. The observed linear relationship between accuracy and pulse spacing was used to determine that reductions in detection accuracy of 5% and 10% corresponded to pulse densities of 4.4 and 2.2 $Pu.m^{-2}$. A marked increase in tree detection error was observed below 2 $Pu.m^{-2}$ which aligns with reported minimum pulse densities from other studies. For example Wang et al. (2016) concluded 2 points per m^2 could be adequate for the detection of dominant trees, in a study that included coniferous stands in southern Finland. In another study on boreal forest in southern Finland, reduction of point density from 12 to 0.5 points m^{-2} was found to have only a moderate effect on the accuracy of estimates for individual tree properties (Vauhkonen et al. 2008). However in that study tree detection and delineation had been carried out using full point density and so the effect of these important steps were not included in the study. The authors concluded that 3 $Pu.m^{-2}$ were adequate for deriving useful three-dimensional crown metrics, based on alpha shapes, given that accurate detection and delineation were already available. They also noted prior work which showed pulse densities of 5 to 10 $Pu.m^{-2}$ are usually required for detecting and delineating trees in boreal forests (Persson et al. 2002). Accurate tree detection is essential to the subsequent derivation of crown metrics and estimates of values such as genetic parameters. On the basis of results, 2 $Pu.m^{-2}$ should be considered an absolute minimum to avoid rapidly escalating errors in the detection of radiata pine trees in research trials, but higher pulse density is desirable to achieve corresponding increases in accuracy. A LiDAR resolution of 6 $Pu.m^{-2}$ is indicated to achieve automated tree detection rates near 90%.

5.4.2 Crown size

The study area was a forest genetics trial, containing young (age 7) radiata pine trees, planted on a regular grid. Tree spacing was 3.2 by 3.2 m and apart from intermittent gaps caused by missing trees, the trial had reached canopy closure. Detection of trees in even-aged conifer stands is generally agreed as representing a relatively simple case, and it can be argued that a regularly planted trial area is an even closer to an ideal case. Crown areas of detected trees, determined from delineation on the CHM image averaged 10.4 m^2. This is slightly greater than the 10.2 m^2 area theoretically available to each tree due to the 3.2 by 3.2 m grid spacing, and has occurred as a result of crowns occupying space left by missing trees. Crown areas ranged from 1.4 to 29.0 m^2, reflecting a large range of variation in crown sizes within the trial. The observed variability of crown sizes, largely of genetic origin in this trial, therefore presented more of a challenge to tree-based analysis than might be expected for a trial established with a regular grid layout.

Pulse spacing is related to pulse density by an inverse square relationship. The initial pulse density of 6.1 $Pu.m^{-2}$ corresponded to a pulse spacing of 0.41 m, and a point spacing of 0.25 m. It is interesting to note that detection of tree crowns with average diameters of 3.2 m was imperfect, even with such closely spaced returns. In fact it is more instructive to consider the limiting case as being the smallest crowns able to be detected. In this study, crowns as small as 1.6 m in diameter were detected, representing more than a six-fold ratio of crown size to point spacing at 6.1 $Pu.m^{-2}$. It is suggested such a ratio, relating crown diameter with LiDAR point spacing, may be a useful metric expressing the marginal resolution of LiDAR required to detect the smallest crowns in an area, taking into account LiDAR resolution and variations in crown size due to spacing, silviculture and age. It is still useful to express resolution in terms of pulse density, as this is a parameter that can be specified when planning LiDAR capture, but it is also instructive to think about point spacing when considering the potential for image analysis to detect tree crowns. On the basis of the ratio observed in this study between crown size and point spacing, and the inverse square relationship between spacing and density, the required point spacing and point density for a given minimum crown size can be estimated. Estimates

for two different minimum crown sizes are depicted in Figure 5.11, showing the required point spacings and densities, and illustrating the linear decrease in point spacing and the exponential decrease in point density necessary to detect larger crowns.

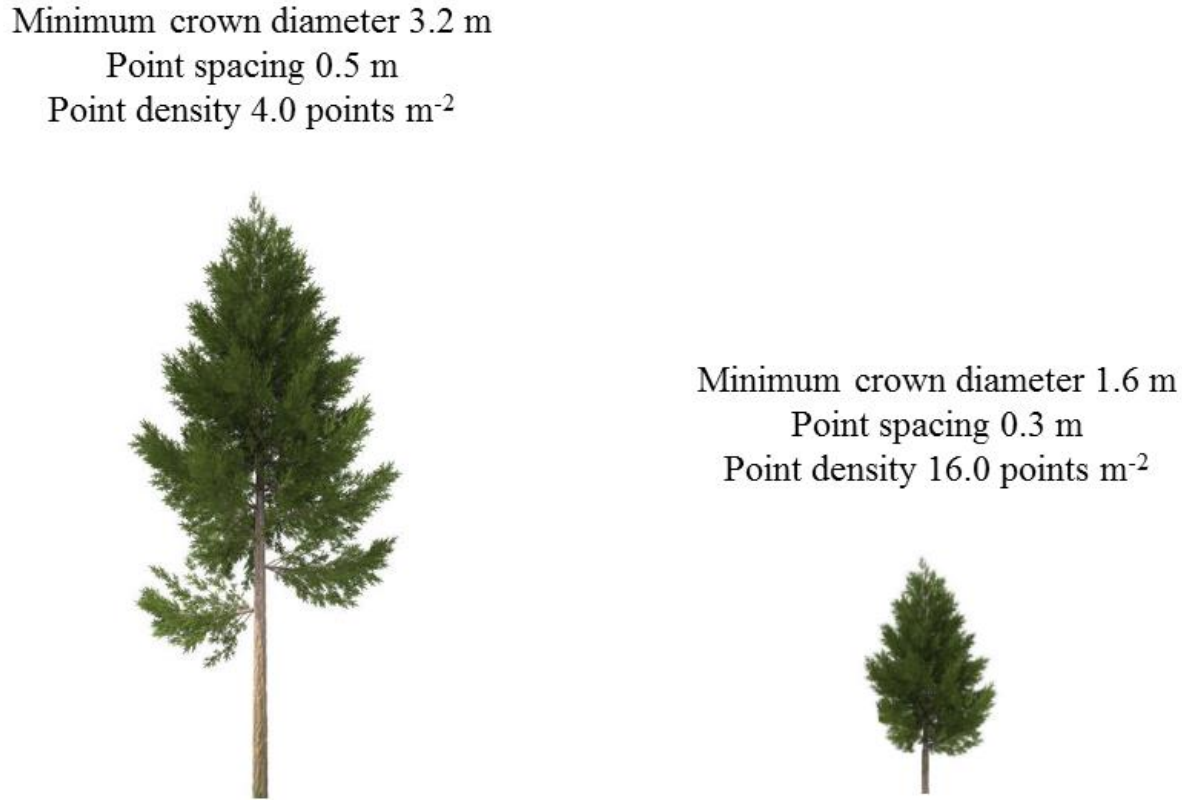

Figure 5.11. The relationship between minimum crown size and point spacing required for tree detection. The observed ratio between minimum crown size and point spacing was used to estimate the required point spacing and corresponding point density for detection of different crown sizes. A minimum crown size of 3.2 m (left) equates to a required point spacing of 0.5 m and a point density of 4 points m^{-2}. Halving crown size to 1.6 m (right) halves required point spacing to 0.3 m and increases point density by a factor of four, to 16 points m^{-2}.

5.4.3 Correlations, heritabilities and genetic gains

In this study the effect of pulse density on correlations between crown metrics and ground measurements of trees, and on estimates of genetic parameters, were considered. In all cases reducing pulse density diminished the ability to estimate these quantities. It was observed that maximum accuracy of tree detection was desirable for subsequent tree-based analyses, and

demonstrated that maintaining estimates within 5 or 10% of original values required higher pulse densities for tree detection than for the other derived values evaluated (Table 5.3). This indicates that although tree detection accuracy falls at lower pulse densities, useable correlations with crown metrics, and useable estimates of genetic parameters for tree attributes such as height and diameter can still be obtained. As with tree detection, a marked decline in estimates generally occurred below 2 $Pu.m^{-2}$, and a linear decline was observed with increasing pulse spacing. The observed linear relationships between accuracy and pulse spacing were used to determine that reductions in estimates of 5% and 10% corresponded to pulse densities of around 3-4 and 2-3 $Pu.m^{-2}$ respectively. Those results support a conclusion that a pulse density of 4 $Pu.m^{-2}$ should be considered a minimum for determination of correlations with crown metrics and estimation of genetic parameters. It is also noted that the assessment of research trials demands high quality data, and in practice higher pulse density would be advised to obtain the best possible estimates.

5.4.4 Pulse density and pulse spacing

The observed linearity between pulse spacing and accuracies for tree-based analyses of LiDAR has important implications. A linear relationship with spacing supports an exponential relationship with pulse density, agreeing with theoretical relationships between density and spacing. Those relationships were confirmed in this study, over a range of densities and spacings. Using tree detection as an example, results demonstrated that a fourfold reduction in pulse density only resulted in a doubling of point spacing and a doubling of detection error. Equally, results indicated that in order to halve error it is necessary to halve pulse spacing, requiring a four-fold increase in pulse density. The first implication of the study results is that accuracies decline but are relatively insensitive to moderate reductions in pulse densities down to a level of 2 $Pu.m^{-2}$. The second implication is that accuracies cannot be easily increased by increasing pulse density, because exponential increases in density are required to make incremental gains in accuracy. It is therefore concluded that to achieve small gains in the accuracies achieved in this study, pulse densities greatly in excess of 6 $Pu.m^{-2}$ would have been

required. To generalise, lower densities incur gradual but undesirable increases in error, and higher densities incur increasing costs for diminishing gains in accuracies.

5.4.5 Higher resolution from new technologies

Other researchers have noted that higher point (and thus pulse) density was more critical for point-based detection methods, and that those methods are able to better utilise increased point density, compared to raster-based methods as was used in this thesis study (Wang et al. 2016). They also noted that three dimensional analyses of high-density LiDAR has important potential benefits, notably for more complex forest types. Ongoing improvements in technologies are delivering LiDAR with higher pulse densities. Multi-laser LiDAR systems already exist, for example the Optech Pegasus incorporates two lasers, effectively doubling achieved pulse densities (Optech 2014). Surface models extracted from highly-overlapping imagery can be used to produce very high density point clouds, on the order of one hundred or more points m^{-2} (St-Onge et al. 2015; St-Onge and Audet 2015; Wallace et al. 2016). However these point clouds lie solely on the upper surface of the canopy, lacking the penetration of LiDAR. Therefore they might be used for raster-based analyses, as applied in this study, but will lack the detail utilised in point-based methods. Processing of waveform LiDAR data is still an active area of research, with a lack of standardised methods. One approach is to analyse the waveform data to extract increased numbers of discrete returns compared to standard processing by vendor systems, although increases are in the order of ten-fold at best (Adams et al. 2012; Allouis et al. 2013). Another example is a multi-laser LiDAR system able to be carried by unmanned aerial vehicles which can provide pulse densities over 100 $Pu.m^{-2}$, due in part to multiple lasers, and to the ability to operate at lower height above ground and lower flight speeds, compared to systems in manned aircraft (Routescene 2015). New LiDAR systems such as Geiger-mode could provide pulse densities hundreds of times higher than existing systems but it could be some time before such systems are readily available (Lemmens 2015). The results of the current study indicate that incremental increases in LiDAR pulse densities might provide only moderate benefits, and that exponential increases in pulse densities, possible with some new technologies, will be required to deliver useful improvements in results from tree-

based analyses of LiDAR. New studies with different forms of higher density LiDAR will be required to quantify the trade-offs between pulse densities, computational demands, operational costs, and achieved accuracies.

5.5 Conclusions

This study has provided useful insight into the effects of pulse density on tree-based analysis of ALS data. The effects of pulse density on tree detection, and on correlations of crown metrics with ground measures, have been evaluated, meeting the first two objectives: *"Quantify the effect of reducing pulse densities on the accuracy of tree detection"* and *"Quantify the effect of reducing pulse densities on correlations between crown metrics and ground measurements of key tree attributes"*. Effects have also been evaluated in practical terms by examining effects on estimates of genetic parameters, thereby meeting the third objective *"Quantify the effect of reducing pulse densities on estimates of heritabilities and genetic gains"*. The research results have addressed the research question "**What is the effect of varying pulse density on the accuracy of estimates obtained from the analysis of discrete return LiDAR?"** by quantifying effects and thereby providing practical guidance for operational applications of tree-based analyses of ALS.

Chapter 6 Summary

The use of ALS data has already had a significant impact on international and local forest management and research. The development of methods to analyse ALS data at the individual tree level was identified as having a number of potential benefits. The research carried out in this thesis was aimed at developing and evaluating methods to estimate a number of key individual tree attributes from ALS data for plantation-grown New Zealand radiata pine, with the aim of advancing the international knowledge and providing methods to support innovative research and forest management practices. Important applications identified were in precision forestry and in phenotyping trees for tree growth and tree breeding research. Gaps identified in the international literature led to the formulation of three key research questions, with associated objectives, which were addressed in the research carried out. The success in addressing those objectives and questions is summarised below.

6.1 Can methods be developed to estimate key attributes of individual trees using airborne laser scanning data?

International literature indicated potential for crown metrics derived from ALS data to be used in estimating tree size attributes, and there was some limited research or discussion of possibilities for estimating other attributes. In the research carried out, a broad set of crown metrics were developed, including a number of novel metrics, to evaluate for use in estimating tree attributes, meeting the first objective "*Derive a set of individual crown metrics from raster-based analysis of ALS data in which individual trees have been detected*". This study was also the first known example where estimates for a range of key tree attributes, representing tree size, form, wood quality, and disease expression, were made in a single study. The best correlations with those ground measured attributes were determined using the crown metrics, meeting the second objective "*Quantify correlations between LiDAR crown metrics and ground-based measures of tree size, form, wood quality, and disease expression*". The crown metrics evaluated provided strong correlations with tree size attributes, and weak or absent correlations for the other tree attributes. An interesting finding was a moderate negative

correlation between crown size, which was correlated positively with tree size, and the degree of disease infection. This was interpreted as reflecting reduced tree growth due to the effects of the disease and could offer potential for indirectly assessing the presence and levels of disease in individual trees and areas of trees. This also indicates genetic gains in disease resistance will be obtained if selecting on tree size. Results supported an affirmative answer to the research question, by demonstrating strong relationships between measures of crown metrics and tree size.

6.2 Can methods be developed to estimate variance components of individual trees using airborne laser scanning data to elucidate the genetic and environmental drivers of tree growth?

In the introduction, the need for tree-based analysis of ALS was established. Such methods could be beneficial for precision forestry applications but they were identified as being critical to the use of remotely sensed data, such as ALS, in research trials in general and tree breeding research in particular. Tree breeders have developed specialised analytical approaches in order to separate genetic and environmental determinants of tree growth. A need was identified to evaluate the ability to apply these analytical methods to individual tree metrics derived from ALS data to ensure the applicability of a tree-based approach in tree breeding research. The benefits of applying such analytical methods in tree growth research were also identified, supporting the development of individual tree phenotyping methods, with benefits to the next generation of research into tree breeding, tree growth, and wood quality, as well as supporting development of precision forestry methods. This led to the formulation of the objective: "*Estimate genetic parameters for measures of tree size, form, wood quality, and disease expression using crown metrics and compare these with estimates from ground measurements".* Review of the literature and local research experience also identified that accurate tree detection was an important prerequisite to generating useful tree crown metrics for use in such research. Therefore a second objective "*Evaluate the effect of errors in tree detection and delineation by comparing estimates of genetic parameters from automatic and*

manual segmentation of individual trees" was posed in order to evaluate sensitivity to the accuracy of tree detection. Tree crown metrics were derived from an initial automated tree detection result, and from a manually corrected set of tree crowns. The two sets of metrics were then used to evaluate the ability to estimate a set of genetic parameters.

This was the first known example of using tree crown metrics from ALS to estimate genetic and environmental sources of variation. It was also the first known example of evaluating the effects of tree segmentation accuracy on the results of ALS analyses. Results showed the ability to accurately estimate genetic parameters for the tree size attributes and not the other attributes. Those results were attributed to strong correlations between crown size metrics and ground measurements of tree size. Results also showed the correction of an automated crown segmentation had a negligible effect on accuracy of estimated variance components and genetic parameters. This was an important finding, indicating manual correction would not be necessary in operational use of the methods evaluated. It was observed that strong relationships between crown metrics and tree attributes were more important than the effects of correcting the tree segmentation.

6.3 What is the effect of varying pulse density on the accuracy of estimates obtained from the analysis of discrete return LiDAR?

The resolution of ALS data necessary to derive accurate estimates from tree-based analysis is an important theoretical and operational consideration. Increased pulse density potentially yields more data for analyses, but increases the costs of data collection. Review of the literature showed some studies have quantified the effects of pulse density on estimates from area-based analysis of LAS, but there was a lack of research for tree-based analysis. Investigation of the effects of pulse density were thus seen as an important issue to consider when evaluating tree-based analysis of ALS for forestry research and operational applications. The original ALS data was thinned to create data sets representing a wide range of pulse densities. Those data were then processed using the methodologies presented and developed in this thesis. The effects of reducing pulse densities were then evaluated for tree detection,

correlations with crown metrics, and estimates of heritabilities and genetic gains, meeting the three corresponding objectives defined for this phase of the research: "*Quantify the effect of reducing pulse densities on the accuracy of tree detection"*, "*Quantify the effect of reducing pulse densities on correlations between crown metrics and ground measurements of key tree attributes*", and "*Quantify the effect of reducing pulse densities on estimates of heritabilities and genetic gains*".

The results of the investigations showed that in general an exponential decline in estimates occurred in relation to reducing pulse density. This was evident in reductions in accuracies which were initially moderate but which declined rapidly at pulse densities below 1 or 2 $Pu.m^{-2}$. The accuracy of tree detection was found to be most sensitive (see Table 5.3). Overall detection accuracy was 90% at the unthinned pulse density of 6.1 $Pu.m^{-2}$. Accuracy was reduced by 5% with a relatively small reduction in pulse density to 4.4 $Pu.m^{-2}$. Accurate tree detection is a prerequisite to obtaining accurate crown metrics and a reduction to 85% in tree detection is seen as unsuitable for use in research or management applications for, counting or assessing trees. Therefore a minimum pulse density of 6 $Pu.m^{-2}$, the highest evaluated, is recommended for accurate tree detection.

Estimates of correlations and genetic parameters, evaluated for tree height and diameter, were slightly less sensitive, permitting a recommended minimum pulse density of 4 $Pu.m^{-2}$. The exponential relationship demonstrated between estimates and pulse densities were noted as having two important implications: estimates decline rapidly with reducing pulse density; and improvements in estimates require exponential increases in pulse density.

6.4 Conclusions

The research carried out has used a number of novel approaches to evaluate the utility of ALS data for applications in precision forestry, forestry research, and tree breeding. The ability to derive individual tree crown metrics for New Zealand plantation-grown radiata pine using ALS data, a form of data which is becoming increasing available in the New Zealand forestry sector,

has been demonstrated. The tree crown metrics developed and evaluated in this research have been shown to correlate well with tree size attributes, allowing accurate estimation of these important measures of tree growth. The methods developed can be used to estimate tree heights, diameters and stem volumes using the same ALS data obtained for operational uses with conventional area-based analysis. The ability to partition genetic and environmental sources of variation in measures of tree size derived from ALS data has also been demonstrated. These findings have important implications for general forest inventory and in the assessment of research and genetics trials, where the ability to characterise trees from remotely sensed data can have benefits in terms of cost-savings and improved safety by reducing time spent on the ground in the forest. Finally, the effects of pulse density on the tree-based analyses of the ALS data have been carried out. The research results indicate that the methodologies developed and presented in this thesis, namely tree-based analysis of ALS data, of around 6 $Pu.m^{-2}$, using a raster-based approach to derive crown metrics, provide a parsimonious and effective approach to characterising individual trees.

In conclusion the research carried out in this thesis has contributed to the international body of research into individual tree methods for ALS data. Methods to estimate attributes of individual trees from ALS data were evaluated for New Zealand plantation-grown radiata pine trees in the setting of genetics trials. The tree attributes included measures of tree size, form, wood quality and disease, representing an operationally relevant set of attributes. The methods developed will have applications in precision forest management and in phenotyping trees for innovative research into tree growth and the development of elite tree breeds.

References

Adams, T., Beets, P., & Parrish, C. (2012). Extracting more data from LiDAR in forested areas by analyzing waveform shape. *Remote Sensing, 4*, 682-702

Adams, T., Brack, C., Farrier, T., Pont, D., & Brownlie, R. (2011). So you want to use LiDAR? - A guide on how to use LiDAR in forestry. *New Zealand Journal of Forestry, 55*, 19-23

Allouis, T., Durrieu, S., Vega, C., & Couteron, P. (2013). Stem volume and above-ground biomass estimation of individual pine trees from LiDAR data: Contribution of full-waveform signals. *IEEE Journal of Selected Topics in Applied Earth Observations and Remote Sensing, 6*, 924-934

Bakula, M., Przestrzelski, P., & Kazmierczak, R. (2015). Reliable technology of centimeter GPS/GLONASS surveying in forest environments. *IEEE Transactions on Geoscience and Remote Sensing, 53*, 1029-1038

Balenović, I., Jazbec, A., Marjanović, H., Paladinić, E., & Vuletić, D. (2015). Modeling tree characteristics of individual Black Pine (Pinus nigra Arn.) trees for use in remote sensing-based inventory. *Forests, 6*, 492-509

Barth, A., Möller, J.J., Wilhelmsson, L., Arlinger, J., Hedberg, R., & Söderman, U. (2014). A Swedish case study on the prediction of detailed product recovery from individual stem profiles based on airborne laser scanning. *Annals of Forest Science, 72*, 47-56

Becker, G. (2001). Precision forestry in central Europe - new perspectives for a classical management concept. In D. Briggs (Ed.), *The first international precision forestry cooperative symposium*. Seattle, Washington: University of Washington

Beets, P.N., Brandon, A.M., Goulding, C.J., Kimberley, M.O., Paul, T.S.H., & Searles, N. (2012). The national inventory of carbon stock in New Zealand's pre-1990 planted forest using a LiDAR incomplete-transect approach. *Forest Ecology and Management, 280*, 187-197

Beets, P.N., Reutebuch, S., Kimberley, M.O., Oliver, G.R., Pearce, S.H., & McGaughey, R.J. (2011). Leaf area index, biomass carbon and growth rate of Radiata Pine genetic types and relationships with LiDAR. *Forests, 2*, 637-659

Bilker, M., & Kaartinen, H. (2001). The quality of real-time kinematic (RTK) GPS positioning. *Reports of the Finnish Geodetic Institute, 2001*

Blanchette, D., Fournier, R.A., Luther, J.E., & Côté, J.-F. (2015). Predicting wood fiber attributes using local-scale metrics from terrestrial LiDAR data: A case study of Newfoundland conifer species. *Forest Ecology and Management, 347*, 116-129

Bogaert, J., Rousseau, R., Van Hecke, P., & Impens, I. (2000). Alternative area-perimeter ratios for measurement of 2D shape compactness of habitats. *Applied Mathematics and Computation, 111*, 71-85

Bouvier, M., Durrieu, S., Fournier, R.A., & Renaud, J.-P. (2015). Generalizing predictive models of forest inventory attributes using an area-based approach with airborne LiDAR data. *Remote Sensing of Environment, 156*, 322-334

Brandtberg, T., Warner, T.A., Landenberger, R.E., & McGraw, J.B. (2003). Detection and analysis of individual leaf-off tree crowns in small footprint, high sampling density lidar data from the eastern deciduous forest in North America. *Remote Sensing of Environment, 85*, 290-303

Breda, N.J. (2003). Ground-based measurements of leaf area index: a review of methods, instruments and current controversies. *J Exp Bot, 54*, 2403-2417

Breidenbach, J., Næsset, E., Lien, V., Gobakken, T., & Solberg, S. (2010). Prediction of species specific forest inventory attributes using a nonparametric semi-individual tree crown approach based on fused airborne laser scanning and multispectral data. *Remote Sensing of Environment, 114*, 911-924

Bribiesca, E. (2008). An easy measure of compactness for 2D and 3D shapes. *Pattern Recognition, 41*, 543-554

Brosofske, K.D., Froese, R.E., Falkowski, M.J., & Banskota, A. (2014). A review of methods for mapping and prediction of inventory attributes for operational forest management. *Forest Science, 60*, 733-756

Burdon, R.D. (2001). Pinus radiata. In F.T. Last (Ed.), *Ecosystems of the World, Vol. 19. Tree Crop Ecosystems* (pp. 99-161). Amsterdam, The Netherlands: Elsevier

Burdon, R.D. (2008). Trees: Structural marvels but very imperfect wood factories. In, *IUFRO-Canadian Tree Improvemnt Conference, CTIA Wood Quality Workshop*. Quebec City, Canada

Burdon, R.D., Bannister, M.H., & Low, C.B. (1992). Genetic survey of Pinus radiata. 3: Variance structures and narrow-sense heritabilities for growth variables and morphological traits in seedlings. *New Zealand Journal of Forestry Science, 22*, 160-186

Burdon, R.D., & Low, C.B. (1992). Genetic survey of Pinus radiata. 6. Wood properties: variation, heritabilities, and interrelationships with other traits. *New Zealand Journal of Forestry Science, 22*, 228-245

Butler, D.G., Cullis, B.R., Gilmour, A.R., & Gogel, B.J. (2009). *ASReml-R reference manual*. Queensland, Australia: Queensland Department of Primary Industries

Carson, M.J., Inglis, C.S., & Shelbourne, C.J.A. (1988). Genotype and location effects on internode length of Pinus radiata in New Zealand. *New Zealand Journal of Forestry Science, 18*, 267-279

Carson, S.D., Cown, D.J., McKinley, R.B., & Moore, J.R. (2014). Effects of site, silviculture and seedlot on wood density and estimated wood stiffness in radiata pine at mid-rotation. *New Zealand Journal of Forestry Science, 44*, 1-12

Chen, Q., Gong, P., Baldocchi, D., & Tian, Y.Q. (2007). Estimating basal area and stem volume for individual trees from lidar data. *Photogrammetric Engineering and Remote Sensing, 73*, 1355-1365

Chen, Y., & Zhu, X. (2012). Site quality assessment of a Pinus radiata plantation in Victoria, Australia, using LiDAR technology. *Southern Forests: a Journal of Forest Science, 74*, 217-227

Cobb, J.N., Declerck, G., Greenberg, A., Clark, R., & McCouch, S. (2013). Next-generation phenotyping: requirements and strategies for enhancing our understanding of genotype-phenotype relationships and its relevance to crop improvement. *Theor Appl Genet, 126*, 867-887

Coops, N.C., Varhola, A., Bater, C.W., Teti, P., Boon, S., Goodwin, N., & Weiler, M. (2014). Assessing differences in tree and stand structure following beetle infestation using lidar data. *Canadian Journal of Remote Sensing, 35*, 497-508

Costa, E.S.J., Borralho, N.M., & Potts, B.M. (2004). Additive and non-additive genetic parameters from clonally replicated and seedling progenies of *Eucalyptus globulus*. *Theor Appl Genet, 108*, 1113-1119

Cullis, B.R., Jefferson, P., Thompson, R., & Smith, A.B. (2014). Factor analytic and reduced animal models for the investigation of additive genotype-by-environment interaction in outcrossing plant species with application to a Pinus radiata breeding programme. *Theor Appl Genet, 127*, 2193-2210

De Reffye, P., Houllier, F., Blaise, F., Barthelemy, D., Dauzat, J., & Auclair, D. (1995). A model simulating above- and below-ground tree architecture with agroforestry applications. *Agroforestry Systems, 30*, 175-197

Dean, T.J. (2004). Basal area increment and growth efficiency as functions of canopy dynamics and stem mechanics. *Forest Science, 50*, 106-116

Dean, T.J., Jerez, M., & Cao, Q.V. (2013). A simple stand growth model based on canopy dynamics and biomechanics. *Forest Science, 59*, 335-344

Dhondt, S., Wuyts, N., & Inze, D. (2013). Cell to whole-plant phenotyping: the best is yet to come. *Trends Plant Sci, 18*, 428-439

Dungey, H., S, Pont, D., Li, Y., Wilcox, P., L, Telfer, E., J, Watt, M., S, & Jefferson, P., A (2013). Novel remote sensing phenotyping platform and genomic selection will boost the delivery of genetic gain of radiata pine in New Zealand. In, *Forest Genetics 2013*. Whistler, British Columbia, Canada

Dungey, H.S., Brawner, J.T., Burger, F., Carson, M., Henson, M., Jefferson, P., & Matheson, A.C. (2009). A new breeding strategy for pinus radiata in New Zealand and New South Wales. *Silvae Genetica, 58*, 28-38

Dungey, H.S., Matheson, A.C., Kain, D., & Evans, R. (2006). Genetics of wood stiffness and its component traits in Pinus radiata. *Canadian Journal of Forest Research, 36*, 1165-1178

Dungey, H.S., Russell, J.H., Costa e Silva, J., Low, C.B., Miller, M.A., Fleet, K.R., & Stovold, G.T. (2012). The effectiveness of cloning for the genetic improvement of Mexican white cypress Cupressus lusitanica (Mill.). *Tree Genetics & Genomes, 9*, 443-453

Enquist, B.J., West, G.B., & Brown, J.H. (2009). Extensions and evaluations of a general quantitative theory of forest structure and dynamics. *Proc Natl Acad Sci U S A, 106*, 7046-7051

Ferraz, A., Mallet, C., Jacquemoud, S., Goncalves, G.R., Tome, M., Soares, P., Pereira, L.G., & Bretar, F. (2015). Canopy Density Model: A New ALS-Derived Product to Generate Multilayer Crown Cover Maps. *IEEE Transactions on Geoscience and Remote Sensing, 53*, 6776-6790

Filipescu, C.N., Groot, A., MacIsaac, D.A., Cruickshank, M.G., & Stewart, J.D. (2012). Prediction of diameter using height and crown attributes: a case study. *Western Journal of Applied Forestry, 27(1)*, 30-35

Fins, L., Friedman, S.T., & Brotschol, J.V. (1992). *Handbook of quantitative forest genetics*. Springer Science & Business Media

Flewelling, J.W. (2006). Forest inventory predictions from individual tree crowns: Regression modeling within a sample framework. In R.E. McRoberts, G.A. Reams, P.C. Van Deusen, & W.H. McWilliams (Eds.), *Proceedings of the Eighth Annual Forest Inventory and Analysis Symposium* (pp. 203-210). Monterey, CA: U.S. Department of Agriculture, Forest Service

Fournier, M., Dlouha, J., Jaouen, G., & Almeras, T. (2013). Integrative biomechanics for tree ecology: beyond wood density and strength. *J Exp Bot, 64*, 4793-4815

Fu, Y.B. (2003). On implementation of incomplete block designs in forest genetic field trials. *Forest Genetics, 10*, 23-33

Gadgil, P.D. (1967). Infection of Pinus radiata needles by Dothistroma pini. *New Zealand Journal of Botany, 5*, 498-503

Gatziolis, D., & Andersen, H.E. (2008). A guide to LIDAR data acquisition and processing for the forests of the Pacific Northwest. *USDA Forest Service - General Technical Report PNW-GTR*, 1-32

Gilmour, A.R., Cullis, B.R., & Verbyla, A.P. (1997). Accounting for Natural and Extraneous Variation in the Analysis of Field Experiments. *Journal of Agricultural, Biological, and Environmental Statistics, 2*, 269-293

Gilmour, A.R., Gogel, B.J., Cullis, B.R., & Thompson, R. (2009). *ASReml User Guide Release 3.0*. Hemel Hempstead, HP1 1ES, UK www.vsni.co.uk: VSN International Ltd

Gilmour, A.R., Thompson, R., & Cullis, B.R. (1995). Average Information REML: An Efficient Algorithm for Variance Parameter Estimation in Linear Mixed Models. *Biometrics, 51*, 1440

Girard, M.C. (2003). *Processing of Remote Sensing Data*. London: Taylor & Francis

Gobakken, T., & Næsset, E. (2008). Assessing effects of laser point density, ground sampling intensity, and field sample plot size on biophysical stand properties derived from airborne laser scanner data. *Canadian Journal of Forest Research, 38*, 1095-1109

Gonzalez-Benecke, C.A., Gezan, S.A., Samuelson, L.J., Cropper, W.P., Leduc, D.J., & Martin, T.A. (2014). Estimating Pinus palustris tree diameter and stem volume from tree height, crown area and stand-level parameters. *Journal of Forestry Research, 25*, 43-52

González-Ferreiro, E., Diéguez-Aranda, U., Barreiro-Fernández, L., Buján, S., Barbosa, M., Suárez, J.C., Bye, I.J., & Miranda, D. (2013). A mixed pixel- and region-based approach for using airborne laser scanning data for individual tree crown delineation in Pinus radiata D. Don plantations. *International Journal of Remote Sensing, 34*, 7671-7690

Goulding, C.J. (1986). *Forestry handbook*. New Zealand Institute of Foresters (Inc.)

Goulding, C.J. (1998). The forest as a warehouse. In M. Hansen, & T. Burk (Eds.), *SAF / IUFRO S4.02 conference* (pp. 276-282). Boise, Idaho, USA: USDA

Groot, A. (2014). Tree crown-fibre attribute relationships for adding wood quality information to forest inventories in Canada. In, *Precision Forestry Symposium*. March 3, 2014, Stellenbosch

Groot, A., Cortini, F., & Wulder, M.A. (2015). Crown-fibre attribute relationships for enhanced forest inventory: Progress and prospects. *The Forestry Chronicle, 91*, 266-279

Groot, A., & Schneider, R. (2011). Predicting maximum branch diameter from crown dimensions, stand characteristics and tree species. *Forestry Chronicle, 87*, 542-551

Hadaś, E., & Estornell, J. (2016). Accuracy of tree geometric parameters depending on the LiDAR data density. *European Journal of Remote Sensing, 49*, 73-92

Hansen, E., Gobakken, T., & Næsset, E. (2015). Effects of pulse density on digital terrain models and canopy metrics using airborne laser scanning in a tropical rainforest. *Remote Sensing, 7*, 8453-8468

Hauglin, M., Astrup, R., Gobakken, T., & Næsset, E. (2013a). Estimating single-tree branch biomass of Norway spruce with terrestrial laser scanning using voxel-based and crown dimension features. *Scandinavian Journal of Forest Research, 28*, 456-469

Hauglin, M., Dibdiakova, J., Gobakken, T., & Næsset, E. (2013b). Estimating single-tree branch biomass of Norway spruce by airborne laser scanning. *ISPRS Journal of Photogrammetry and Remote Sensing, 79*, 147-156

Hauglin, M., Gobakken, T., Astrup, R., Ene, L., & Næsset, E. (2014a). Estimating single-tree crown biomass of norway spruce by airborne laser scanning: A comparison of methods with and without the use of terrestrial laser scanning to obtain the ground reference data. *Forests, 5*, 384-403

Hauglin, M., Lien, V., Næsset, E., & Gobakken, T. (2014b). Geo-referencing forest field plots by co-registration of terrestrial and airborne laser scanning data. *International Journal of Remote Sensing, 35*, 3135-3149

Heinimann, H.R., & Breschan, J. (2012). Pre-Harvest Assessment based on LiDAR Data. *Croatian Journal of Forest Engineering, 33*, 169-180

Hilker, T., Coops, N.C., Culvenor, D.S., Newnham, G., Wulder, M.A., Bater, C.W., & Siggins, A. (2012). A simple technique for co-registration of terrestrial LiDAR observations for forestry applications. *Remote Sensing Letters, 3*, 239-247

Hilker, T., Frazer, G.W., Coops, N.C., Wulder, M.A., Newnham, G.J., Stewart, J.D., van Leeuwen, M., & Culvenor, D.S. (2013). Prediction of wood fiber attributes from LiDAR-derived forest canopy indicators. *Forest Science, 59*, 231-242

Holmgren, J., Barth, A., Larsson, H., & Olsson, H. (2012). Prediction of stem attributes by combining airborne laser scanning and measurements from harvesters. *Silva Fennica, 46*, 227-239

Holmgren, J., & Lindberg, E. (2014). Tree crown segmentation based on a geometric tree crown model for prediction of forest variables. *Canadian Journal of Remote Sensing, 39*, S86-S98

Holopainen, M., Vastaranta, M., & Hyyppä, J. (2014). Outlook for the next generation's precision forestry in Finland. *Forests, 5*, 1682-1694

Holopainen, M., Vastaranta, M., Liang, X., Hyyppä, J., Jaakkola, A., & Kankare, V. (2013). Estimation of Forest Stock and Yield Using LiDAR Data. *Remote Sensing of Natural Resources* (pp. 259-290): CRC Press

Hudak, A.T., Crookston, N.L., Evans, J.S., Falkowski, M.J., Smith, A.M.S., Gessler, P.E., & Morgan, P. (2006). Regression modeling and mapping of coniferous forest basal area and tree density from discrete-return lidar and multispectral satellite data. *Canadian Journal of Remote Sensing, 32*, 126-138

Hyyppä, J., & Inkinen, M. (2002). Detecting and estimating attributes for single trees using laser scanner. *The Photogrammetric Journal of Finland, 18*, 43-53

Jakubowski, M.K., Guo, Q., & Kelly, M. (2013a). Tradeoffs between lidar pulse density and forest measurement accuracy. *Remote Sensing of Environment, 130*, 245-253

Jakubowski, M.K., Li, W., Guo, Q., & Kelly, M. (2013b). Delineating individual trees from lidar data: A comparison of vector- and raster-based segmentation approaches. *Remote Sensing, 5*, 4163-4186

Jayawickrama, K.J.S. (2001). Genetic parameter estimates for radiata pine in New Zealand and New South Wales: A synthesis of results. *Silvae Genetica, 50*, 45-53

Jayawickrama, K.J.S., & Carson, M.J. (2000). A breeding strategy for the New Zealand Radiata Pine Breeding Cooperative. *Silvae Genetica, 49*, 82-90

Kaartinen, H., & Hyyppa, J. (2008). EuroSDR/ISPRS Project, Commission II "Tree Extraction"; Final Report; Official Publication No. 53;. In. Dublin, Ireland: EuroSDR (European Spatial Data Research)

Kaartinen, H., Hyyppä, J., Vastaranta, M., Kukko, A., Jaakkola, A., Yu, X., Pyörälä, J., Liang, X., Liu, J., Wang, Y., Kaijaluoto, R., Melkas, T., Holopainen, M., & Hyyppä, H. (2015). Accuracy of kinematic positioning using global satellite navigation systems under forest canopies. *Forests, 6*, 3218-3236

Kaartinen, H., Hyyppä, J., Yu, X., Vastaranta, M., Hyyppä, H., Kukko, A., Holopainen, M., Heipke, C., Hirschmugl, M., Morsdorf, F., Næsset, E., Pitkänen, J., Popescu, S., Solberg, S., Wolf, B.M., & Wu, J.-C. (2012). An international comparison of individual tree detection and extraction using airborne laser scanning. *Remote Sensing, 4*, 950-974

Kane, V.R., McGaughey, R.J., Bakker, J.D., Gersonde, R.F., Lutz, J.A., & Franklin, J.F. (2010). Comparisons between field- and LiDAR-based measures of stand structural complexity. *Canadian Journal of Forest Research, 40*, 761-773

Kankare, V., Liang, X., Vastaranta, M., Yu, X., Holopainen, M., & Hyyppä, J. (2015). Diameter distribution estimation with laser scanning based multisource single tree inventory. *ISPRS Journal of Photogrammetry and Remote Sensing, 108*, 161-171

Kankare, V., Vastaranta, M., Holopainen, M., Räty, M., Yu, X., Hyyppä, J., Hyyppä, H., Alho, P., & Viitala, R. (2013). Retrieval of forest aboveground biomass and stem volume with airborne scanning LiDAR. *Remote Sensing, 5*, 2257-2274

Kankare, V., Vauhkonen, J., Tanhuanpa¨a¨, T., Holopainen, M., Vastaranta, M., Joensuu, M., Krooks, A., Hyyppa¨, J., Hyyppa¨, H., Alho, P., & Viitala, R. (2014). Accuracy in estimation of timber assortments and stem distribution - A comparison of airborne and terrestrial laser scanning techniques. *ISPRS Journal of Photogrammetry and Remote Sensing, 97*, 89-97

Kantola, T., Vastaranta, M., Lyytikäinen-Saarenmaa, P., Holopainen, M., Kankare, V., Talvitie, M., & Hyyppä, J. (2013). Classification of needle loss of individual Scots Pine trees by means of airborne laser scanning. *Forests, 4*, 386-403

Kantola, T., Vastaranta, M., Yu, X., Lyytikainen-Saarenmaa, P., Holopainen, M., Talvitie, M., Kaasalainen, S., Solberg, S., & Hyyppa, J. (2010). Classification of defoliated trees using tree-level airborne laser scanning data combined with aerial images. *Remote Sensing, 2*, 2665-2679

Kato, A., Morgenroth, J., Kelbe, D., Gomez, C., & Van Aardt, J. (2013). Ground truth measurement of trees using terrestrial laser for satellite remote sensing. In, *International Geoscience and Remote Sensing Symposium (IGARSS)* (pp. 2106-2109)

Kaufman, L., & Rousseeuw, P.J. (2008). *Finding groups in data: An introduction to cluster analysis*. John Wiley & Sons, Inc.

Ke, Y., Zhang, W., & Quackenbush, L.J. (2010). Active contour and hill climbing for tree crown detection and delineation. *Photogrammetric Engineering and Remote Sensing, 76*, 1169-1181

Kempes, C.P., West, G.B., Crowell, K., & Girvan, M. (2011). Predicting maximum tree heights and other traits from allometric scaling and resource limitations. *PLoS ONE, 6*, e20551

Kennedy, S.G., Cameron, A.D., & Lee, S.J. (2013). Genetic relationships between wood quality traits and diameter growth of juvenile core wood in Sitka spruce. *Canadian Journal of Forest Research, 43*, 1-6

Kennedy, S.G., Yanchuk, A.D., Stackpole, D.J., & Jefferson, P.A. (2014). Incorporating non-key traits in selecting the Pinus radiata production population. *New Zealand Journal of Forestry Science, 44*, 1-9

Khosravipour, A., Skidmore, A.K., Isenburg, M., Wang, T., & Hussin, Y.A. (2013). Development of an algorithm to generate a Lidar pit-free canopy height model. In, *Silvilaser 2013*. Beijing

Khosravipour, A., Skidmore, A.K., Isenburg, M., Wang, T., & Hussin, Y.A. (2014). Generating pit-free canopy height models from airborne Lidar. *Photogrammetric Engineering & Remote Sensing, 80*, 863-872

Kim, Y., Chang, A., & Eo, Y. (2012). Estimation of forest biomass based on segmentation using airborne LiDAR data. In (pp. 309-312)

Kimberley, M.O., Cown, D.J., McKinley, R.B., Moore, J.R., & Dowling, L.J. (2015a). Modelling variation in wood density within and among trees in stands of New Zealand-grown radiata pine. *New Zealand Journal of Forestry Science, 45*, 1-13

Kimberley, M.O., Moore, J.R., & Dungey, H.S. (2015b). Quantification of realised genetic gain in radiata pine and its incorporation into growth and yield modelling systems. *Canadian Journal of Forest Research, 45*, 1676-1687

Kleinbaum, D., Kupper, L., Nizam, A., & Rosenberg, E. (2013). *Applied regression analysis and other multivariable methods*. Cengage Learning

Korhonen, L., & Mosdorf, F. (2014). Estimation of canopy cover, gap fraction and leaf area index with airborne laser scanning. In M. Maltamo, E. Naesset, & J. Vauhkonen (Eds.), *Forestry Applications of Airborne Laser Scanning* (p. 484): Springer

Korhonen, L., Vauhkonen, J., Virolainen, A., Hovi, A., & Korpela, I. (2013). Estimation of tree crown volume from airborne lidar data using computational geometry. *International Journal of Remote Sensing, 34*, 7236-7248

La, H.P., Eo, Y.D., Chang, A., & Kim, C. (2015). Extraction of individual tree crown using hyperspectral image and LiDAR data. *KSCE Journal of Civil Engineering, 19*, 1078-1087

Larsen, M., Eriksson, M., Descombes, X., Perrin, G., Brandtberg, T., & Gougeon, F.A. (2011). Comparison of six individual tree crown detection algorithms evaluated under varying forest conditions. *International Journal of Remote Sensing, 32*, 5827-5852

Larson, P.R. (1962). A biological approach to wood quality. *Tappi, 45*, 443-448

Larson, P.R. (1963). Stem form development of forest trees. *Forest Science Monographs, 5*, 42

Larson, P.R. (1969). *Wood formation and the concept of wood quality*. Yale University

Leech, J.W. (1984). Estimating crown width from diameter at breast height for opengrown radiata pine trees in South Australia. *Australian Forest Research, 14*, 333-337

Lefsky, M.A., Hudak, A.T., Cohen, W.B., & Acker, S.A. (2005). Patterns of covariance between forest stand and canopy structure in the Pacific Northwest. *Remote Sensing of Environment, 95*, 517-531

Legendre, P., & Legendre, L. (2012). Numerical Ecology. *3rd English Edition*

Lemmens, M. (2015). Photon Lidar, a promising advance in mapping applications. In, *GIM International*

Lenz, P., Bernier-Cardou, M., Mac, J., & Beaulieu, J. (2012). Can wood properties be predicted from the morphological traits of a tree? A canonical correlation study of plantation-grown white spruce. *Canadian Journal of Forest Research, 42*, 1518-1529

Lindberg, E., Holmgren, J., Olofsson, K., & Olsson, H. (2012). Estimation of stem attributes using a combination of terrestrial and airborne laser scanning. *European Journal of Forest Research, 131*, 1917-1931

Lindberg, E., Holmgren, J., Olofsson, K., Olsson, H., & Wallerman, J. (2008). Estimation of tree lists from airborne laser scanning data using a combination of analysis on single tree and raster cell level. *Proceedings of the SilviLaser 2008 Conference, Edinburgh, UK*

Lindberg, E., Holmgren, J., Olofsson, K., Wallerman, J., & Olsson, H. (2010). Estimation of tree lists from airborne laser scanning by combining single-tree and area-based methods. *International Journal of Remote Sensing, 31*, 1175-1192

Lindberg, E., Holmgren, J., Olofsson, K., Wallerman, J., & Olsson, H. (2013). Estimation of tree lists from airborne laser scanning using tree model clustering and k-MSN imputation. *Remote Sensing, 5*, 1932-1955

Liu, H., & Dong, P. (2014). A new method for generating canopy height models from discrete-return LiDAR point clouds. *Remote Sensing Letters, 5*, 575-582

Liu, H., Wang, L., Sherman, D., Gao, Y., & Wu, Q. (2010). An object-based conceptual framework and computational method for representing and analyzing coastal morphological changes. *International Journal of Geographical Information Science, 24*, 1015-1041

Liu, S.M., Constable, G.A., Cullis, B.R., Stiller, W.N., & Reid, P.E. (2014). Benefit of spatial analysis for furrow irrigated cotton breeding trials. *Euphytica, 201*, 253-264

Lo, C.S., & Lin, C. (2013). Growth-competition-based stem diameter and volume modeling for tree-level forest inventory using airborne LiDAR data. *IEEE Transactions on Geoscience and Remote Sensing, 51*, 2216-2226

Lu, X., Guo, Q., Li, W., & Flanagan, J. (2014). A bottom-up approach to segment individual deciduous trees using leaf-off lidar point cloud data. *ISPRS Journal of Photogrammetry and Remote Sensing, 94*, 1-12

Luther, J.E. (2013). Predicting and mapping forest inventory attributes in NL using airborne LiDAR. In, *CIF Inventory Workshop*. Corner Brook, NL

Luther, J.E., Skinner, R., Bowers, W.W., Fournier, R.A., van Lier, O.R., & Côté, J.-F. (2012). Predicting forest structure and fibre attributes of insular Newfoundland using airborne laser scanner (ALS) data. In, *Promoting science-based applications of remote sensing, ForestSAT 2012*. Corvallis, Oregon, USA

Luther, J.E., Skinner, R., Fournier, R.A., Van Lier, O.R., Bowers, W.W., Coté, J.F., Hopkinson, C., & Moulton, T. (2014). Predicting wood quantity and quality attributes of balsam fir and black spruce using airborne laser scanner data. *Forestry, 87*, 313-326

Madgwick, H.A.I. (1994). *Pinus radiata - biomass, form and growth*. Rotorua

Magnusson, M., Fransson, J.E.S., & Holmgren, J. (2007). Effects on estimation accuracy of forest variables using different pulse density of laser data. *Forest Science, 53*, 619-626

Maltamo, M., Naesset, E., & Vauhkonen, J. (2014). *Forestry applications of airborne laser scanning*. Springer

McGaughey, R.J., & Carson, W.W. (2003). Fusing LIDAR data, photographs, and other data using 2D and 3D visualization techniques. In A.S.f.P.R. Sensing (Ed.), *Proceedings of Terrain Data: Applications and Visualization – Making the Connection* (pp. 16-24). Charleston, South Carolina: American Society for Photogrammetry and Remote Sensing

McRoberts, R.E., Cohen, W.B., Næsset, E., Stehman, S.V., & Tomppo, E.O. (2010). Using remotely sensed data to construct and assess forest attribute maps and related spatial products. *Scandinavian Journal of Forest Research, 25*, 340-367

Mead, D.J. (2013). *Sustainable management of Pinus radiata plantations*. Rome: FAO

Mikita, T., Klimánek, M., & Cibulka, M. (2013). Evaluation of interpolation methods of airborne laser scanning data for detection of trees and their heights. *Hodnocení metod interpolace dat leteckého laserového skenování pro detekci stromů a měření jejich výšek, 58*, 99-106

Moore, J.R., Cown, D.J., McKinley, R.B., & Sabatia, C.O. (2015). Effects of stand density and seedlot on three wood properties of young radiata pine grown at a dry-land site in New Zealand. *New Zealand Journal of Forestry Science, 45*, 1-15

Næsset, E. (2002). Predicting forest stand characteristics with airborne scanning laser using a practical two-stage procedure and field data. *Remote Sensing of Environment, 80*, 88-99

Næsset, E. (2004). Practical large-scale forest stand inventory using a small-footprint airborne scanning laser. *Scandinavian Journal of Forest Research, 19*, 164-179

Næsset, E., Bollandsås, O.M., & Gobakken, T. (2005). Comparing regression methods in estimation of biophysical properties of forest stands from two different inventories using laser scanner data. *Remote Sensing of Environment, 94*, 541-553

Næsset, E., Gobakken, T., Holmgren, J., Hyyppä, H., Hyyppä, J., Maltamo, M., Nilsson, M., Olsson, H., Persson, Å., & Söderman, U. (2004). Laser scanning of forest resources: The nordic experience. *Scandinavian Journal of Forest Research, 19*, 482-499

Næsset, E., & Økland, T. (2002). Estimating tree height and tree crown properties using airborne scanning laser in a boreal nature reserve. *Remote Sensing of Environment, 79*, 105-115

NZ Forest Owners Association (2012). *New Zealand forestry science and innovation plan*. Wellington, New Zealand: NZ Forest Owners Association

Optech (2014). Optech PEGASUS HA500 summary specification sheet. In (p. 2). Canada: Optech Incorporated

Oshio, H., Asawa, T., Hoyano, A., & Miyasaka, S. (2015). Estimation of the leaf area density distribution of individual trees using high-resolution and multi-return airborne LiDAR data. *Remote Sensing of Environment, 166*, 116-125

Packalen, P., Vauhkonen, J., Kallio, E., Peuhkurinen, J., Pitkänen, J., Pippuri, I., Strunk, J., & Maltamo, M. (2013). Predicting the spatial pattern of trees by airborne laser scanning. *International Journal of Remote Sensing, 34*, 5154-5165

Paris, C., & Bruzzone, L. (2014). A Three-Dimensional Model-Based Approach to the Estimation of the Tree Top Height by Fusing Low-Density LiDAR Data and Very High Resolution Optical Images. *IEEE Transactions on Geoscience and Remote Sensing*

Paris, C., Valduga, D., & Bruzzone, L. (2016). A Hierarchical Approach to Three-Dimensional Segmentation of LiDAR Data at Single-Tree Level in a Multilayered Forest. *IEEE Transactions on Geoscience and Remote Sensing, 54*, 4190-4203

Persson, Å., Holmgren, J., & Söderman, U. (2002). Detecting and measuring individual trees using an airborne laser scanner. *Photogrammetric Engineering and Remote Sensing, 68*, 925-932

Peuhkurinen, J., Mehtätalo, L., & Maltamo, M. (2011). Comparing individual tree detection and the area based statistical approach for the retrieval of forest stand characteristics using airborne laser scanning in Scots pine stands. *Canadian Journal of Forest Research, 41*, 583-598

Pont, D. (2003). A model of secondary growth For Radiata Pine: Stem ring width and basic density variation in relation to crown structure. In, *School of Forestry* (p. 183). Christchurch, New Zealand: University of Canterbury

Pont, D., Holt, L., Brownlie, R., Goulding, C., & Kimberley, M. (2012a). Improved tree counts from remotely sensed images of planted forests. In, *ForestSAT 2012*. Oregon State University, Corvallis, Oregon, USA

Pont, D., Kimberley, M., Brownlie, R., Morgenroth, J., & Watt, S.M. (2015a). Tree counts from airborne LiDAR. *New Zealand Journal of Forestry, 60*, 45-60

Pont, D., Kimberley, M.O., Brownlie, R.K., Sabatia, C.O., & Watt, M.S. (2015b). Calibrated tree counting on remotely sensed images of planted forests. *International Journal of Remote Sensing, 36*, 3819-3836

Pont, D., & Lorraine, I. (2015). Slam Dunk. In, *GeoConnexion International* (pp. 30-31). Cambridge, United Kingdom: GeoConnexion Limited

Pont, D., Morgenroth, J., & Watt, M.S. (2013). Tree-based analysis of ALS to estimate tree size and quality. In, *MeMoWood - Measurement Methods and Modelling Approaches for Predicting Desirable Future Wood Properties*. Nancy, France

Pont, D., Watt, M.S., Adams, T., Marshall, H., Lee, J., Crawley, D., & Watt, P.J. (2012b). Modelling variation in Pinus radiata stem velocity from area- and crown- based LiDAR metrics. In N. Coops, & M. Wulder (Eds.), *SilviLaser 2012* Vancouver, Canada: Silvilaser 2012 Organizing Committee

Prieditis, G., Šmits, I., Arhipova, I., Daģis, S., & Dubrovskis, D. (2012). Tree diameter models from field and remote sensing data. *International Journal of Mathematical Models and Methods in Applied Sciences, 6*, 707-714

R Core Team (2014). R: A language and environment for statistical computing. In. Vienna, Austria: R Foundation for Statistical Computing

Roberts, S.D., Dean, T.J., Evans, D.L., McCombs, J.W., Harrington, R.L., & Glass, P.A. (2005). Estimating individual tree leaf area in loblolly pine plantations using LiDAR-derived measurements of height and crown dimensions. *Forest Ecology and Management, 213*, 54-70

Ronse, C., & Heijmans, H.J.A.M. (1991). The algebraic basis of mathematical morphology: II. Openings and closings. *CVGIP: Image Understanding, 54*, 74-97

Routescene (2015). Routescene LidarPod user guide 5 June 2015. In. Edinburgh: Mapix Technologies Ltd

Scion (2014). *Growing confidence in forestry's future: Research programme 2013-2019.* Rotorua, New Zealand: Forest Research Institute Ltd

Silva, C.A., Hudak, A.T., Vierling, L.A., Loudermilk, E.L., O'Brien, J.J., Hiers, J.K., Jack, S.B., Gonzalez-Benecke, C., Lee, H., Falkowski, M.J., & Khosravipour, A. (2016).

Imputation of Individual Longleaf Pine (Pinus palustris Mill.) Tree Attributes from Field and LiDAR Data. *Canadian Journal of Remote Sensing*, 1-20

Smith, D.M. (1954). Maximum moisture content method for determining specific gravity of small wood samples [R]. *US Forest Service, Forest Products Laboratory. 1954, Report No: 2014*

Smyrnaios, M., Schön, S., & Liso Nicolás, M. (2013). Multipath propagation, characterization and modeling in GNSS. *Geodetic Sciences - Observations, Modeling and Applications*, 99-125

Solberg, S., Naesset, E., & Bollandsas, O.M. (2006a). Single tree segmentation using airborne laser scanner data in a structurally heterogeneous spruce forest. *Photogrammetric Engineering and Remote Sensing, 72*, 1369-1378

Solberg, S., Næsset, E., Hanssen, K.H., & Christiansen, E. (2006b). Mapping defoliation during a severe insect attack on Scots pine using airborne laser scanning. *Remote Sensing of Environment, 102*, 364-376

St-Onge, B., Audet, F.-A., & Bégin, J. (2015). Characterizing the Height Structure and Composition of a Boreal Forest Using an Individual Tree Crown Approach Applied to Photogrammetric Point Clouds. *Forests, 6*, 3899-3922

St-Onge, B., & Audet, F.A. (2015). Comparing Photogrammetric and Airborne-LiDAR Point Clouds in Individual Tree Crown Delineation and Species Identification. In

Stone, C., Penman, T., & Turner, R. (2011). Determining an optimal model for processing lidar data at the plot level: Results for a Pinus radiata plantation in New South Wales, Australia. *New Zealand Journal of Forestry Science, 41*, 191-205

Suárez, J.C. (2010). An Analysis of the Consequences of Stand Variability in Sitka Spruce Plantations in Britain using a combination of airborne LiDAR analysis and models. In (p. 295). Sheffield: University of Sheffield

Swetnam, T.L., & Falk, D.A. (2014). Application of metabolic scaling theory to reduce error in local maxima tree segmentation from aerial LiDAR. *Forest Ecology and Management, 323*, 158-167

Tang, H., Brolly, M., Zhao, F., Strahler, A.H., Schaaf, C.L., Ganguly, S., Zhang, G., & Dubayah, R. (2014). Deriving and validating Leaf Area Index (LAI) at multiple spatial scales through lidar remote sensing: A case study in Sierra National Forest, CA. *Remote Sensing of Environment, 143*, 131-141

Tang, S., Dong, P., & Buckles, B.P. (2013). Three-dimensional surface reconstruction of tree canopy from lidar point clouds using a region-based level set method. *International Journal of Remote Sensing, 34*, 1373-1385

Telfer, E.J., Pont, D., Dash, J., Dungey, H.S., & Moore, J.R. (2015). Whole forest modelling: Reconstructing the past, present and future performance of trees with big data. In, *QMB: Computational Genomics Satellite meeting*. Queenstown, New Zealand

Turner, R., Stone, C., Kathuria, A., & Penman, T. (2011). Towards an operational lidar resource inventory process in Australian softwood plantations. In, *34th International Symposium for Remote Sensing of the Environment*. Sydney, Australia

Valbuena, R. (2014). Integrating airborne laser scanning with data from global navigation satellite systems and optical sensors. In M. Maltamo, E. Naesset, & J. Vauhkonen (Eds.), *Forestry Applications of Airborne Laser Scanning* (p. 484): Springer

Valbuena, R., Mauro, F., Rodriguez-Solano, R., & Manzanera, J.A. (2010). Accuracy and precision of GPS receivers under forest canopies in a mountainous environment. *Exactitud y precisiońn de receptores GPS bajo cubiertas forestales en ambientes montañosos, 8*, 1047-1057

van der Pas, J.B. (1981). Reduced early growth rates of Pinus radiata caused by Dothistroma pini. *New Zealand Journal of Forestry Science, 11*, 210-220

van der Pas, J.B., Bulman, L., & Slater-Hayes, J.D. (1984). Evaluation of the assessment of Dothistroma needle blight in stands of Pinus radiata. *New Zealand Journal of Forestry Science, 14*, 3-13

van Diggelen, F. (2007). GNSS accuracy: Lies, damn lies, and statistics. *GPS World, 18*, 26-32

Van Leeuwen, M., Hilker, T., Coops, N.C., Frazer, G., Wulder, M.A., Newnham, G.J., & Culvenor, D.S. (2011). Assessment of standing wood and fiber quality using ground and airborne laser scanning: A review. *Forest Ecology and Management, 261*, 1467-1478

van Rossum, G. (1995). Python tutorial, Technical Report CS-R9526. In. Amsterdam: Centrum voor Wiskunde en Informatica (CWI)

Vastaranta, M., Kankare, V., Holopainen, M., Yu, X., Hyyppä, J., & Hyyppä, H. (2012). Combination of individual tree detection and area-based approach in imputation of forest variables using airborne laser data. *ISPRS Journal of Photogrammetry and Remote Sensing, 67*, 73-79

Vastaranta, M., Kantola, T., Lyytikäinen-Saarenmaa, P., Holopainen, M., Kankare, V., Wulder, M., Hyyppä, J., & Hyyppä, H. (2013). Area-based mapping of defoliation of Scots Pine stands using airborne scanning LiDAR. *Remote Sensing, 5*, 1220-1234

Vauhkonen, J., Ene, L., Gupta, S., Heinzel, J., Holmgren, J., Pitkanen, J., Solberg, S., Wang, Y., Weinacker, H., Hauglin, K.M., Lien, V., Packalen, P., Gobakken, T., Koch, B., Naesset, E., Tokola, T., & Maltamo, M. (2011). Comparative testing of single-tree detection algorithms under different types of forest. *Forestry, 85*, 27-40

Vauhkonen, J., Korpela, I., Maltamo, M., & Tokola, T. (2010). Imputation of single-tree attributes using airborne laser scanning-based height, intensity, and alpha shape metrics. *Remote Sensing of Environment, 114*, 1263-1276

Vauhkonen, J., & Mehtätalo, L. (2015). Matching remotely sensed and field-measured tree size distributions. *Canadian Journal of Forest Research, 45*, 353-363

Vauhkonen, J., Rombouts, J., & Maltamo, M. (2014). Inventory of forest plantations. In M. Maltamo, E. Naesset, & J. Vauhkonen (Eds.), *Forestry Applications of Airborne Laser Scanning* (p. 484): Springer

Vauhkonen, J., Tokola, T., Maltamo, M., & Packalén, P. (2008). Effects of pulse density on predicting characteristics of individual trees of Scandinavian commercial species using alpha shape metrics based on airborne laser scanning data. *Canadian Journal of Remote Sensing, 34*, S441-S459

Vega, C., Hamrouni, A., El Mokhtari, A., Morel, M., Bock, J., Renaud, J.P., Bouvier, M., & Durrieue, S. (2014). PTrees: A point-based approach to forest tree extraction from lidar data. *International Journal of Applied Earth Observation and Geoinformation, 33*, 98-108

Visscher, P.M., Hill, W.G., & Wray, N.R. (2008). Heritability in the genomics era - Concepts and misconceptions. *Nature Reviews Genetics, 9*, 255-266

Waff, C.B. (1976). Isaac Newton, the motion of the lunar apogee, and the establishment of the inverse square law. *Vistas in Astronomy, 20*, 99-103

Waghorn, M.J., Watt, M.S., & Mason, E.G. (2007). Influence of tree morphology, genetics, and initial stand density on outerwood modulus of elasticity of 17-year-old Pinus radiata. *Forest Ecology and Management, 244*, 86-92

Wallace, L., Lucieer, A., Malenovský, Z., Turner, D., & Vopěnka, P. (2016). Assessment of Forest Structure Using Two UAV Techniques: A Comparison of Airborne Laser Scanning and Structure from Motion (SfM) Point Clouds. *Forests, 7*, 62

Wallace, L., Lucieer, A., & Watson, C.S. (2014a). Evaluating tree detection and segmentation routines on very high resolution UAV LiDAR ata. *IEEE Transactions on Geoscience and Remote Sensing, 52*, 7619-7628

Wallace, L., Watson, C., & Lucieer, A. (2014b). Detecting pruning of individual stems using airborne laser scanning data captured from an Unmanned Aerial Vehicle. *International Journal of Applied Earth Observation and Geoinformation, 30*, 76-85

Wallace, L.O., Lucieer, A., & Watson, C.S. (2012). Assessing the feasibility of UAV-based Lidar for high resolution forest change detection. *ISPRS - International Archives of the Photogrammetry, Remote Sensing and Spatial Information Sciences, XXXIX-B7*, 499-504

Wang, F., Letort, V., Lu, Q., Bai, X., Guo, Y., de Reffye, P., & Li, B. (2012). A functional and structural Mongolian Scots pine (Pinus sylvestris var. mongolica) model integrating architecture, biomass and effects of precipitation. *PLoS ONE, 7*, 1-13

Wang, Y., Hyyppa, J., Liang, X., Kaartinen, H., Yu, X., Lindberg, E., Holmgren, J., Qin, Y., Mallet, C., Ferraz, A., Torabzadeh, H., Morsdorf, F., Zhu, L., Liu, J., & Alho, P. (2016). International benchmarking of the individual tree detection methods for modeling 3-D canopy structure for silviculture and forest ecology using airborne laser scanning. *IEEE Transactions on Geoscience and Remote Sensing*

Watt, M., Bulman, L., & Palmer, D. (2011). The economic cost of Dothistroma needle blight to the New Zealand forest industry. *New Zealand Journal of Forestry, 56*, 20-22

Watt, M.S., Adams, T., Aracil, S.G., Marshall, H., & Watt, P. (2013a). The influence of LiDAR pulse density and plot size on the accuracy of New Zealand plantation stand volume equations. *New Zealand Journal of Forestry Science, 43*, 1-10

Watt, M.S., Adams, T., Marshall, H., Pont, D., Lee, J., Crawley, D., & Watt, P. (2013b). Modelling variation in Pinus radiata stem volume and outerwood stress-wave velocity from LiDAR metrics. *New Zealand Journal of Forestry Science, 43*, 1-7

Watt, M.S., & Kirschbaum, M.U.F. (2011). Moving beyond simple linear allometric relationships between tree height and diameter. *Ecological Modelling, 222*, 3910-3916

Watt, M.S., Meredith, A., Watt, P., & Gunn, A. (2013c). Use of LiDAR to estimate stand characteristics for thinning operations in young douglas-fir plantations. *New Zealand Journal of Forestry Science, 43*, 1-10

Watt, M.S., Meredith, A., Watt, P., & Gunn, A. (2014). The influence of LiDAR pulse density on the precision of inventory metrics in young unthinned Douglas-fir stands during initial and subsequent LiDAR acquisitions. *New Zealand Journal of Forestry Science, 44*, 1-9

Watt, M.S., & Zoric, B. (2010). Development of a model describing modulus of elasticity across environmental and stand density gradients in plantation-grown Pinus radiata within New Zealand. *Canadian Journal of Forest Research, 40*, 1558-1566

Watt, P. (2005). An evaluation of LiDAR and optical satellite data for the measurement of structural attributes in British upland conifer plantation forestry. In, *Department of Geography*: University of Durham, England

Watt, P.J., & Watt, M.S. (2013). Development of a national model of Pinus radiata stand volume from LiDAR metrics for New Zealand. *International Journal of Remote Sensing, 34*, 5892-5904

Wehr, A., & Lohr, U. (1999). Airborne laser scanning—an introduction and overview. *ISPRS Journal of Photogrammetry and Remote Sensing, 54*, 68-82

White, J.C., Wulder, M.A., Varhola, A., Vastaranta, M., Coops, N.C., Cook, B.D., Pitt, D., & Woods, M. (2013). A best practices guide for generating forest inventory attributes from airborne laser scanning data using an area-based approach (Version 2.0). In. Victoria, British Columbia: Canadian Wood Fibre Centre

White, T.L., Adams, W.T., & Neale, D.B. (2007). *Forest genetics*. Oxfordshire, UK: CABI Publishing, CAB International

Wilcox, M.D. (1982). Genetic variation and inheritance of resistance to Dothistroma needle blight in Pinus radiata. *New Zealand Journal of Forestry Science, 12*, 14-35

Williams, E.R., John, J.A., & Whitaker, D. (1999). Example of block designs for plant and tree breeding trials. *Australian and New Zealand Journal of Statistics, 41*, 277-284

Wing, M.G., & Eklund, A. (2007). Performance comparison of a low-cost mapping grade global positioning systems (GPS) receiver and consumer grade GPS receiver under dense forest canopy. *Journal of Forestry, 105*, 9-14

Wing, M.G., Eklund, A., & Kellogg, L.D. (2005). Consumer-grade global positioning system (GPS) accuracy and reliability. *Journal of Forestry, 103*, 169-173

Woollons, R.C., & Hayward, W.J. (1984). Growth losses in Pinus radiata stands unsprayed for Dothistroma pini. *New Zealand Journal of Forestry Science, 14*, 14-22

Wu, B., Yu, B., Wu, Q., Huang, Y., Chen, Z., & Wu, J. (2016). Individual tree crown delineation using localized contour tree method and airborne LiDAR data in coniferous forests. *International Journal of Applied Earth Observation and Geoinformation, 52*, 82-94

Wulder, M.A., White, J.C., Nelson, R.F., Næsset, E., Ørka, H.O., Coops, N.C., Hilker, T., Bater, C.W., & Gobakken, T. (2012). Lidar sampling for large-area forest characterization: A review. *Remote Sensing of Environment, 121*, 196-209

Xu, Q., Hou, Z., Maltamo, M., & Tokola, T. (2014). Calibration of area based diameter distribution with individual tree based diameter estimates using airborne laser scanning. *ISPRS Journal of Photogrammetry and Remote Sensing, 93*, 65-75

Yu, X., Hyyppä, J., Vastaranta, M., Holopainen, M., & Viitala, R. (2011). Predicting individual tree attributes from airborne laser point clouds based on the random forests technique. *ISPRS Journal of Photogrammetry and Remote Sensing, 66*, 28-37

Zas, R. (2006). Iterative kriging for removing spatial autocorrelation in analysis of forest genetic trials. *Tree Genetics & Genomes, 2*, 177-185

Zhang, J., Sohn, G., & Brédif, M. (2014). A hybrid framework for single tree detection from airborne laser scanning data: A case study in temperate mature coniferous forests in Ontario, Canada. *ISPRS Journal of Photogrammetry and Remote Sensing, 98*, 44-57

Zhang, W., Quackenbush, L.J., Im, J., & Zhang, L. (2012). Indicators for separating undesirable and well-delineated tree crowns in high spatial resolution images. *International Journal of Remote Sensing, 33*, 5451-5472

Zhao, D., Pang, Y., Li, Z., & Liu, L. (2014). Isolating individual trees in a closed coniferous forest using small footprint lidar data. *International Journal of Remote Sensing, 35*, 7199-7218

Zhen, Z., Quackenbush, L., & Zhang, L. (2016). Trends in automatic individual tree crown detection and delineation - Evolution of LiDAR data. *Remote Sensing, 8*, 333

Zhen, Z., Quackenbush, L.J., Stehman, S.V., & Zhang, L. (2015). Agent-based region growing for individual tree crown delineation from airborne laser scanning (ALS) data. *International Journal of Remote Sensing, 36*, 1965-1993

Appendix A Positional Error under Forest Canopy

A.1 Introduction

The ability to obtain accurate positional information on the ground is essential for precision forestry applications (Holopainen et al. 2013; Kaartinen et al. 2015) and GNSS systems are widely used when positional information is needed in the forest. Published accuracy statements by GNSS equipment manufacturers and vendors are often for idealised conditions with an unobstructed view of the sky (Bakula et al. 2015). Such accuracy statements are therefore of little relevance in forestry conditions where terrain and canopy cover can cause satellite signals to be blocked or attenuated, and deflections can cause multipath problems, resulting in increased positional error (Kaartinen et al. 2015; Smyrnaios et al. 2013; Valbuena 2014). It was thus seen as necessary to quantify GNSS error under New Zealand forest conditions in order to understand the implications for tree-based analyses of LiDAR.

A.2 Methods

A forest stand due for operational harvest was selected to evaluate GNSS accuracy using a novel approach that has not been used in the reviewed literature. The stand contained a research trial where treatment blocks were marked with corner pegs. The co-ordinates of 11 pegs were determined using a number of GNSS devices prior to harvest. Accurate reference locations were determined subsequently, using a mapping-grade differentially-corrected GNSS at the test positions, after the stand was clearfelled.

A.2.1. Study area

The investigation of GNSS positional error was carried out at a polycross progeny trial (R 664/2) in compartment 327 at Kaingaroa forest in the central North Island of New Zealand. The trial and surrounding stand were planted in 1975, with mean tree height of 48.9 m and age 39 years at the time of measurement. The trial and the surrounding area were flat, sloping slightly to the west at less than 5 degrees, with no significant topographic barriers to GNSS signals.

Photographs taken looking straight up from each of the test peg locations illustrate the high degree of canopy cover typical at the test locations within the trial (Figure A.1).

Figure A.1. Vertical photograph showing degree of canopy cover at a test trial peg.

Trees were located in blocks within the trial, with a grid layout of 8 by 6 trees and spacing of 5 m x 4 m respectively. Block corners were marked with wooden pegs located in mid-row positions. Selected pegs were used as test positions where GNSS coordinates were collected. Test measurements were carried out before harvest in March and September 2014 using different combinations of receiver, antenna, residency time, and differential correction. Not all combinations of the factors were evaluated in the tests. For example, the Garmin 64S receiver cannot be fitted with an external antenna so this test was not made, and tests of longer residency time were only made with the Geo7X fitted with an external antenna to avoid onerous data collection time in the field. After harvest, in December 2014, reference locations were established at the test positions.

This trial was used specifically to evaluate GNSS error under canopy as it offered the opportunity to determine positions before and after clearfelling of the stand. Analyses in this thesis research were carried out using measurements of tree attributes in another genetics trial in Kaingaroa forest. The canopy conditions at this trial site represented a relatively high level of GNSS signal blocking and resultant positional error due to the mature age of the stand. Therefore estimates of horizontal error and precision are expected to be conservative with respect to younger stands

A.2.2. GNSS equipment

Three GNSS receivers were used in this study. The GPS Pathfinder ProXRT and Geo7X (both Trimble Navigation Ltd., Sunnyvale, CA, United States) are GLONASS (Russian GNSS satellite system) capable mapping-grade receivers able to deliver decimetre accuracy in open-sky conditions and capable of differential correction by post-processing. The Geo7X receiver also incorporates Trimble Floodlight satellite shadow (multipath) reduction technology. The Garmin 64S receiver (Garmin International Inc. Lenexa, Kansas, United States) is a GLONASS capable recreational grade receiver, for which the manufacturer claims 2 - 3 m accuracy in ideal conditions. Fitting of an external antenna, and differential correction by post-processing, are not possible for the Garmin 64S. A Tornado antenna (Trimble Navigation Ltd., Sunnyvale, CA, United States) mounted 2 m above ground on a tripod was used for tests with an external antenna with the Geo7X and ProXRT receivers. The term device is used to refer to a combination of a GNSS receiver and antenna (internal or external). Corrections were carried out by post processing using Trimble GPS Pathfinder Office version 5.6 for data recorded by the Trimble devices.

A.2.3. GNSS test field surveys

A set of 11 pegs within the trial were selected as test positions. The GNSS receiver, or external antenna when used, was centred over the test pegs. For the ProXRT and Geo7X receivers, GNSS epochs (positions) were logged at one second intervals until the number of positions required for the test, 300 or 500 positions, were recorded. With the Garmin 64S receiver

positions were recorded until the device reported 100% accuracy. The time taken for this averaged approximately five minutes, and was therefore considered comparable with recording of 300 positions with the Trimble receivers. An initial survey carried out with the ProXRT on 28th March gave a set of locations designated as tests 8 and 9. Further tests carried out on the 8th, 9th and 15th of September gave locations for designated test numbers 1 to 7. Key characteristics of the tests are described in Table A.1.

Table A.1. Characteristics of GNSS devices and configurations tested.

Test	Receiver	Mount	Antenna	Residency time (s)	Correction
1	Garmin 64S	Hand-held	Internal	300*	N
2	Trimble Geo7X	Hand-held	Internal	300	N
3	Trimble Geo7X	Hand-held	Internal	300	Y
4	Trimble Geo7X	Tripod	External	300	N
5	Trimble Geo7X	Tripod	External	300	Y
6	Trimble Geo7X	Tripod	External	500	N
7	Trimble Geo7X	Tripod	External	500	Y
8	Trimble ProXRT	Tripod	External	300	N
9	Trimble ProXRT	Tripod	External	300	Y

*Points were collected until the receiver reported 100% complete, approximately 300 seconds on average, and therefore considered equivalent to collection of 300 epochs with the Trimble receivers.

A.2.4. Determination of reference locations

In preparation for the survey to be carried out after the trees were felled, the surveyed peg locations were permanently marked using each of four different methods. A 20 cm length of steel rebar was driven into the ground at the base of the post to a depth of 5 cm below the ground surface. A length of yellow tape attached to the rebar remained visible above the ground surface. The bases of three or four adjacent trees were painted with white paint facing the peg location. Additionally the original labelled peg post was painted white at the top.

The trees were felled in late November 2014 and the site re-visited in early December to determine accurate reference locations. The original under-canopy GNSS locations were used as the initial guide to locating the test positions. Error on the original under-canopy locations

and the extensive site disruption resulting from the felling operation made the task difficult. By clearing debris with a spade and using a metal detector to locate the buried rebar the reference peg locations were identified. The re-located peg position was re-surveyed using the Geo7X with internal antenna, a residency time of 120 epochs and differential correction was carried out. This provided accurate reference locations obtained under open sky for determination of error on the earlier locations determined under canopy conditions.

A.2.5. Determination of error measures

Error was derived as horizontal error (e_h) in metres, being the Euclidean distance between the test positions (x_t, y_t) and reference positions (x_r, y_r):

$$e_h = \sqrt{(x_t - x_r)^2 + (y_t - y_r)^2} \qquad A.1$$

Precision of positions was given by the GPS Pathfinder Office software, for tests with the ProXRT and Geo7X receivers (tests 2-9). Precision is computed as the standard deviation in the horizontal component:

$$\sigma_h = \sqrt{\frac{1}{n-1}\left(\sum_{i=1}^{n}(x_i - \bar{x})^2 + (y_i - \bar{y})^2\right)} \qquad A.2$$

Tests for significant pair-wise differences between mean error values were carried out in R (R Core Team 2014) using a Tukey 'Honest Significant Differences' (HSD) test. Analysis of variance was also carried out using R in order to examine the effects of a number of factors on horizontal error and precision.

Expected horizontal error can be determined at different confidence levels using the observed standard deviations from the different tests made. This error is expressed as the radius of a circle within which a given percentage of observations are expected to fall. For example observed GNSS positions will be expected to fall within $1.177\sigma_H$ at the 50% probability level, where σ_H is the standard deviation of the horizontal errors. Multipliers, obtained from a two

dimensional Rayleigh distribution, for the four probability levels evaluated in this study were as follows: 50% = 1.177, 90% = 2.146, 95% = 2.447, and 99% = 3.035 (van Diggelen 2007).

A.3 Results

Though canopy cover was not quantified, visual inspection of the overhead photographs taken at each test peg location (see Figure A.1 for an example) showed the degree of canopy cover was uniform across all test positions. Horizontal error was calculated using Equation A.1 and results by test are presented in Figure A.2. Horizontal precision estimated by the Trimble® GPS Pathfinder® Office software is presented in Figure A.3. Results for mean horizontal error, and horizontal precision determined for each GNSS test (except for tests with the Garmin 64S) are presented in Table A.2.

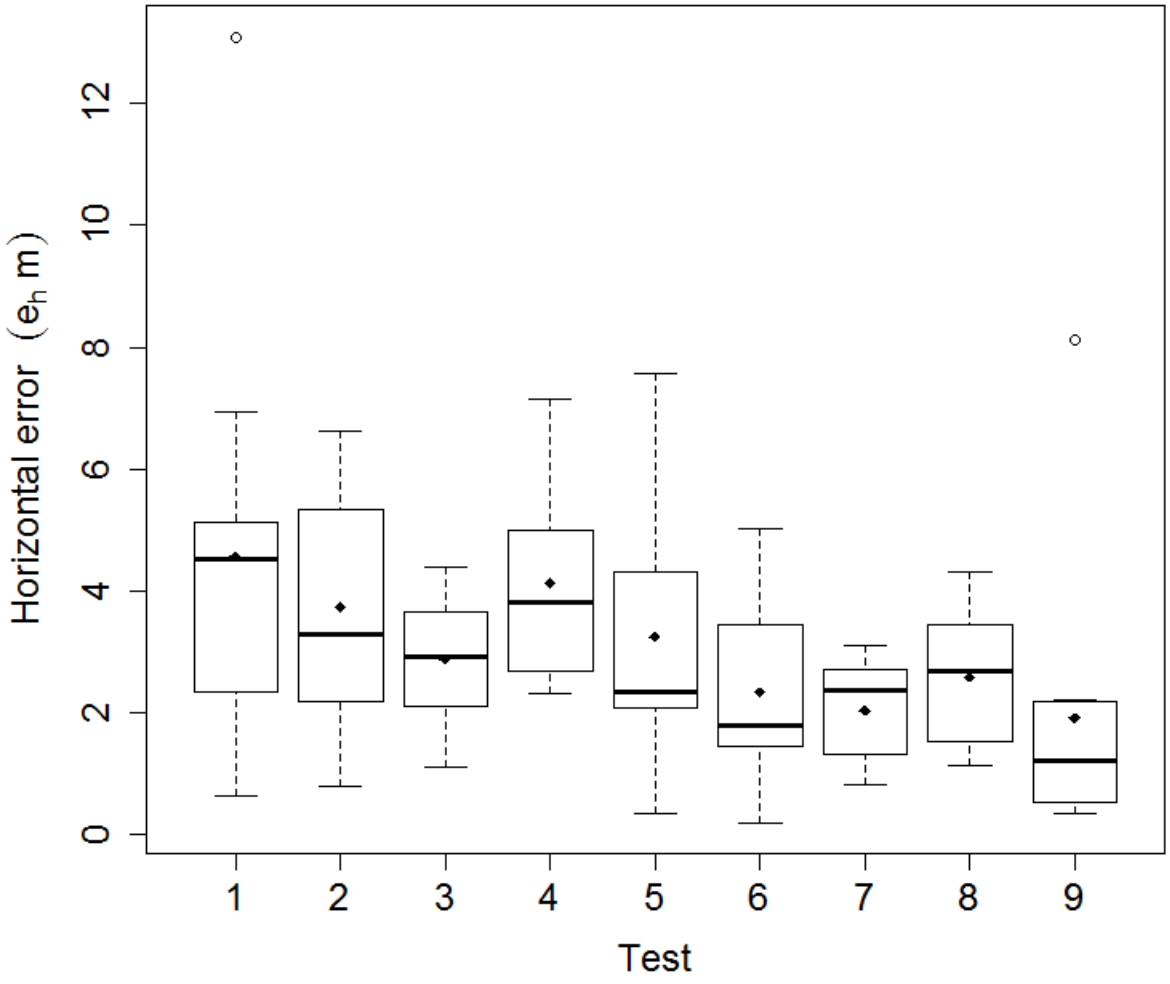

Figure A.2. Horizontal error by GNSS test. The lower end of the box indicates the 25th percentile, a line within the box marks the median, the solid point marks the mean, and the upper boundary of the box indicates the 75th percentile. Error bars above and below the box indicate the nominal data range, defined as the lower and upper quartile minus and plus (resp.) 1.5 times the interquartile range. Points falling outside the nominal data range are represented with open circles.

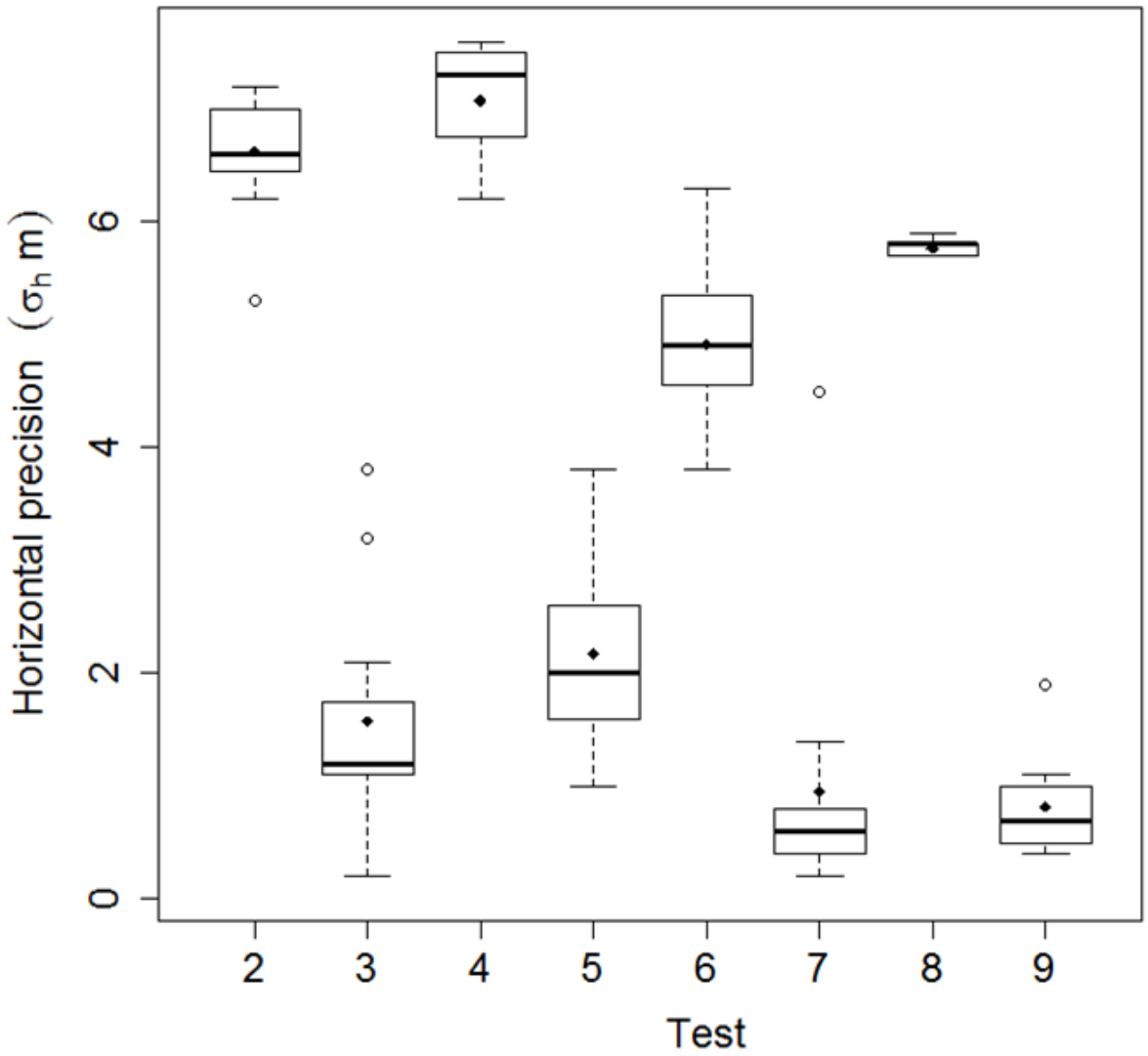

Figure A.3. Horizontal precision by GNSS test. Precision estimates were not available for test 1 with the Garmin 64S. The lower end of the box indicates the 25th percentile, a line within the box marks the median, the solid point marks the mean, and the upper boundary of the box indicates the 75th percentile. Error bars above and below the box indicate the nominal data range, defined as the lower and upper quartile minus and plus (resp.) 1.5 times the interquartile range. Points falling outside the nominal data range are represented with open circles.

Table A.2. Mean and standard deviation of measured horizontal error and precision for the GNSS device tests. Values were obtained from Trimble Pathfinder Office. Precision was not available for test 1 with the Garmin 64S.

Test	Mean error (m)	Standard deviation (m)	Mean precision (m)
1	4.6	3.4	NA
2	3.7	1.9	6.6
3	2.9	1.1	1.6
4	4.1	1.7	7.1
5	3.3	2.3	2.2
6	2.3	1.5	4.9
7	2.0	0.9	1.0
8	2.6	1.1	5.8
9	1.9	2.3	0.8

The largest mean error of 4.6 m came from the Garmin 64S with an internal antenna and no ability to carry out correction (test 1). The smallest mean error of 1.9 m came from the ProXRT with an external antenna and correction by post-processing (test 9). Standard deviations estimated from test measurements were somewhat variable with no obvious pattern related to correction or device except for a higher standard deviation with the consumer grade device in test 1. Precision estimated for positions by the Trimble Pathfinder Office software was significantly better (lower values) after differential correction. Results from analysis of variance are presented in Table A.3. Tests examined the effects of residency time, device, test locations, correction, test date, and external antenna on e_h and σ_h.

Table A.3. Summary of analysis of variance (ANOVA) for the horizontal error (e_h) and horizontal precision (σ_h) of global navigation satellite system (GNSS) tests.

	Horizontal error (e_h)				Horizontal precision (σ_h)			
Source of variation	Df	F value	Pr(>F)		Df	F value	Pr(>F)	
Residency	1	9.089	0.00435	**	1	5.29	0.0265	*
Device	3	3.341	0.0239	*	2	1.149	0.323	(ns)
Location	10	1.971	0.0462	*	10	0.039	1.00	(ns)
Correction	1	2.980	0.0892	(ns)	1	526.9	<0.0001	***
Date	3	1.906	0.134	(ns)	4	7.286	<0.0001	***
Antenna	1	0.489	0.488	(ns)	1	0.430	0.515	(ns)

Results for the Geo7X with external antenna and with 300 and 500 seconds residency time (tests 4, 5, 6 and 7) were analysed to determine the effects of residency time on accuracy and precision. Results showed a statistically highly significant effect of increasing residency time from 300 to 500 epochs (p=0.0044) for e_h, with reductions of 44% and 39% before and after correction respectively. Reductions in σ_h were 31% and 55% before and after correction respectively, but they were marginally statistically insignificant (p=0.0265).

To examine error from different devices (receiver and antenna combinations) analysis of all tests with residency time of 300 seconds (tests 1, 2, 3, 4, 5, 8 and 9) were made. Analysis of variance showed device to be significant (p=0.0239) for e_h but not for σ_h. A Tukey HSD pairwise test by device revealed only a single statistically significant difference of 59% in e_h, between the Garmin 64S with internal antenna (test 1) and the ProXRT with external antenna (test 9) with p=0.0205.

Analysis of variance showed a moderately significant effect of test location (peg) within the trial (p=0.0462) on e_h but a Tukey HSD pairwise test did not show any significant differences in e_h between pairs of test locations (pegs). Test location did not have a significant effect on σ_h.

Results for the three devices with 300 seconds residency, before and after correction by post processing (tests 2, 3, 4, 5, 8 and 9) were analysed to determine the effects of differential correction by post processing. Analysis of variance showed no significant effect for e_h and a highly significant effect on σ_h ($p<0.0001$), with reductions in σ_h averaging 75%.

Analysis of variance showed no significant effect of survey date ($p=0.1340$) on e_h and a highly significant ($p<0.0001$) effect on σ_h. A Tukey HSD pairwise test showed σ_h on a single survey date to differ significantly from the other dates. Results from the Geo7X with 300 seconds residency time (tests 2, 3, 4 and 5) were analysed to determine the effect of external antenna. Analysis of variance showed no significant effect of external antenna for e_h or σ_h.

In order to evaluate the relevance of the GNSS accuracy results obtained in this study it was necessary to consider the accuracy required to identify individual trees on the ground. This was done using a simple theoretical approach, taking into account variation in tree spacing at typical operational stand densities. In a research trial or in an idealised stand with trees located on a uniform grid, individual trees could be located with a position having error less than half the tree spacing (see Figure A.4). Trees in the trial where the tests were carried out were planted on a 4 by 5 m grid and accurate tree location in that situation would require positional error less than 2 m.

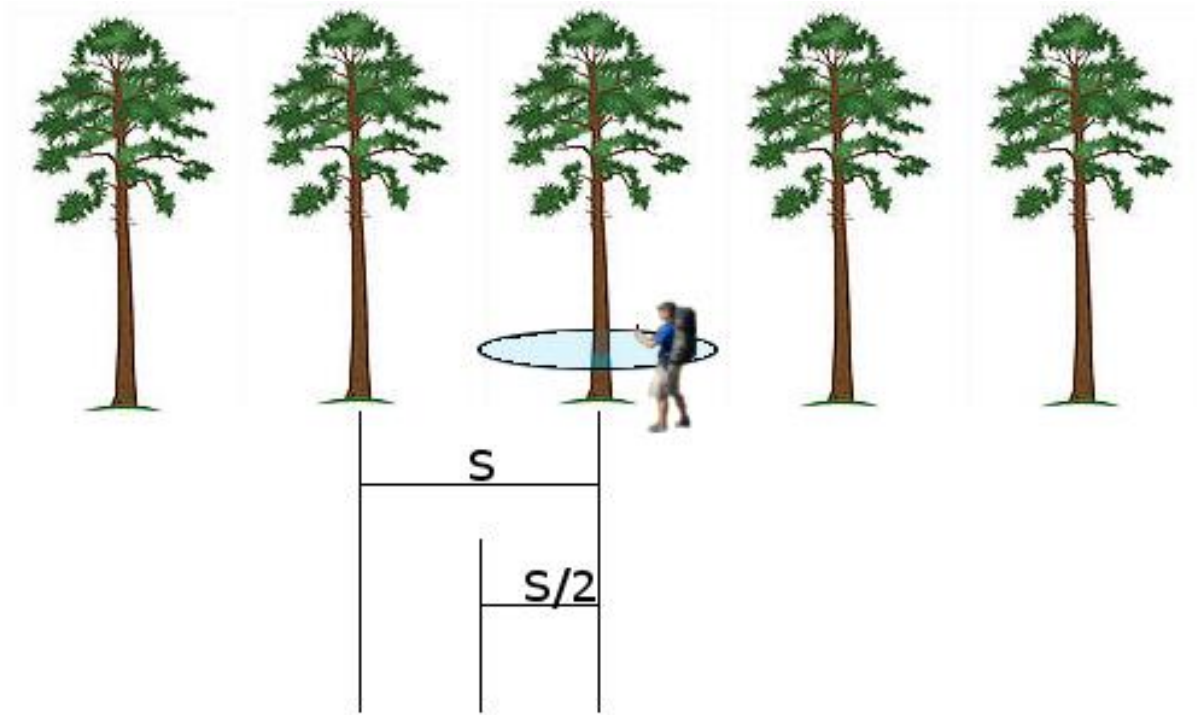

Figure A.4. Acceptable positional error to identify individual trees. In an idealised stand trees are spaced at a distance *S*. To correctly identify individual trees unambiguously would require determination of position with error lower than *S*/2.

Tree spacing can be quite variable in typical New Zealand forest stands, being affected by variations in tree spacing at planting, subsequent thinning and windthrow. An extensive set of tree locations manually digitised by experienced operators on images (D. Pont 2015, pers. comm.), generated during earlier work on development of tree detection methods (Pont et al. 2015b), were used to fit a linear model to estimate minimum tree spacing from stand density. The model used to estimate minimum tree spacing D_{min} in metres from mean tree spacing S in metres is:

$$D_{min} = 0.4038S - 0.0642 \qquad A.3$$

where mean tree spacing S is derived from stand density in stems per hectare D:

$$S = \frac{100}{\sqrt{D}} \qquad A.4$$

This model reflects the fact that some trees within a stand will be closer together than others due to variable spacing, and the shorter distance estimated by the model (D_{min}) is a better estimate of the accuracy required to locate trees than the mean distance between trees (S). Table A.4 presents tree spacing estimates across a wide range of stand densities that would be encountered in New Zealand plantation forest stands. The table shows that minimum tree spacing values estimated from the empirical model are lower than the mean spacing estimated from stand density. In order to separate two trees at the minimum spacing, positional error must be less than half that distance. For example at 400 stems ha^{-1} mean tree spacing is 5 m and half that distance (2.5 m) represents a simplistic estimate of the desired accuracy to identify individual trees at that stand density. The model was then used to estimate a minimum spacing of 2 m for stands at 400 stems ha^{-1}, half that distance (1 m), being a more realistic estimate of the accuracy needed to locate individual trees.

Table A.4. Estimated mean and minimum tree spacing, with corresponding half distances, at different stand densities.

Stand density (Stems ha^{-1})	Tree spacing (m)			
	Mean	Half mean	Minimum	Half minimum
1200	2.9	1.5	1.1	0.6
1000	3.2	1.6	1.2	0.6
800	3.5	1.8	1.4	0.7
600	4.1	2.1	1.6	0.8
400	5.0	2.5	2.0	1.0
200	7.1	3.6	2.8	1.4
100	10.0	5.0	4.0	2.0

The probabilistic nature of GNSS error, discussed in the introduction and detailed in van Diggelen (2007), means that even stricter error tolerances are required to ensure individual trees could be identified to a given confidence level. For individual tree analysis of ALS a 99%

confidence level would be desirable, implying GNSS error could result in one tree in a hundred being incorrectly identified. The standard deviations of our test observations (Table A.2) were used to estimate the radii of circles expected to contain 50%, 90%, 95%, and 99% of GNSS positions, presented in Table A.5.

Table A.5. Radii of circles estimated to include given percentages of GNSS positions for different test devices.

	Error radius at given probability level (m)			
Test	50%	90%	95%	99%
1	4.0	7.3	8.3	10.3
2	2.2	4.1	4.6	5.8
3	1.3	2.4	2.7	3.3
4	2.0	3.6	4.2	5.2
5	2.7	4.9	5.6	7.0
6	1.8	3.2	3.7	4.6
7	1.1	1.9	2.2	2.7
8	1.3	2.4	2.7	3.3
9	2.7	4.9	5.6	7.0

A.4 Conclusions

Results have shown that mean error of the best GNSS device tested exceeded target levels significantly (by 35%) even at the lower end of the stocking range (200 stems ha^{-1}). For a desired 99% confidence level in positional estimates, error of a mapping grade receiver with an external antenna and 500 seconds residency time is estimated to be 2.7 m, which is two and five times higher than necessary at the lower and higher ends of expected stand densities (200 and 1200 stems ha^{-1} respectively). It is concluded that GNSS error under mature New Zealand forest canopy conditions exceeds desired accuracy levels for individual tree location by a significant margin.

This study has shown that the method of using GNSS measurements before and after felling of the stand is an effective approach for quantifying the effects of canopy cover and other factors

on GNSS accuracy. Results confirm the general findings of other researchers that the degree of canopy cover and residency time are the principal effects on accuracy. Further research would be useful to quantify error in different conditions, focusing on canopy cover, related principally to stand age and density, and to evaluate a wider range of residency times.

This study has also confirmed the observation of some other researchers that precision values reported by GNSS devices and software are not useful indicators of horizontal error. These precision values have contributed to a general belief that GNSS accuracy is better than it is in fact, particularly under forest canopy conditions. The individual tree-level analyses of ALS to be carried out in the planned research require methods to identify individual trees accurately. This capability is also required to utilise tree-based methods in operational precision forestry. Results show currently available GNSS devices used in forestry applications cannot deliver sufficient accuracy to reliably identify individual trees in New Zealand forest conditions.

Appendix B Dissemination of Research

The research in this thesis was aimed at developing and evaluating methods to characterise individual trees using remote sensing for applications in precision forestry, in New Zealand and internationally. Results of the research have been presented at a number of national and international forums, and have provided the basis for an upcoming invited keynote speech at an international conference. These outputs, comprising a total of 5 presentations at international conferences, 3 presentations at national conferences, a technical report, and 9 presentations to New Zealand forestry sector groups and governmental agencies, are evidence of the novelty, relevance, and impact of the research.

B.1 International conferences

Dungey, H., S, Pont, D., Li, Y., Wilcox, P., L, Telfer, E., J, Watt, M., S, Jefferson, P., A. (2013). Novel remote sensing phenotyping platform and genomic selection will boost the delivery of genetic gain of radiata pine in New Zealand. In, Forest Genetics 2013. Whistler, British Columbia, Canada, 22-25 July.

Pont, D., Morgenroth, J., & Watt, M.S. (2013). Tree-based analysis of ALS to estimate tree size and quality. In, MeMoWood - Measurement Methods and Modelling Approaches for Predicting Desirable Future Wood Properties. Nancy, France, 1-4 October.

Telfer, E. J., Pont, D., Dash, J., Dungey, H.S., & Moore, J.R. (2015) Whole forest modelling: Reconstructing the past, present and future performance of trees with big data. Paper presented at Queenstown Research Week, QMB Computational Genomics Satellite meeting. Queenstown, New Zealand, 3-4 September.

Pont, D. (2016). The use of LiDAR for Phenotyping Trees. Keynote paper at the international conference: Forest Genetics for Productivity, the next generation, Rotorua, New Zealand, 14-18 March.

Pont, D., Watt, M.S., Morgenroth, J., & Dungey, H. (2016). Correlating tree size and quality with crown metrics from airborne laser scanning. In, WoodQC – Modelling Wood Quality, Supply and Value Chain Networks. Quebec, Canada, 12-17 June.

B.2 National conferences

Pont, D., Watt. M.S., Dash, J., & Brownlie, R. (2014). Remote Sensing for Phenotyping. Presented to the: Forest Owners Association, Forest Growing Research Conference "More income, less risk", Rotorua, New Zealand, 29-31 October.

Pont, D., Dungey, H., Watt, M.S., Morgenroth, J., & Stovold, G. (2015). Can we remotely sense phenotypic information from genetics trials? Presented at the: Second Annual Conference of the GCFF research programme - "First glimpse at results", Christchurch, New Zealand, 24-25 March.

Pont, D., Watt, M.S., Morgenroth, J., Dungey, H., & Stovold, G. (2015). Phenotyping from remote sensing. Presented to the Radiata Pine Breeding Company, Rotorua, New Zealand, 21 May.

B.3 Technical reports

Pont, D., Watt, M.S., Morgenroth, J., Dungey, H., Brownlie, R.K., & Stovold, G. (2015). Locating individual trees within a forest genetics trial. (GCFF TN-06). Rotorua, New Zealand; Growing Confidence in Forestry's Future.

B.4 Research presentations

Pont, D., Watt, M.S., & Paul, T. (2013). LiDAR and remote sensing. Presented to a representatives of the Ministry for the Environment, Rotorua, New Zealand, 18 December.

Pont, D., Dash, J., & Watt, M.S. (2014). Remote Sensing. Presented to representatives of Ballance Agri-Nutrients, Rotorua, New Zealand, 4 February.

Pont, D. (2014). Remote Sensing and LiDAR. Presented to representatives of the NZ Drylands Forest Initiative, Rotorua, New Zealand, 12 March.

Pont, D. (2014). Tree-Level Analysis of Aerial LiDAR for Phenotyping. Presented at School of Forestry, University of Canterbury during Mid-thesis defence, Christchurch, New Zealand, 28 April.

Pont, D., & Graham, B.P. (2014). Remote sensing and phenotyping platform and UAVs, big data and informatics. Presented to Callaghan Innovation, Rotorua, New Zealand, 31 July.

Pont, D. (2015). Remote Sensing and new tools for forest managers. Presented to Minister of Parliament, Hon. Todd McClay, Rotorua, New Zealand, 23 April.

Pont, D. , Watt, M.S., Morgenroth, J., Dungey, H., & Stovold, G. (2015). Phenotyping from remote sensing, first steps. Presented to Representatives of the Forest Owners Association, Rotorua, New Zealand, 6 May.

Pont, D. (2015). Remote sensing and new tools for forest managers. Presented to Member of Parliament, Fletcher Tabuteau, Rotorua, New Zealand, 31 July.

Pont, D., Dungey, H., Watt, M.S., Morgenroth, J., & Stovold, G. (2016). Genetic parameters from airborne LiDAR. Presented to Growing Confidence in Forestry's Future Technical committee quarterly meeting, Rotorua, New Zealand, 16 February.